Ph.D. FLASH PRESENTATIONS SESSIONS

FpS B: Risks

M. Bouvet, D. Francois, C. Schwartz
Role of road soils in retention of lead leached from municipal solid waste incinerator bottom ash used in road construction

V. Cappuyns, R. Swennen, K. de Nil
Risk assessment of heavy metal pollution in alluvial soils and sediments of the Grote Beek River (Belgium)

A. Emonet, M.A. Buès, C. Oltean, O. Bour, P. le Thiez
Experimental and numerical studies of Trichlorethylene migration

K. Poggel, R. Breiter, T. Neeße
A new SPME-based concept for studying chlorinated hydrocarbon degradation in microcosms

G. Lespagnol, J.L. Bouchardon, B. Guy, E.M.S.E., France
Chromium, copper, and arsenic distribution and leaching from soil contaminated with timber preservative

T. Boucard, R.D. Bardgett, K.C. Jones, K.T. Semple
Temporal changes in extractability and mineralization of 2,4-dichlorophenol in plant-amended soil

S. Gaw, G. Palmer, N. Kim, A. Wilkins
Impact of copper based fungicides on the degradation of 4,4 DDT to 4,4 DDE in pip and stonefruit orchard soils in the Waikato region, New Zealand

C.M. Bürger, M. Finkel, G. Teutsch
Data worth analysis in remediation systems planning

FpS C: Remediation Technologies and Concepts

M. Gozan, A. Müller, H. Lorbeer, P. Werner, A. Tiehm
Stimulated biodegradation of chlorinated hydrocarbons in biological activated carbon barriers

M.S.M. Chan, R.J. Lynch
Photocatalytic remediation of MTBE in groundwater

M. Vaccari, R. Bellini, C. Collivignarelli, P. Forzatti, L. Lietti, V. Riganti
Study on the applicability of the thermal desorption process to alkyl-lead contaminated soils

U. Hiester, T. Theurer, A. Winkler, H.-P. Koschitzky, A. Färber
Technical scale investigations for the in situ remediation of low volatile contaminants by thermal wells

S. Gödeke, M. Schirmer, C. Vogt, R. Trabitzsch, H. Weiß
Stimulating natural attenuation at a BTEX-contaminated megasite: The SAFIRA Zeitz project

F.A. Shakweer, C.P. Nathanail
LCA methodology for remediation strategy selection

Ph.D. FLASH PRESENTATIONS

Ph.D Flash Presentations:

FpS B
Risks

ROLE OF ROAD SOILS IN RETENTION OF LEAD LEACHED FROM MUNICIPAL SOLID WASTE INCINERATOR BOTTOM ASH USED IN ROAD CONSTRUCTION

Mickael BOUVET[1-2], Denis FRANÇOIS[1] and Christophe SCHWARTZ[2]

[1] Laboratoire Central des Ponts et Chaussées, route de Bouaye, BP4129, 44321 Bouguenais, France.
[2] Laboratoire Sols et Environnement, ENSAIA-INPL/INRA UMR 1120, BP 172, 54000 Nancy, France.

Phone: (33) 02 40 84 56 89 **Fax:** (33) 02 40 84 59 98 **E-mail:** mickael.bouvet@lcpc.fr

1- Introduction

Economic stakes on raw materials and harmful effects linked to waste landfill, lead to the re-use of alternative materials like municipal solid waste incinerator bottom ash in road construction [1]. MSWI bottom ash represents a production of 3 million tons per year in France, an important part of which is re-used in road construction [2]. This alternative material has a high heavy metal content, which can, under the effect of rainfall infiltration through road, leache and infiltrate into the underlying soil. The assessment of eco-compatibility of MSWI bottom ash re-use implies to study the solubility and the retention of heavy metals in road soil. Road soil is the natural soil underlying the road, previously scraped down to 30 cm and compacted (figure 1). It can act as a pollution filter.

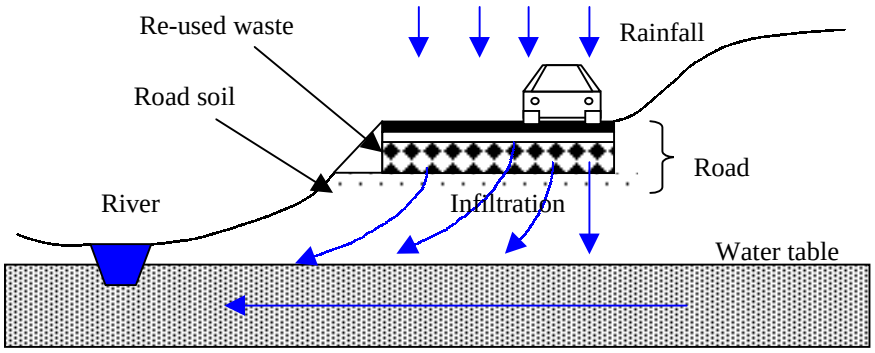

Figure 1: Road – soil – water system

This study is dedicated to Pb transfers into the soil-waste-water system. Lead has a long residence time in environment and tend to accumulate into soil. It is known for being poisonous for mammals [3]. MSWI bottom ash has a high lead content, which can leach, and possibly relegate this material to dump, in accordance with the regulation [4].

2- Methodology

The study is split in three stages.

(i) First, a series of batch tests to highlight the chemical interaction between soils and the MSWI bottom ash leachate.

(ii) Second, unsaturated column tests on selected soils, more or less compacted, to combine the hydrodynamic with the chemistry;

(iii) Third, *in situ* validation.

The paper deals with batch tests. It presents the results of mass-balance and physico-chemical characterisation of some model materials. The aims of batch tests were to select some materials for the column tests and to understand their reactivity with the MSWI bottom ash leachate.

The batch test consists to shake materials and leachate from MSWI bottom ash. The first stage was to determine the right mixing time between materials and the leachate. It has been determine thanks to batch test on which the conductivity and the pH were monitored. When, these parameters were both stable during three consecutive measurements, the reaction was considered as finished. In a second step, the final mixing time was used to carry out a set of batch tests (3 replicates) for each mixture (material-solution) into centrifuge tubes. The dry weight of soil was 10 g and the solution volume was 200 ml for each (L/S=20). After the batch test, the replicates were directly centrifuged for 2500 G and for 15 min. Them, the solution was filtered through a 0,45 µm filter and acidified to pH 2 with HNO_3. The pH and the conductivity were measured and that indicates that the equilibrium between the solid and the leachate was reached. The mass-balance was carried out between the leachate and the solution after test.

Model materials

These materials were characterised through their particle size distribution, CEC, specific surface (BET), pH and their carbonate content. Results are presented in table 1. Their characteristics show that the sandy materials have the lowest CEC and specific surface, unlike the clay materials, which have the highest.

All materials show neutral or basic pH. M2 and M3 are carbonate materials. The buffer power for OH^- was determined to understand the capacity of these materials to neutralize a basic solution. This basic neutralization was very poor for all the materials. Smectites presented the highest with 71 meq/kg.

Mineralogical characteristics of model materials play a very important role in chemical reaction with MSWI bottom ash leachate. All the results of table 2 have been obtained by x-ray diffraction. Two materials (M2 and M3) were dominated by carbonate minerals (calcite and dolomite). M1 was only made of quartz, M4 of kaolinite, quartz and illites, M5 of quartz, smectites and kaolinite, and M6 of hematite.

Table 1: Physico-chemical characteristic of materials

Name		M1	M2	M3	M4	M5	M6
Nature		Siliceous sand	Calcareous sand	Calcareous silt	Kaolinite	Montmorillonite	Iron oxide
Particle size distribution	> 50 µm	100,0	74,3	4,8	5,8	1,6	0,1
	2 – 50 µm	0,0	22,4	84,3	89,3	83,8	86,3
	< 2 µm	0,0	3.3	10,9	4,9	14,6	13.,6
CaCO3	g/kg	0	804	880	0	0	0
CEC	meq/g	0,4	0,3	2,2	4,3	22,7	0,4
Specific surface	m²/g	<0,1	0,5	1,2	11,8	80,9	1,6
pH	-	8,6	9,1	12,4	8,8	7,8	7,2
Buffer power	meq/kg (OH^-)	34	15	0	26	71	12

Table 2: Mineralogical composition of model materials

	M1	M2	M3	M4	M5	M6
quartz	++++		++	++	+++	
calcite		++++	++++			
dolomite		++				
kaolinite				+++	++	
smectites	tr	tr	tr		++	
illite				++	tr	
hematite				tr		++++

++++ dominant ++ abundant

+++ very abundant tr trace

The bottom ash leachate

For this study, a no valuable MSWI bottom ash has been chosen for its high lead content thanks to very basic leachate. Chemical composition of the MSWI bottom ash is presented in table 3. These results show that the element concentration have values close to the MSWI bottom ash mean composition [5].

Table 3: Chemical composition of MSWI bottom ash.

Element	Al	Fe	Ca	K	Mg	Mn
g/kg	52,1	33,8	120,1	11,0	10,1	0,6

Element	Cd	Cr	Cu	Ni	Pb	Zn
mg/kg	1,7	257	2206	127	917	4036

A leachate is first produced in a column with a liquid / solid ratio of 0,7 in 3 days with de-ionised water. The pH is 13,2, due to $Ca(OH)_2$ dissolution ([Ca]= 634 mg/l). It favours the Pb solubility ([Pb]= 5,4 mg/l). These characteristics represent a “fresh” product. To represent the progressive exhaustion of the pollutant source, as the natural pH decrease, a dilution rate of 10 has been used (table 4). Consequently, the second solution has a pH of 12 and a lead concentration of 0,53 mg/l. This concentration value can be compared to lead concentration value of the French regulation, which is 1 mg/l after a 24 hours leaching test for valuable bottom ash (“V class”)[4].

Table 4: Chemical composition and pH of leachates

	Al	Pb	Ca	Si	pH
	mg/l				-
solution A	< 0,10	5,34	634	0,6	13,2
solution B	< 0,10	0,53	52	0,5	12
French regulation	-	1	-	-	-

The buffer capacity of solutions plays an important role in maintaining the pH level of the mixture. Figure 2 shows the acid neutralisation capacity of the solutions which was very high for solution A with an acid neutralisation capacity of 57 meq/l, and smaller for solution B (6,4 meq/l) virtually divided by 10, like the dilution rate from A to B.

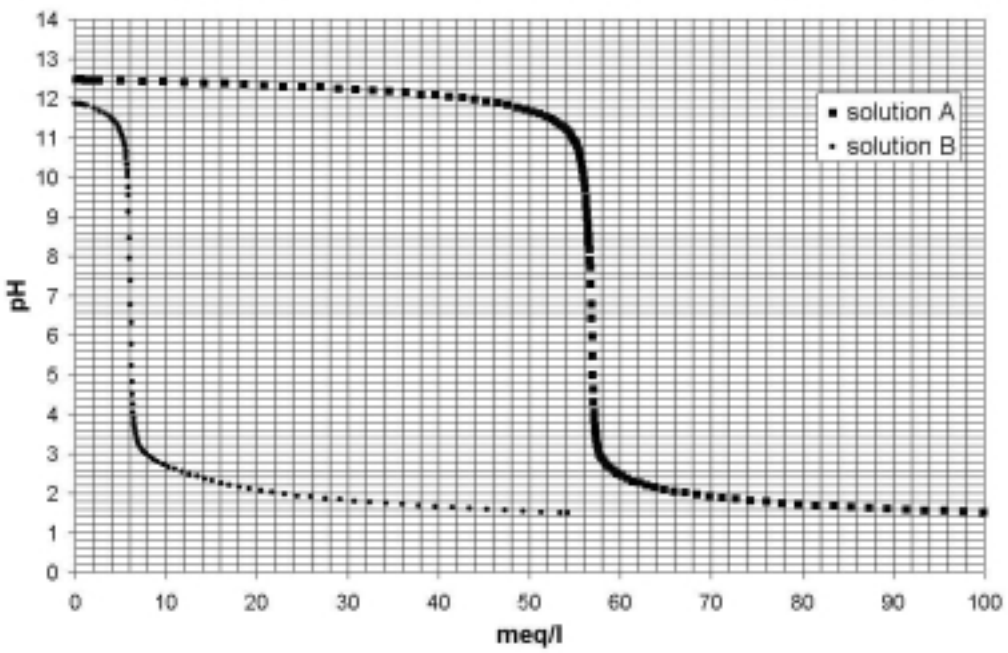

Figure 2: Acid titration of the two solutions from MSWI bottom ash

Analyses

Both materials and the filtered water were analysed by ICP. Analyses of Pb content was made with atomic absorption with graphite furnace depending on concentration. Furthermore, the solution was analysed for pH with the pH-meter TitraLab® TIM 900, and for conductivity with the conductivity-meter MeterLab® CDM 210.

3- Results and discussion

The first stage of the batch test experiment was to determine the right mixing time between model materials and the leachates from MSWI bottom ash. Results for pH and conductivity monitoring are presented in figures 3 and 4. The results for pH and conductivity are similar.

For all mixtures (materials and solutions), the pH and the electric conductivity changed very quickly and stabilised after three hours. To be sure that the equilibrium was reached a mixing time of six hours was applied.

For solution A, the pH is very stable and determined by the solution, which has a very high acid neutralisation capacity. In solution B, the pH is always determined by the solution but the buffer power of M3 and M5 can influence it. Conductivity and pH increased for the calcareous silt (M3) and decreased for the montmorillonite (M5). Sandy materials (M1 and M2) and iron oxide are not really reactive.

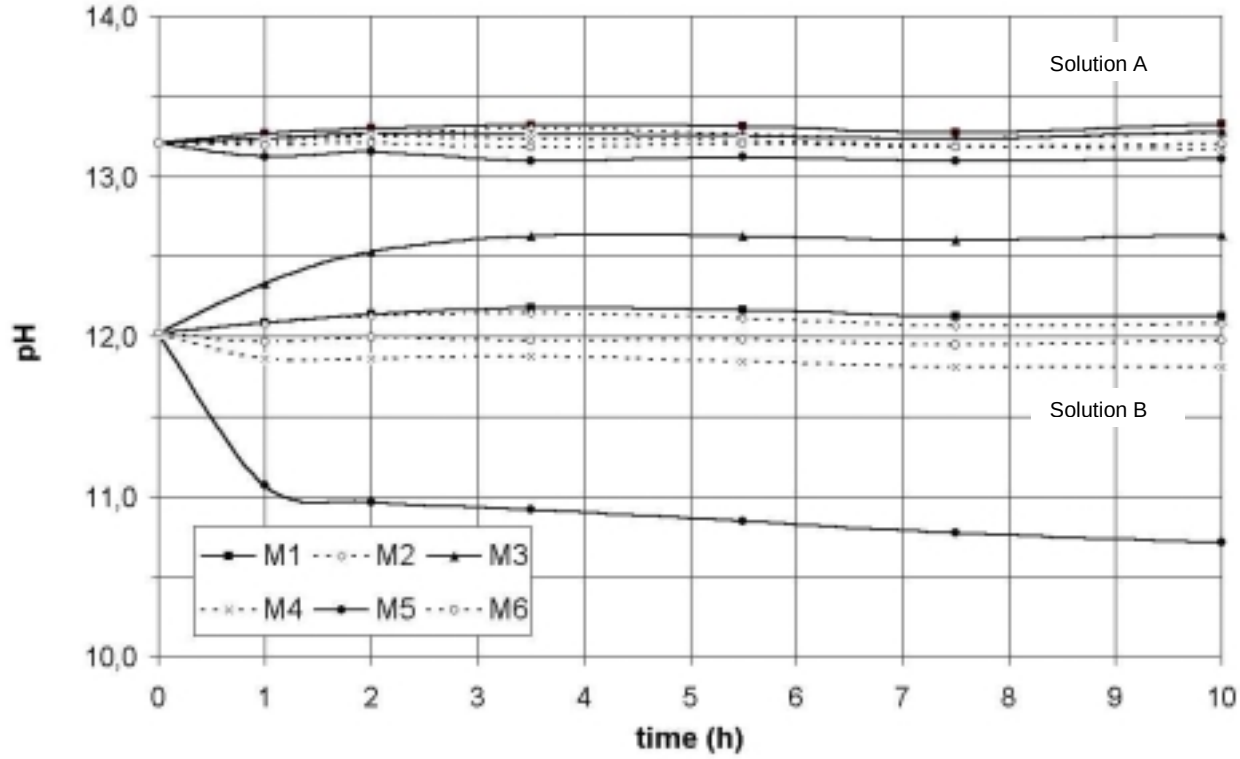

Figure.3: Evolution of pH for model materials and two solutions.

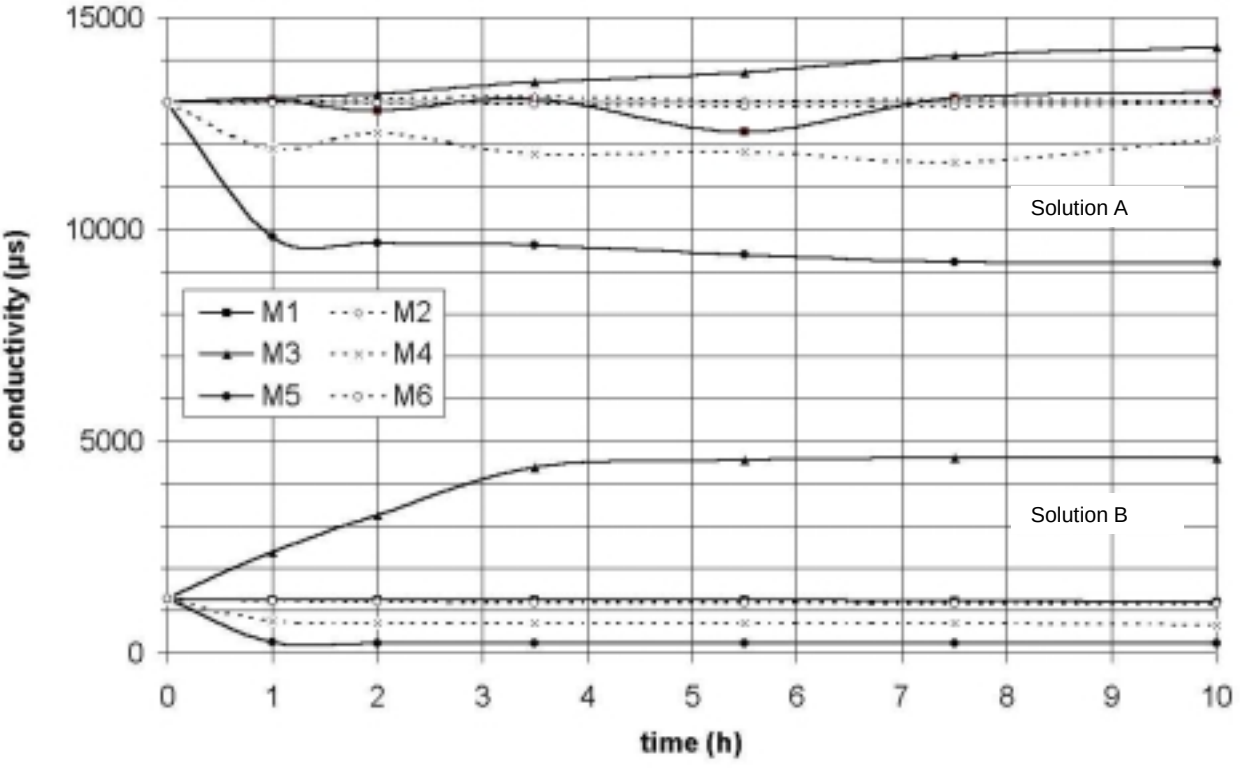

Figure.4: Evolution of conductivity for model materials and two solutions.

Mass balance

Results of the mass balance for Pb are presented in figure 5. For solution A, M1 and M2 (sandy materials) are not really reactive. On the opposite, M3, M4 and M6 adsorb up to 80 % of the Pb initially in the solution. M5 absorbs nearly all the Pb. Sandy materials can not absorb all of the Pb of solution A. On the opposite clayey materials, in particular M5, adsorb all the Pb for each solution. These can be link to their high CEC and specific surface.

For solution B, M1 and M2 adsorbed the same quantity of Pb compare to solution A which represents, in that case, 80 % of the initially Pb. The other materials adsorbed all the Pb. Sandy materials show the lower retention capacity for Pb. The poor retention capacity of sandy materials in contact with leachate from MSWI bottom ash has been pointed up on an actual road after more 20 years of service [6].

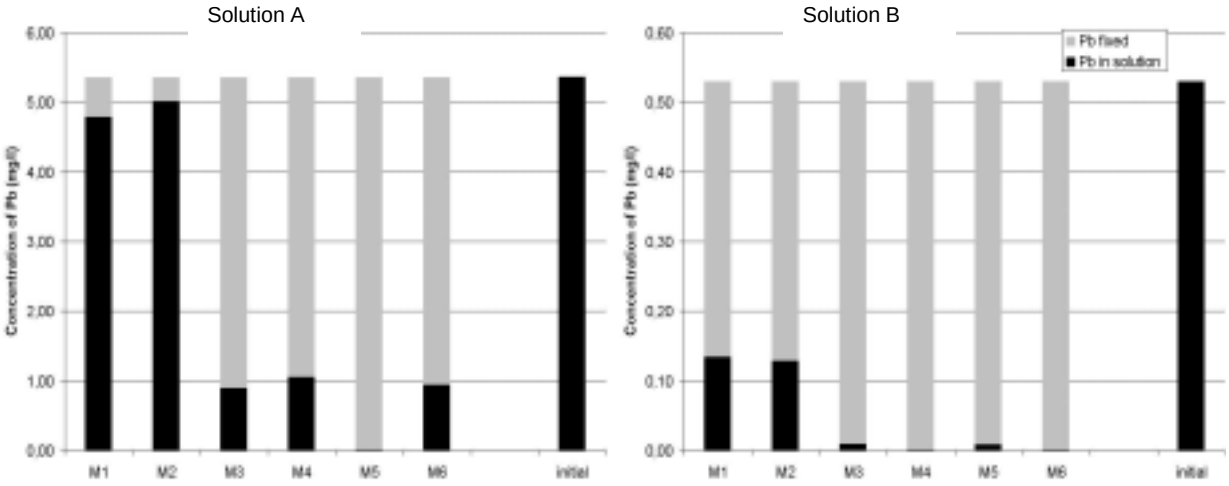

Figure 5: Mass balance for Pb

Exchanges of Ca, Al and Si have also been observed to understand the whole geochemical system evolution (figure 6).

The absorption of elements by some soils (M4, M5) and the release from another (M3) can be explain the electric conductivity evolution (Figure 4). Materials M3 and M5 show different buffer powers which can be explained by the Ca^{2+} exchange. Compared to the initial concentration, we can see that Ca do not exchange in the case of M1, M2 and M6. The calcium is adsorbed by M4 and M5 (clay materials) and released by M3 (calcareous silt). Montmorillonite releases Al and Si. This can be seen in a smaller extend for M3 and M4. Soil chemical behaviours show the same tendency for the evolution of Al, Ca and Si concentrations. But relatively speaking exchanges for these elements were higher for solution B due to the pH decrease with the dilution rate.

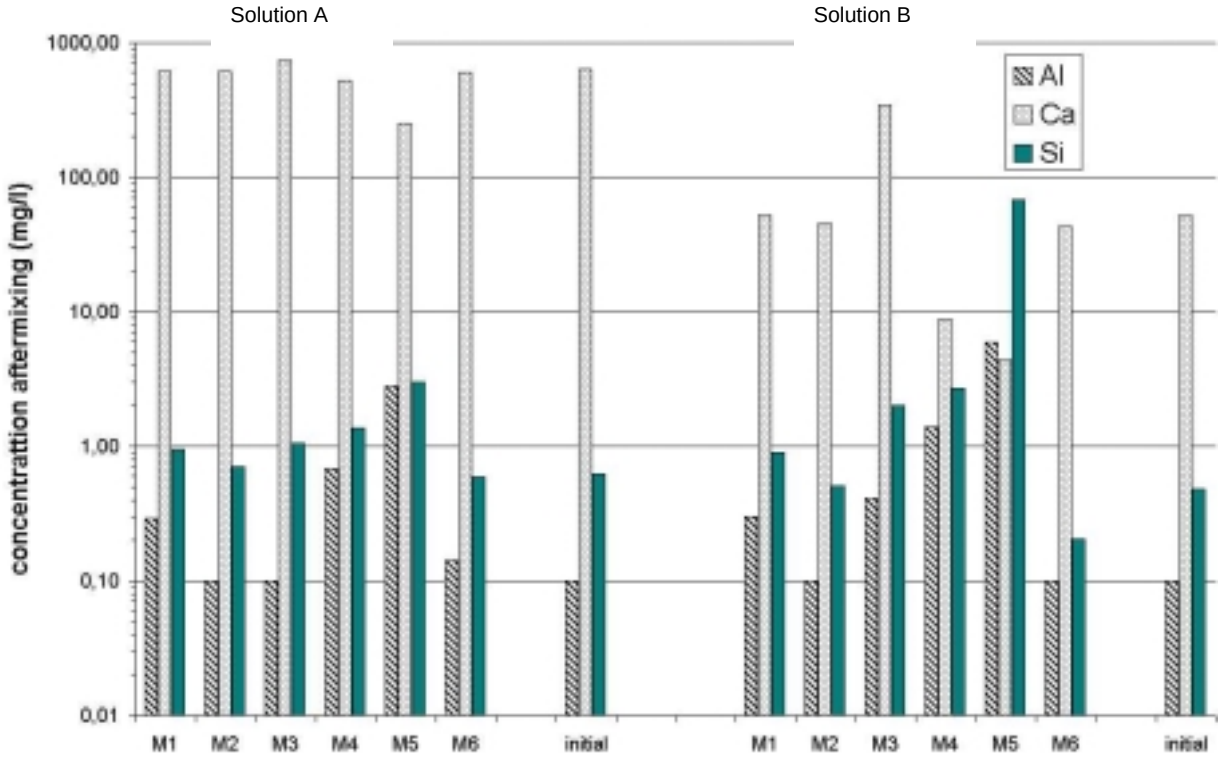

Figure 6: Retention of Ca, Si and Al for model materials

4- Conclusions and perspectives

These experiments show uneven results on the interaction between different materials and MSWI bottom ash leachates representative of a “fresh” product and older MSWI bottom ash. Natural sandy materials do not strongly adsorb the Pb, contrary to clayey materials. This work shows that Pb may, sometimes, not be fixed by the road soil. Moreover, soil capacity to neutralize MSWI bottom ash leachates and soil capacity to adsorb Pb have been linked to soil physico-chemical characteristics like particle size distribution, CEC or buffer power.

Batch test will be carried out on natural soils and for different dilutions, in order to represent the ageing of the source. They will help in the selection of soils for the column tests.

The final objective of the study is to check whether interactions between heavy metal loaded leachates with road soil can have practical consequences in the field of road construction with alternative materials, and soil and ground water conservation.

References

[1] ADEME. Evaluation de l'écocompatibilité de scénarios de stockage et de valorisation des déchets. Principes généraux. *ADEME*, Paris, 2000.

[2] ADEME. Techniques de gestion des déchets ménagers. *ADEME*, Paris, 2000.

[3] Alloway, B.J. Heavy metals in soils. *Blackie Academic , Professional*, London, Second edition, 1995a.

[4] Ministère de l'environnement français. Circulaire 94-IV-1, 1994.

[5] The International Ash Working Group. Municipal solid waste incinerator residues. Studies in Environmental Science 67, *Elsevier*, 1997.

[6] Francois, D., Legret, M., Demare, D., Fraquet, P., Berga, P. Comportement mécanique et environnemental de deux chaussées anciennes réalisées avec des mâchefers d'incinération d'ordure ménagères. *Bulletin des Laboratoires des Ponts et Chaussées*, v. 227, p. 15-30, 2000.

RISK ASSESSMENT OF HEAVY METAL POLLUTION IN ALLUVIAL SOILS AND SEDIMENTS OF THE GROTE BEEK RIVER (BELGIUM)

Valérie Cappuyns, Rudy Swennen and Katrien De Nil

Katholieke Universiteit Leuven, Fysico-chemische Geologie, Celestijnenlaan 200C, 3001 Heverlee, Belgium
Tel. +3216327297, Fax. +3216327981, e-mail: Valerie.Cappuyns@geo.kuleuven.ac.be

1. Introduction

Wastewater discharge from the processing of phosphate ores has contributed to pollution by heavy metals and As in soils adjoining the Grote Beek river (15km long) (Central Belgium). Moreover, elevated chloride concentrations comparable to concentrations in seawater are discharged into the river. The study area is characterized by sandy soils and underlain by the Diestian Formation, containing between 30-40% glauconite. Organic- and iron-rich wetland soils have developed along this stream. The river follows a very meandering path and is characterised by several flooding zones that are inundated a few times a year. The analysis of soil and porewater samples from the area indicated a severe contamination of the floodplain soils and sediments with Cd, Cu, Ni, Zn, Ba and As (up to 276, 531, 172, 7507, 523 and 496 mg/kg respectively) (Cappuyns et al, 2002). The porewater contained elevated concentrations of Cd, Cu, Ni, Zn and Ba (up to 43, 187, 138, 1034 and 4432 µg/l respectively), while As did not seem of immediate environmental concern.
However, porewater composition only gives an indication on the availability and mobility of heavy metals in soils on one specific moment, yet fluctuations in porewater compositions often occur. To perform a risk assessment, predictions about the long-term behaviour of pollutants are necessary, which cannot only rely on porewater analysis. Also the capacity controlling parameters (CCP's) have to be taken into account since they control geochemical and microbiological processes that determine the fate of pollutants in soils and sediments (Stigliani et al., 1991). CEC, pH, redox potential, soil organic matter, salinity and microbiological activity are the CCP's of soils and sediments for heavy metals. In this study, different extractions and leaching tests were used to assess the influence of CCP's on heavy metal behaviour and to estimate the potential (long-term) mobility of heavy metals. Present discussion focuses on the results obtained for two samples (an overbank sediment rich in Fe and organic matter and a dredged sediment that was disposed on the riverbank) representative for the studied area.

2. Material and methods

Physico-chemical analysis, extractions and leaching tests were performed on two oven-dry samples, one representative for overbank sediments (O) and the second for dredged sediments (D). pH(H_2O) was measured in a soil/water suspension (1/2.5). Organic carbon was determined according to the Walkey and Black method (Nelson and Somers, 1982); effective cation exchange capacities (ECEC) were analyzed applying the 'silver thiourea method' (Van Reeuwijk, 1992). Total element concentrations (Al, As, Ba, Cd, Co, Cr, Cu, Ni, Pb, Zn, Fe, Mn, K, P and Ca) were determined after dissolution of the samples with a mixture of 3 concentrated acids (4 ml HCl_{conc}, 2 ml HNO_{3conc} and 2 ml HF_{conc}). These solutions were analyzed by AAS (Varian® Techtron AA6) for Ca, Fe, K and Al. For As, Ba, Cd, Co, Cr, Cu, Ni, Pb, Zn, Mn and P a multi element analysis by ICP-MS (HP 4500 series) was carried out. A certified reference material (Montana Soil 2710) and sample duplicates were used for quality assurance of the analytical data. A mineralogical sample characterization was conducted by X-ray diffraction.
The influence of reducing conditions on heavy metal mobility was assessed by making use of a reducing agent ($NH_2OH.HCl$ in 25% CH_3COOH) at different concentrations (Davranche and Bollinger, 2002). 30 ml of $NH_2OH.HCl$ in 25% CH_3COOH (0.01, 0.05, 0.1, 0.2 and 0.5 M) was added to 0.2 g of oven dry soil in a 50 ml centrifuge tube. The experiment was conducted at 96 °C with a 5 h equilibration time as determined by Tessier et al. (1979). After reaction, the suspension was centrifuged (2500 r.p.m., 10 min.), decanted off and filtered (Millipore 0.45 µm).

To investigate the impact of elevated Cl^- concentrations in the floodwater on heavy metal mobility, extractions with Cl^- solutions at different concentrations (0, 250, 500, 1000, 2000, 4000 and 6000 mg/l) were performed. 20 ml of a NaCl solution was added to 1 g of sample in a polyethylene centrifuge tube, shaken on a reciprocal shaker during 10 h, centrifuged (3500 r.p.m, 10 min.), decanted off and filtered (Millipore 0.45µm). The samples were acidified and stored at 4°C until their analysis (ICP-MS)

A modified BCR-extraction scheme was applied (Table 1). Because of the elevated Fe-content of the samples, a reducing extraction with $NH_2OH.HCl$ 0.5 M was added to the original sequence. pH_{stat} leaching tests with continuous setpoint titration (pH 2, 4, 6, 8 en 10) were used to assess long-term effects of pH on heavy metal mobility and predict possible chemical time bombs (cfr. Van Herreweghe et al., 2002*).* The pH_{stat} tests were conducted during 96 h. However the pH_{stat} test for sample O was prolonged to 176 h because a sudden increase in the BNC curve at pH 10 after 71 h. Reaction kinetics was also considered by mathematical fitting of leaching curves as a function of time (Schwarz et al., 1999).

A Cascade Leaching Test (NEN 7341) was used to estimate the actual leachability of heavy metals in the samples. The extractions were carried out in triplicate in acid rinsed 50 ml polyethylene centrifuge tubes with screw caps. 30 ml of distilled water, acidified to pH 4 with ultrapure HNO_3 was added to 1.5 g of dry sediment sample. The suspension was shaken during 22 h on a reciprocal shaker, centrifuged (3000 rpm, 10 min), decanted off and filtered (0.45 µm). This extraction was repeated until five fractions, with a solid/liquid ratios ranging from 20 to 100 were obtained. The cascade leaching test was also performed on $Ca_3(PO_4)_2$ (sample C) en Fe-oxide (sample F) subsamples that were separated from the dredged sediment (sample D). Element concentrations in the leachates of the pH_{stat} and cascade leaching tests were measured with ICP-MS. SO_4^{2-} was determined by turbidimetry (Vogel, 1961).

Table 1: Modified BCR extraction scheme

	Fraction	Chemical agents	Duration
Step 1	Acid-extractable	CH_3COOH 0.11M	16 h
Step 2a	Reducible	$NH_2OH.HCl$ 0.1M, pH 2	16 h
Step 2b	Reducible	$NH_2OH.HCl$ 0.5M in CH_3COOH 25%, 90°C	5 h
Step 3	Oxidisable	H_2O_2 15%, pH 2, 80°C; CH_3COONH_4	2x evaporate; 16 h
Step 4	Residual	HNO_3/HCl/HF $_{conc}$	

3. Results

Total concentrations of heavy metals are shown in Table 2. Intervention Values for Soil Contamination (Anonymous, 1995) were exceeded for Cd, As (both samples) and Zn (sample D). Quartz, hematite, amorphous Fe-oxides, pyrrhothite and glauconite were identified in the overbank sediment (O) by XRD-analysis. The dredged sediment (D) contained amorphous Fe-oxides, quartz, glauconite and $Ca_3(PO_4)_2$. $Ca_3(PO_4)_2$ and Fe-oxide grains were separated manually from the dredged sediment sample (D), characterised by XRD and analysed for major and trace elements. Amorphous Fe-oxides (F) were enriched in As and Ni. Small white particles which consisted of $Ca_3(PO_4)_2$ (C) contained elevated concentrations of Cd, Zn, Cu and As .

Table 2: Concentrations of heavy metals, As, Fe, organic carbon (org. C), CEC, pH (H_2O) in the 2 samples (D= dredged sediment, O= overbank sediment, C= $Ca_3(PO_4)_2$, F=Fe-oxide). NA = Not Analysed

	Cr	Ni	Cu	Zn	As	Cd	Ba	Pb	P	Ca	Fe	Org. C	CEC	pH
	mg/kg	mg/kg	mg/kg	mg/kg	mg/kg	mg/kg	mg/kg	mg/kg	mg/kg	%	%	%	cmol/kg	
D	84	108	182	4083	254	213	753	84	20521	1.67	8,2	8,8	19.2	6,8
O	44	30	10	265	176	40	292	67	3920	0.53	14.7	9,0	31.2	6,3
C	119	78	462	8025	305	374	516	23	122659	3.43	0.47	NA	NA	NA
F	41	183	67	1773	446	210	350	27	12336	0.93	23.5	NA	NA	NA

3.1 Single Extractions

EDTA was capable of extracting between 50 to 100 % of the total concentrations of Cd, Ni, Zn, Cu an Pb. Only negligible amounts of Ba, As and Cr were released (Fig. 1). Cl^- had the most significant effect on the leaching of Cu, Cd (Fig. 2a), Zn and Ni. In absolute concentrations the metal leachability decreased in the order Cu > Zn > Cd > Ni. Relative to their total concentrations in soil the order was: Cu > Ni, Cd > Zn. Stronger reducing conditions induced a significant increase of the release As (Fig. 2b), Pb, Ba and Cr.

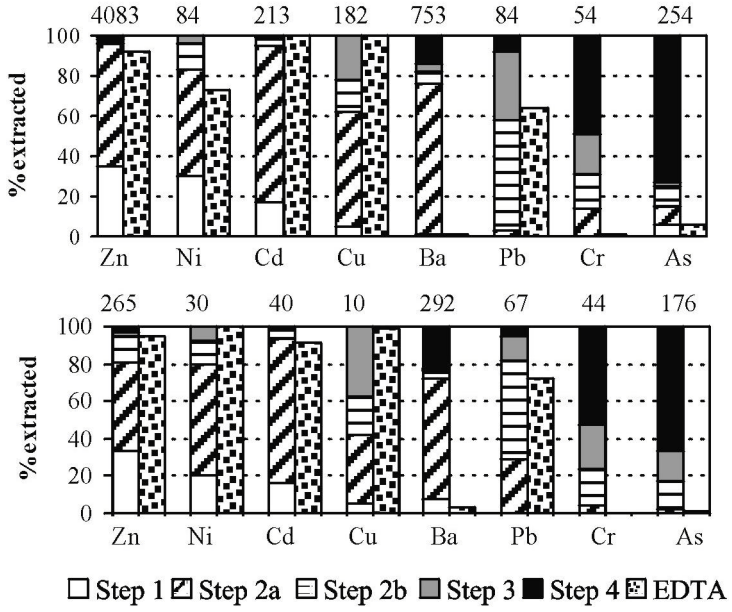

3.2 Sequential extractions

The fractionation of trace elements was very similar for both samples. Zn, Ni and Cd were principally released during the CH_3COOH (Step 1) and the $NH_2OH.HCl$ 0.1M (Step 2) extractions. For Cr an As, the residual fraction prevailed, while Pb was mostly recovered in Step 2b and 3. In the dredged sediment, a low but significant As-concentration (6 mg/kg) was extracted with CH_3COOH (Step 1) and EDTA. Cu and Ba are generally characterized by a considerable reducible fraction (Step 2a) and a significant amount of Cu was also released during the oxidising extraction (Step 3).

Figure 1: Heavy metal and As fractionation according to the BCR extraction (Table 1) in sample D (a) and O (b)

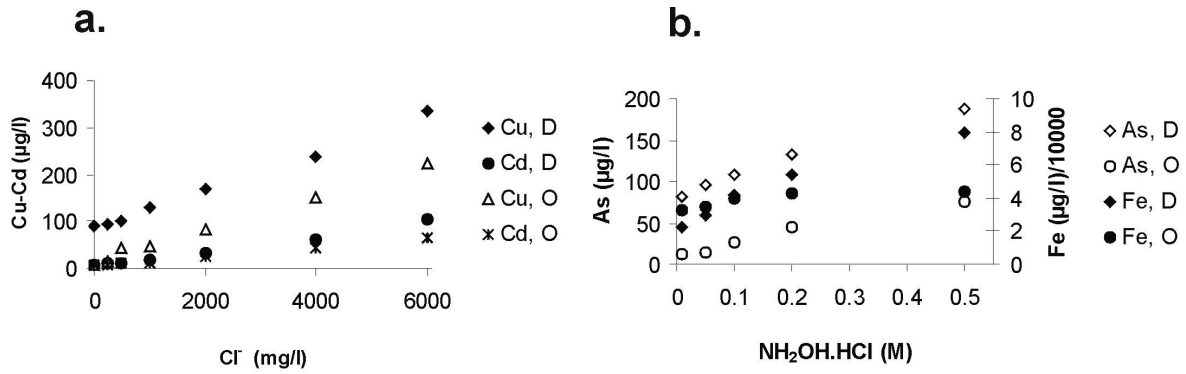

Figure 2: (a) Leaching of Cd and Cu as a function of Cl^- concentration (b) Leaching of As and Fe as a function of $NH_2OH.HCl$ concentrations.

3.3 Leaching tests

Heavy metal concentrations in the leachates of the cascade test performed on the dredged sediment (D) were significantly higher than for the overbank sediment (O) (Table 3). Although Cu, Ni, Zn, As, Cd and Ba-concentrations were in the µg/l range for sample D, only Zn, Ni and Ba were leached from sample O in significant amount. The pH remained more or less constant during the leaching experiment. Nevertheless, sample O had a lower acid neutralizing capacity than sample D, as the pH of the extracts was on the average 0.5 units lower in the overbank sediment than for the dredged sediment.

Element concentrations in the leachates of the pH_{stat} tests after 96 h (D) and 167 h (O) at different pH values are given in Table 4. The dredged sediment is characterised by an elevated acid neutralising capacity (ANC). In general, the highest pollutant concentrations are released at the lowest pH values, except As in sample O, which is only leached at pH 10. In this sample also a considerable SO_4^{2-} and DOC release was observed at pH 10.

Table 3: Concentrations of selected trace elements (µg/l) and pH of the leachates of the cascade leaching test (mean ± standard deviation of three replicates). DL = below detection limit

	L/S	20			40			60			80			100		
D	pH	7	±	0,08	6,97	±	0,04	7,06	±	0,11	7,05	±	0,01	6,95	±	0,13
	Ca	18837	±	1107	6158	±	456	5215	±	505	4658	±	57	3859	±	122
	Fe	107	±	58	447	±	95	151	±	43	351	±	126	320	±	15
	P	1290	±	5	2271	±	130	1692	±	153	1805	±	47	1654	±	46
	Ni	51	±	6,0	35,2	±	2,5	18,8	±	1,2	16,1	±	0,5	11,9	±	0,3
	Cu	59	±	3,1	43,6	±	4,1	20,9	±	6,2	15,9	±	1,6	17,3	±	3,4
	Zn	60	±	11	53	±	14	76	±	32	25	±	5	28	±	9
	As	22	±	0,5	37,9	±	1,8	28,2	±	2,5	29,4	±	0,9	26,8	±	1,0
	Cd	2	±	0,49	1,65	±	0,93	0,18	±	0,16	0,60	±	0,67		DL	
	Ba	10	±	1,46	6,82	±	0,69	3,75	±	0,55	3,89	±	0,87	3,61	±	0,24
O	pH	6,07	±	0,04	6,43	±	0,07	6,62	±	0,14	6,57	±	0,22	6,51	±	0,21
	Ca	35060	±	465	5908	±	153	3328	±	141	3222	±	191	2368	±	98
	Fe	113	±	7	743	±	189	505	±	216	765	±	114	721	±	80
	P		DL			DL			DL			DL			DL	
	Ni	18	±	1,7	15,7	±	1,0	8,0	±	1,2	8,0	±	1,1	5,7	±	3,4
	Cu	0,1	±	0,1		DL			DL			DL		1,0	±	1,8
	Zn	27	±	1	18	±	13	20	±	4	4	±	1	13	±	11
	As		DL		0,2	±	0,2		DL		0,1	±	0,2	0,1	±	0,1
	Cd	0,86	±	0,03		DL			DL			DL			DL	
	Ba	29,04	±	0,80	8,00	±	0,82	3,52	±	0,80	4,63	±	1,36	3,31	±	0,66

Table 4: pH_{stat} leaching of sample D and O. 'Time' gives the time to reach a certain ANC assuming a worst case scenario. DL = below detection limit

		D						O					
		pH2	pH4	pH6	pH_{soil}	pH8	pH10	pH2	pH4	pH6	pH_{soil}	pH8	pH10
Ca	mg/kg	22841	8537	1827	401	113	92	6712	4256	1401	779	299	250
Fe	mg/kg	206	25	4	3	7	160	876	10	<1	<1	12	325
P	mg/kg	7813	1155	48	22	66	504	2	3	2	1	8	128
Ni	mg/kg	99	25	1	1	2	4	38	3	0,39	0,34	1	6
Cu	mg/kg	67	2	DL	1	2	15	1	DL	DL	DL	0,28	2
Zn	mg/kg	4066	347	5	0,19	0,08	3	276	148	4	2	3	8
As	mg/kg	14	6	1	1	1	11	DL	DL	DL	DL	DL	2
Cd	mg/kg	140	10	0,42	0,06	0,08	0,41	40	3	0,1	DL	DL	0,3
Ba	mg/kg	43	7	1	DL	DL	1	205	8	1	1	DL	1
SO_4^{2-}	mg/kg	61	22	20	24	45	192	24	27	43	147	58	489
DOC	mg/kg	174	57	32	32	95	339	46	45	76	90	174	828
ANC/BNC	meq/kg	2331	680	64	-	276	788	994	409	46	-	208	590
Time	year	1485	433	41	-	-	-	633	261	29	-	-	-

4. Discussion

4.1 Sequential extractions and EDTA

The pool of potentially available metals consists of those fractions, which can deliver metals from the solid phase of the soil to the soil solution in a relatively short time period. EDTA extractions are often used to estimate this potentially available pool. Sequential extractions divide the total content of heavy metals in a soil sample in different pools according to their reactivity. Assuming that stronger chemical reagents can be

related to lower potential mobility and availability, metals released at the beginning of the sequence have a higher potential availability then the fractions obtained at the end.
When comparing the information on heavy metal mobility obtained from EDTA-extraction and sequential extraction, (Fig. 1) some apparent incompatibilities can be deduced. Cd, Zn and Ni were mostly extracted in the first two steps of the sequential extraction, pointing to a considerable potential availability. This is confirmed by the almost complete extraction of these elements by EDTA. Cu and Pb displayed a rather low potential availability according to the sequential extraction, still Cu is completely extracted by EDTA and also a significant amount of Pb (50-70% of its total concentration) was released by EDTA, suggesting an important potential availability of these elements. This may indicate that organic matter, which is also dissolved by EDTA, is an important sink for Cu. Another possibility is the readsorption of Pb on Cu on non-dissolved compounds during the sequential extraction, while EDTA forms stable complexes with the extracted elements, keeping them in solution.

4.2 Reducing conditions

Fe-oxides have a high capacity to adsorb heavy metal cations and oxyanions. In poorly drained soils with a high water table, a rise of the piezometric level or flooding of the soil will cause a redistribution or depletion of Fe-oxides and a release of contaminants. Although the reducing conditions brought about by $NH_2OH.HCl$ are not representative for a flooding period of a few days up to a few weeks, they give an indication on the reactivity of Fe-oxides and the potential mobilisation of metals.
Cd, Zn, Ni and Cu leachability do not significantly increase with increasing $NH_2OH.HCl$ concentrations, indicating that they are not incorporated in stable Fe-oxides. Increasing reducing conditions have the most significant effect for As, Pb, Ba and Cr. This suggests that stable (crystalline) Fe-oxides are an important sink for As, Ba, Pb and Cr. These results also show that the modification of the BCR extraction scheme, which consisted on the addition of a strongly reducing extraction step, was most important for As, Ba, Pb and Cr. Although a considerable readsorption of As is possible at the low pH value of the extract, CH_3COOH seems to significantly diminish this readsorption. A different reactivity of Fe-oxides in sample D and O, related to a different crystallinity, was apparent from the amount of Fe extracted by increasing $NH_2OH.HCl$ concentrations.

4.3 Actual availability: Cascade leaching test and influence of chlorides

Although the EDTA extraction indicates a considerable potential availability of Zn, Ni and Cd, the actual leachability of Zn, Cd and Cu (cascade leaching test) is relatively low with respectively less than 1%, 1% and 4% of the potentially extractable pool of the dredged sediment that was released. The amount of Ni and As released in the cascade leaching test represent about 25% of the potentially available pool. A completely different heavy metal mobility is obtained for the overbank sediment, in which only Zn, Ni and Ba have significant but low actually available pool (less than 2% of the potentially available pool for Zn and Ni. 30% for Ba). No As and Cd were released from this sample during the cascade leaching test.
However, when the elevated Cl^- concentrations in the riverwater and the porewater are taken into account, a much higher actual availability of Cd, Cu and to a lesser extend Zn and Ni is observed, pointing to the importance of chlorides towards the mobility of these elements. Increasing the Cl^-- concentration from 0 mg/l to 6000 mg/l resulted in a 9-fold increase in the mobility of Cd and the release of Cu was multiplied by a factor 3 (D) to 10 (O). Doner (1978) studied the mobility of chlorocomplexes through soil and found that Cl^- had a marked effect on the mobility of Cd, and to a lesser extend on Ni and Cu. The mixing of humic bound metals with seawater can release these metals and make them more available for uptake (Lores and Pennock, 1998).

Additional information on the processes that are responsible for heavy metal release in the dredged sediment is obtained from the cascade leaching test on $Ca_3(PO_4)_2$ (C) and Fe-oxides (F). Desorption of Ni from Fe-oxides is more important than from the bulk sample and from $Ca_3(PO_4)_2$. Arsenic on the other hand is principally released from $Ca_3(PO_4)_2$, which thus represents a major sink of As in the dredged sediment.

Notice that very little As is released from the Fe-oxides. More Cd, Zn and Cu are released from the bulk sample than from the Fe-oxides and $Ca_3(PO_4)_2$, indicating that other components of the dredged material (e.g. clays and organic matter) are also responsible for the release of Cd, Zn and Cu.

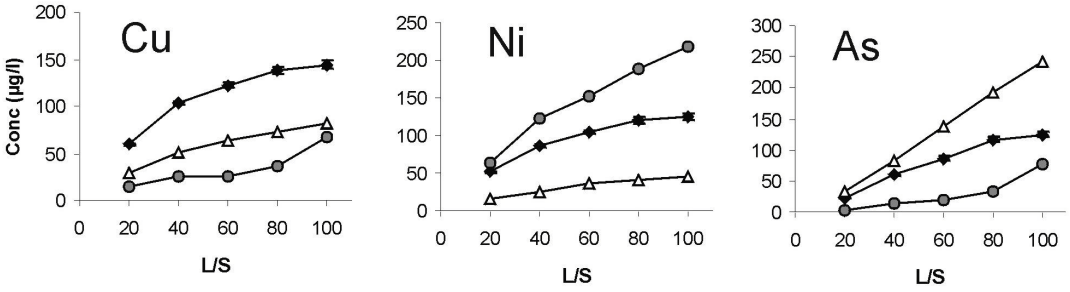

Fig. 3: Cumulative leaching of Cu, Ni and As from sample D (◆),F (Fe-oxide) (●) and C ($Ca_3(PO_4)_2$ (△)

4.4 pH_{stat} leaching tests

The amount of acid added to a soil-water suspension to keep the pH at a predefined constant value gives an estimation of the acid neutralizing capacity (ANC) of this sample. ANC depends on the reference pH chosen and on the duration of the pH_{stat} experiment. Acid buffering capacities of sample D display a different pattern as for sample O. While ANC has an asymptotical behaviour as a function of time in samples D, a steeper curve is obtained for sample O. ANC curves obtained in the pH_{stat} tests with continuous setpoint titration were described according to Schwartz et al. (1999). The proton buffering capacity of soils during pH_{stat} experiments can be described as the sum of two independent first-order reactions:

$$\mathbf{H_b(t) = BC_1\,(1- \exp(-k_1 t)) + BC_2\,(1-\exp(-k_2 t))} \qquad \mathbf{(1)}$$

With: $H_b(t)$ = buffered protons at time t (meq/kg), BC_i = buffering capacity of system i (meq/kg), k_i is the rate coefficient of the buffer system i and t is the time after starting the titration (h). Analogously, heavy metal release as a function of time was described in a similar way as the ANC. The cumulative release of an element m at time t is given by:

$$\mathbf{RL_m = RC_1(1- \exp(-r_1 t)) + RC_2(1- \exp(-r_2 t))} \qquad \mathbf{(2)}$$

With RC_i = the release capacity of buffer system I, r_i is the rate coefficient of the buffersystem i [h^{-1}] and t is the time after starting the titration.

As pH increases from 2→ 4 → 6 in the respective pH_{stat} experiments, the release rate (r_1) of most elements decreases (Fig. 4). In the dredged sediment, Zn, Cd, Ni and Cu show a rapid initial release at pH 2 and 4, (r_1 = 0.4-0.3 h^{-1}) while the second buffer system, according to equation 2, is characterised by a release rate that is an order of magnitude lower (r_2 = 0.02-0.03 h^{-1}). The leaching curve of these elements also follows the same pattern as the ANC curve. The amount of cations released is however higher than the amount of protons introduced into the system (ANC). This was also observed by Schwartz et al. (1999). As, P and Ba have a somewhat different behaviour since the maximal release of these elements occurs after 6 hours, after which their concentrations in the solution start to decrease. Readsorption of negatively charged arsenate and phosphate ions on the positively charged soil surface can explain the behaviour of As and P (Fig. 6a). The decrease in Ba concentrations with time, which is less pronounced than for As and P, seems to be caused by the precipitation of $BaSO_4$. While competition between As (AsO_4^{3-} and $HAsO_4^{2-}$) or P (PO_4^{3-} and HPO_4^{2-}) and OH^- ions, that were added to the system, explains for the release of As and P at pH 10 in the dredged sediment, complexation with DOC is an important release mechanism for Cu.

Desorption of heavy metals in sample O could be described by only 1 exponential equation ('1 buffer system), with a rather slow release rate (r = 0.02-0.08 h^{-1}) compared to sample D. The release of Fe, Cu and Pb at pH 2 is even linear as a function of time, indicating a slow dissolution of Fe-oxides and the concomitant release of associated (coprecipitated) elements. The release rate of Cd displayed a constant decrease, as the sink for Cd is progressively depleted (Fig. 5). At pH 4, only 50 % of the total amount of Cd present in sample O was leached and almost no Fe was released. Both desorption and dissolution processes account for the leaching of Cd in the acid pH range (pH 2). Geochemical modelling (MINTEQA2) suggests that the Cd leached at pH 4 was desorbed from the surface of Fe-oxides. The extra amount of Cd leached at pH 2 was probably released as a result of the dissolution of poorly stable Fe-oxides. Leaching of most elements at pH 10 in sample O started after 48 h (Fig. 6b). While a decrease in Ca-concentrations, because of precipitation reactions and/or sorption to the negatively charged soil surface, was observed in the initial stage of the experiment, an increase in Ca-concentrations also occurred at that time. After 71 h, a break appeared in the BNC curve, suggesting the start of new base neutralizing reactions. The elevated DOC concentrations indicate a considerable dissolution of organic matter. MINTEQA2 modelling however indicates that the speciation of Ni and Zn is dominated by hydroxy-complexes ($Zn(OH)_{2aq}$ en $Ni(OH)_{2aq}$), while Cd mainly occurs as chlorohydroxy-complex (Cd(OH)(Cl)).

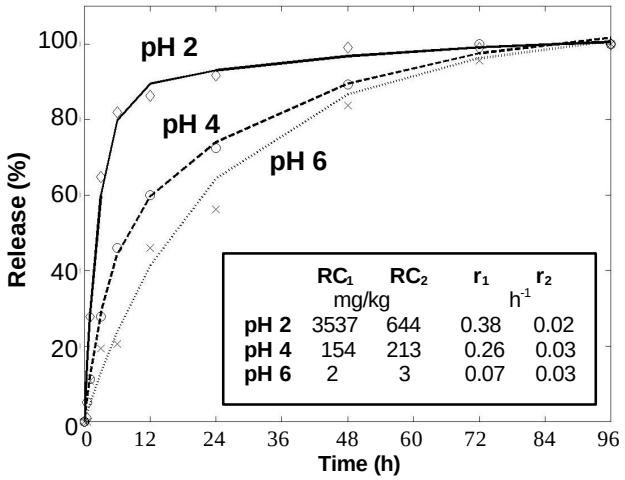

Figure 4: Release (% of concentration after 96 h) of Zn in sample D as a function of time during the pH_{stat} test at pH 2, 4 and 6. (Symbols: experimental results, lines: fitted results according to equation 2)

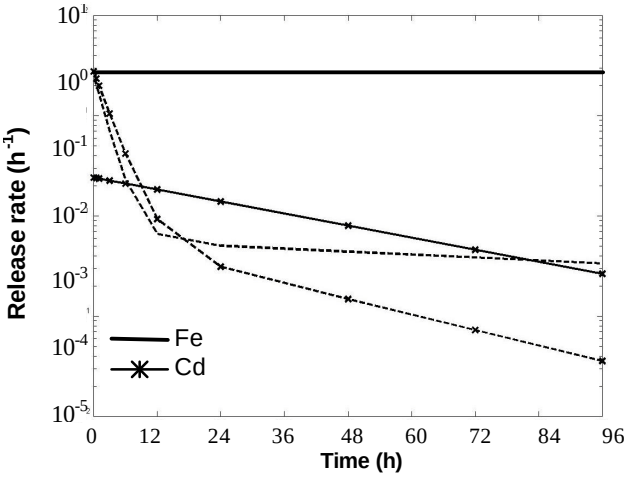

Figure 5: Release rate of Cd, Fe and Ca as a function of time during the pH_{stat} test at pH 2 (full lines: sample O, dotted lines: sample D)

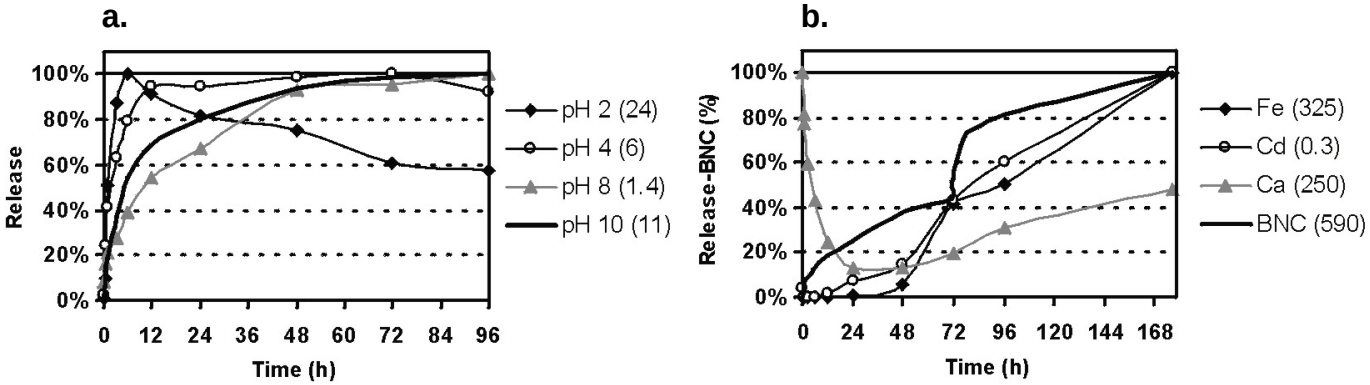

Fig. 6: (a) Leaching behaviour of As in sample D at pH 2, 4, 8 and 10 (b) Leaching behaviour of Fe, Cd and Ca and BNC in sample O at pH 10 (% of maximal concentration, which is given between brackets (in mg/kg)).

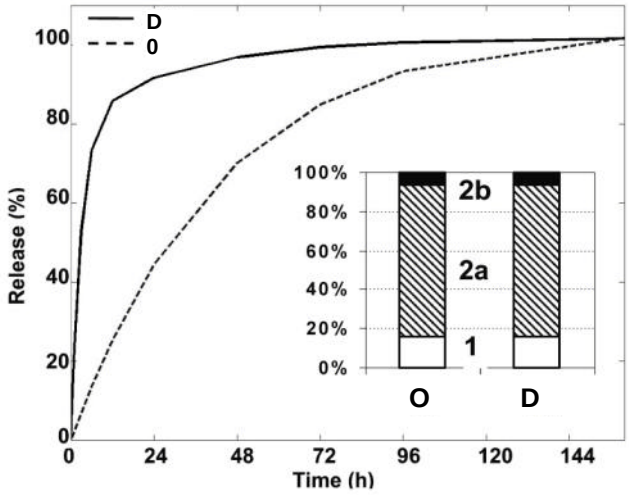

Figure 7: Release (% of concentration at the end of the experiment) of Cd as a function of time during the pH_{stat} test at pH 2 and Cd fractionation according to the BCR sequential extraction

Sequential extractions give a similar fractionation for Cd in samples O and D (Fig. 7) and the EDTA-extract suggests a comparable potential availability of Cd in both samples. At pH 2 (Fig. 7) and 4, a much slower release of Cd was nevertheless observed in the overbank sediment (O) compared to the dredged sediment (D). This different leaching behaviour, related to differences in reaction kinetics, indicates a different speciation of Cd in both samples.

The total acid deposition by rain in Flanders in 1998 amounted to 4082 equivalents of acid per hectare and per year (Mensink et al., 2000). Assuming quasi constant emissions of SO_x, NO_x and NH_x compounds in the coming years and accepting that ANC is correctly estimated by the pH_{stat} leaching tests, future contaminant leaching can to some extent be predicted. The time needed to reach a certain ANC is given in table 3. Assuming a worst case scenario, 2.4 mg/kg Cd will be leached from the dredged sediment and 1.06 mg/kg from the overbank sediment in a timespan of 100 years. The considerable acid neutralizing capacity of the dredged sediment and the elevated Fe-concentrations in sediments of the study area contribute significantly to the immobilization of heavy metals and As.

5. Conclusion

Heavy metal mobility in alluvial sediments of the Grote Beek river was evaluated by using different extractions and leaching techniques. The actual availability of heavy metals (Zn, Cd, Cu, Ni and As) was higher in the dredged sediment than in the overbank sediment. Flooding of the riverbank with Cl^- rich water mainly has an influence on the mobility of Cu and Cd. While Cd was already of concern because its concentrations exceed by far Intervention Values for Soil Contamination, the information on mobility of Cu is very important since this metal doesn't display excessive total concentrations in the sediments.

pH_{stat} leaching tests were applied to study the long-term heavy metal behaviour. They also allowed to assess reaction mechanisms involved in the release of heavy metals and to consider reaction kinetics. pH_{stat} tests indicated a strong binding of As with the soil matrix in the overbank sediment since almost no As was released in the pH range 2-10. Strongly reducing conditions brought about by $NH_2OH.HCl$ caused a substantial release of As, pointing to the incorporation of As in Fe-oxides. A higher As-mobility was found in the dredged sediments, because of the association of As with $Ca_3(PO_4)_2$ particles. Despite some artifacts in sequential and EDTA extractions, additional information on the reactivity of heavy metals was obtained. Although EDTA extractions suggest a considerable potential availability of Cd, Zn, Ni and Cu, pH_{stat} leaching tests indicate that this potentially available pool will only be released very progressively.

6. References

Anonymous (1996). Vlaams reglement betreffende de bodemsanering – VLAREBO. Openbare Afvalstoffenmaatschappij voor het Vlaams Gewest, Publicatienummer D/1996/5024/5, 63 pp.

Cappuyns V., Swennen R., De Nil K. (2002). Heavy metals and arsenic in alluvial sediments of the grote Beek river (N Belgium) : contribution of natural and antropohenic sources. In: Contributions to the geology of Belgium and Northwest Europe. Proceedings of the first Geologica Belgica International Meeting. pp. 227-230.

Davranche M., Bollinger J-C. (2000). Heavy metal desorption from synthesized and natural iron and manganese oxides: effect of reductive conditions. J. Coll. Interf. Sci. 227: 531-539.

Doner H.E. (1978). Chloride as a factor in the mobilities of Ni(II), Cu(II) and Cd(II) in soil. Soil Sci. Soc. Am. J. 42: 882-885.

Lores E.M., Pennock J.R. (1998). The effect of salinity on binding of Cd, Cr, Cu and Zn to dissolved organic matter. Chemosphere 37(5): 861-874.

Mensink C., Colles A., De Schrijver A., Hendriks J., Meykens J., Brouwers J. (2000). Verzuring, In: MIRA-S (2000). Milieu- en natuurrapport Vlaanderen: scenario's. Vlaamse Milieumaatschappij.

Nelson D.W., Sommers L.E. (1982). Total carbon, organic carbon and organic matter. In: Methods of soil analysis, part 2: Chemical and biological properties. Second edition, pp. 516-593.

Schwarz A., Wilcke W., Zech W. (1999). Heavy metal release from batch pH_{stat} experiments. Soil Sci. Soc. Am. J. 63: 290-296.

Stigliani, W.M., Doelman, P., Salomons, W., Schulin, R., Smidt, G.R.B., Van der Zee, S.E.A.T.M., (1991). Chemical time bombs. Environ. 33: 26-30.

Tessier, A., Campbell, P.G.C., Bisson, M. (1979). Sequential extraction procedure for the speciation of particulate trace metals. Anal. Chem. 51 (7): 844-850.

Van Herreweghe S., Swennen R., Cappuyns V., Vandecasteele C. (2002). Speciation of heavy metals and metalloids in contaminated soils: an integrated study near former ore treatment plants with emphasis on pH_{stat}-leaching. J. Geoch. Expl. 76: 113-138.

Van Reeuwijk L.P. (1992). Procedures for soil analysis, third edition. ISRIC, Wageningen, The Netherlands.

Vogel A.I. (1961). Nephelometric determination of sulfate. In : Quantitative inorganic analysis. pp 850-851.

EXPERIMENTAL AND NUMERICAL STUDIES OF TRICHLOROETHYLENE MIGRATION

A. Emonet[1], M.A. Buès[1], C. Oltean[1], O. Bour[2], P. Le Thiez[3]

(1) Laboratoire Environnement Géomécanique et Ouvrages
Ecole Nationale Supérieure de Géologie
Rue du Doyen Marcel Roubault – B.P. 40
F – 54501 Vandoeuvre-lès-Nancy

(2) Institut National de l'Environnement Industriel et des Risques
Parc technologique Alata – B.P. 2
F – 60550 Verneuil-en-Halatte

(3) Institut Français du Pétrole
1 – 4 Rue de Bois Préau
F – 92500 Rueil Malmaison

1 INTRODUCTION

Chlorinated solvents represent one category of the most widespread pollutants in soils and aquifers. Among them, the Tricholoroethylene (TCE) is a DNAPL [Pankow and Cherry, 1996]. Its industrial use as a dry cleaner leads to contaminate plenty of industrial sites and justifies a specific study on its behaviour. In porous media, TCE can be found under different forms: pure, volatile and dissolved in water and adsorbed on the solid matrix. Each form is a risk of pollution for soils and aquifers, at long and short terms. In order to focus our study on the phenomena of volatilisation and dissolution, we will not take into account the adsorbed form of the pollutant. In fact, we try to understand and explain the behaviour of TCE in a soil, in order to determine and apply the most appropriate remediation technique for a contaminated site.
The migration of a pollutant through a porous medium is controlled by its physical and chemical parameters but also by the characteristics of the porous medium. For example, these characteristics can be the capillary pressure, hydraulic conductivity, effective porosity … Moreover, the behaviour of TCE can be different whether it is in the unsaturated zone (at irreducible water saturation) where it can volatilise in contact with gas phase or in the saturated zone, where it can dissolve in water.
Several studies realised since 1980 [Abriola, 1989; Miller *et al.*, 1990; Powers *et al.*, 1991; Powers *et al.*, 1992; Geller and Hunt, 1993 and Powers *et al.*, 1994] have been interested in mass transfer during dissolution. Other authors [Sleep and Sykes, 1989; Griffol and Cohen, 1996; Cho *et al.*, 1993; Jellali *et al.*, 2001] have focused on the volatilisation of NAPL and especially on vapour movements and on the influence of a water infiltration on their dissolution. This study tries to understand and measure the process of volatilisation and dissolution of a DNAPL injected in a homogeneous porous medium.
The aims of this study are:

(i) to dimension, using the numerical results, a 2D experimental set-up allowing to follow the migration of TCE in a variably water saturated sand,
(ii) to compare the experimental and numerical results obtained during an injection of TCE.

2 MATERIAL AND METHODS

2.1 Simulations with SIMUSCOPP

SIMUSCOPP is a numerical modelling software package developed by the Petroleum French Institute (IFP). It permits to determine the fluid velocities, pressures and concentrations of chemical species in multiphase flow by solving a set of coupled flow and transport equations (Tardy et al., 1996). The chemical species can be found in one, two or three fluid phases. The mass transfer between chemical species can be taken into account or not. In our study, the chemical species is represented by the trichloroethylene (TCE).
In a first time, the numerical code was used in order to determine the optimal dimensions of a laboratory model represented by a column. Then, it was used in order to simulate an experiment

involving the injection, in the upper part of the experimental set-up, of 400 ml of TCE for 2 hours. The change of the concentration of vapours and dissolved TCE are followed for one day. The comparison between numerical and experimental data is presented in the last section.

2.2 Experimental set-up

The experimental set-up (figure 1) is represented by a glass column. Its optimal dimensions, chosen according to numerical simulations, are: 0.2 m in diameter and 1.0 m in length. The column is progressively filled with water (each time 6 cm of water are maintained above the ground surface) and sand is added by 800 g fractions. The column is struck several times with a hammer to allow the optimisation of grain sand distribution and to avoid compressive effects between each sand level. Once the column is completely filled with water and sand, it is drained by its base. The drainage is stopped when water level is about 0.2 m. So, the saturated zone is located between 0.0 and 0.2 m, the capillary fringe between 0.2 m and 0.5 m approximately and finally, the unsaturated zone between 0.5 m and 1.0 m. We note that the main characteristics of the sand, *i.e.*, hydraulic conductivity, effective porosity, capillary pressure and relative permeability were experimentally determined. These experiments are presented in the third part of the paper.

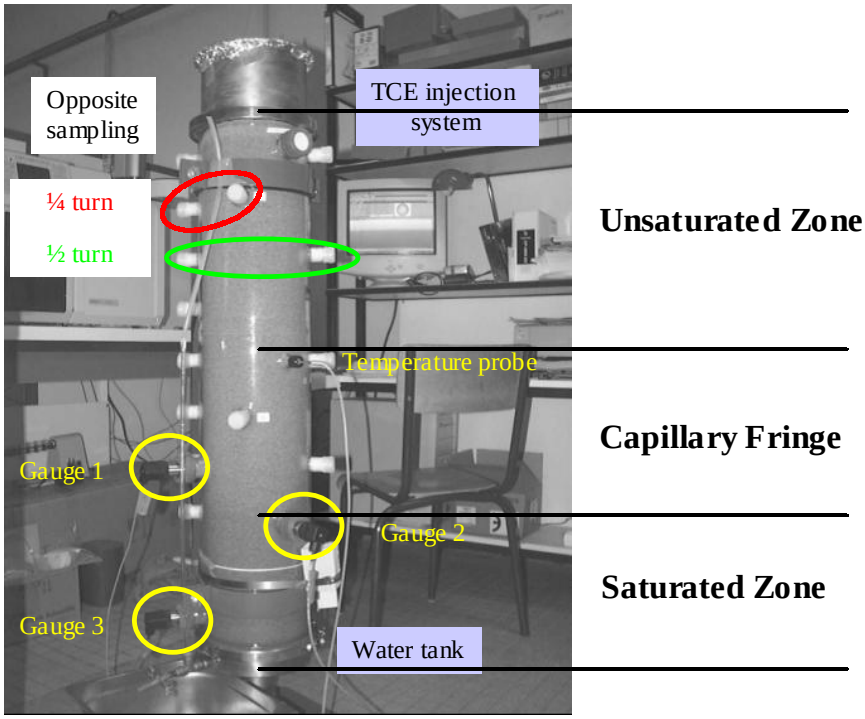

Figure 1: Experimental set-up of TCE injection.

The column is equipped with 3 pressure gauges and 1 temperature probe. In order to allow sampling of gas and water with syringes, 18 holes are located on the column's side. The syringe dimensions permitted sampling at 5.0 cm inside the sand. The samples, mixed with 1 mL of Methanol, which reacts as a trap for pure, volatile and dissolved TCE, are analysed by a gas chromatograph equipped with a flame ionisation detector (FID) and a capillary column. The gases used in the chromatograph are H_2, N_2 and air. The flow rate of N_2 inside the capillary column is about 5 mL/min and its temperature is constant and fixed at 70° C. The temperatures of FID and injector are respectively 250 and 200° C.

3 CHARACTERISATION OF THE POROUS MEDIUM

One sand has been used in our experiments. It is coming from a river located in eastern France. Mainly composed of quartz, the properties of this sand are presented in Table 1.

Table 1: Main characteristics of the sand.

Property	Value
Mean grain diameter (mm)	0.56
Minimal density (g/cm3)	1.43
Maximal density (g/cm3)	1.63
Grain density (g/cm3)	2.635
Hydraulic conductivity(m/s)	1.50E-04

The capillary pressure - water saturation or retention curve is one of the most significant data for SIMUSCOPP package. Consequently, it has been determined using an experimental device (Figure 2). Represented by a column of dimensions: 0.55 m in length and 0.09 m in diameter, this device is made up of a stack of 8 plexiglas cylinders (9.0 cm in diameter and 7.0 cm in height). The column is completely filled with water and the sand is added by fractions of 400 g. The optimal grain sand distribution is obtained in the same way as for the experimental set-up. Once the column is completely filled with water and sand, it is drained by its base until the imposed water level is reached.

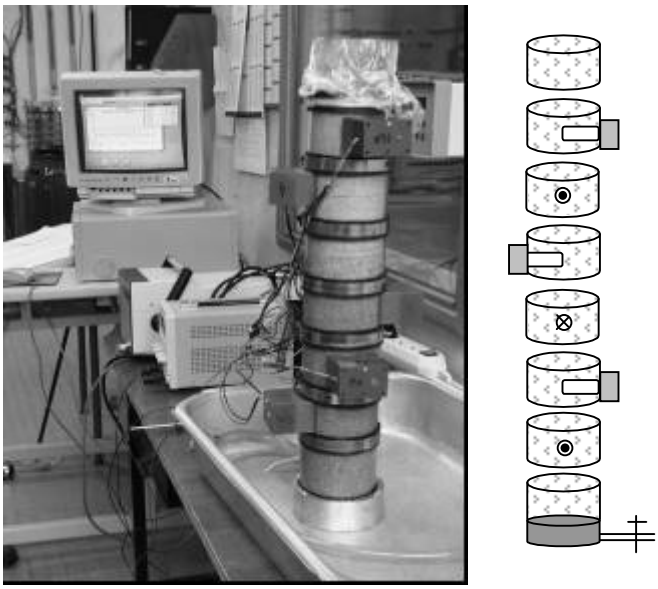

Figure 2: Experimental set-up for determination of retention curve.

In order to measure the pressure evolution in the porous medium, a tensiometer probe is attached to each cylinder. One of its end is buried into the porous medium and the other one is linked to a pressure gauge. At the end of the experiment, the sand is sampled and water saturation is measured. Consequently, for each level corresponding to tensiometer probes, the stabilised recorded pressure in relation to water saturation can be graphically represented (Figure 3). Six experiments have been carried out and all experimental points are plotted on Figure 3.
The interpretation of this figure permits to obtain Van Genuchten model parameters, *i.e.*, α and n [Van Genuchten, 1980] that are listed in table 2.

Table 2: Van Genuchten parameters for the sand.

m	n	α [m^{-1}]
0.70	3.36	0.084

They enable to estimate the relative permeabilities for each two-phase fluid couple in a three-phase system [Van Genuchten, 1980; Parker *et al.*, 1987].
These experimental and analytical data have been implemented in SIMUSCOPP.

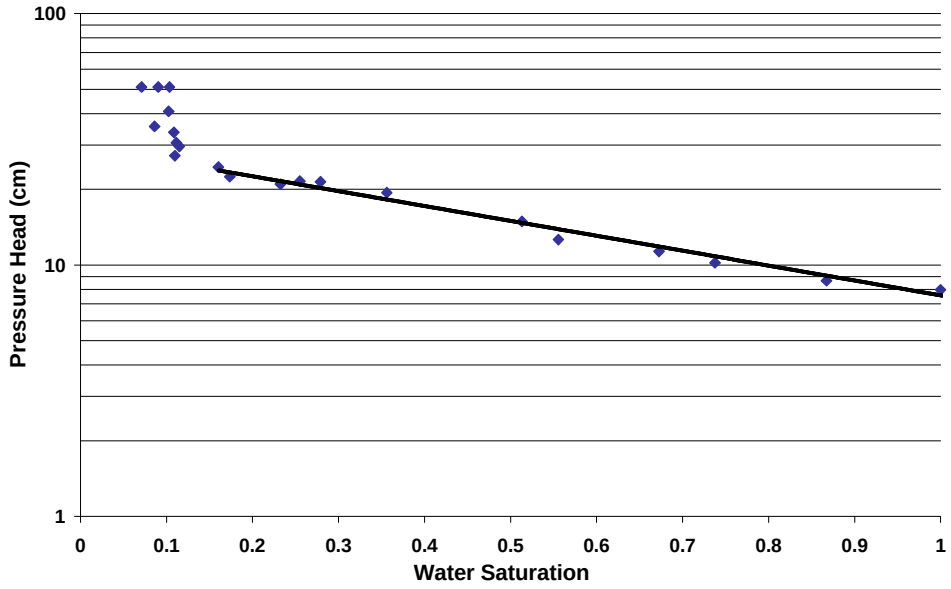

Figure 3: Retention curve for the sand.

4 COMPARISON OF NUMERICAL AND EXPERIMENTAL RESULTS

The experimental data are numerically analysed using SIMUSCOPP package. The simulated domain, similar to the experimental set-up, is divided into 400 bilinear regular elements of dimensions: 0.005 m in X direction (radius) and 0.01 m in Z direction (length). As in experimental data, 400 ml of TCE are injected for 2 hours. The pollutant injection is realised below the upper limit of the domain into an area of 1.5 cm^2 corresponding to 3 elements in X direction and one element in Z direction. The TCE migration is followed for one day. The comparison between the experimental and numerical results is presented by a spatial and temporal concentration evolution of vapours and dissolved TCE.

4.1 Evolution of TCE vapours

Indicated times on the figures correspond, as far as the experiment is concerned, at the time of the first sample taken of a sampling series. For the simulation it is linked to the state of the model at this specific time. It takes approximately half an hour to sample an entire series.
On these graphs, the squares represent the mean value of at least 4 experimental values. These experiments have been conducted according to the same procedure. One uncertainty, due to sampling and analyse, is associated with one experiment. The envelope curves around the mean experimental value result from the mean of the overvaluation (or the undervaluation) of each experimental value by its uncertainty. It gives yellow triangles for the high trend and blue triangles for the low trend.
Lozenges represent numerical results. The blue ones are related to the simulation that takes into account the sand properties: especially the hydraulic conductivity of about 15 10^{-4} m/s. The red lozenges correspond to a simulation realised with a hydraulic conductivity of 75 10^{-4} m/s. These hydraulic conductivities are respectively assimilated to the intrinsic permeabilities: 15 Darcy and 75 Darcy.

We can notice (Figure 4) the increasing evolution of the concentration of TCE vapours, for the experiment as well as for the simulations, in the column with time. This evolution of vapours is related to the migration of pure TCE in the column.
The evolutions of vapours concentration, given by the simulations, are different at the beginning. The blue curve that corresponds to the simulation with the intrinsic permeability experimentally determined presents a slower progression compared with the other and with experiments. On the other hand, the red curve that has been realised with another intrinsic permeability (75 Darcy), has an evolution faster and closer to experimental results.
Moreover, for simulations, once the maximal concentration of TCE vapours is reached, the unsaturated zone of the column is completely saturated by vapours. After 3 hours, one can notice the

decreasing of vapours concentrations in the upper part of the column. This phenomenon reproduces the experimental trend that can be seen at each time, for the upper level.
Although the numerical results are quickly stabilised in the column, this equilibrium state is not so evident for the experimental ones.

4.2 Evolution of dissolved TCE

Another graphic representation has been adopted to illustrate the evolution of dissolved TCE in the water of the column. For three levels situated at z= 35, 25 and 15 cm from the base of the column the evolution of dissolved TCE concentration is followed versus time. As for as the evolution of TCE vapours, blue circles correspond to the mean of 4 to 6 experimental results. Two trends are defined considering the mean of the addition or the removal of the uncertainty related to each experiment (yellow and blue triangles).
The numerical results are represented with lozenges: blue ones for the simulation with an intrinsic permeability of 15 Darcy and red ones for the simulation with intrinsic permeability of 75 Darcy.

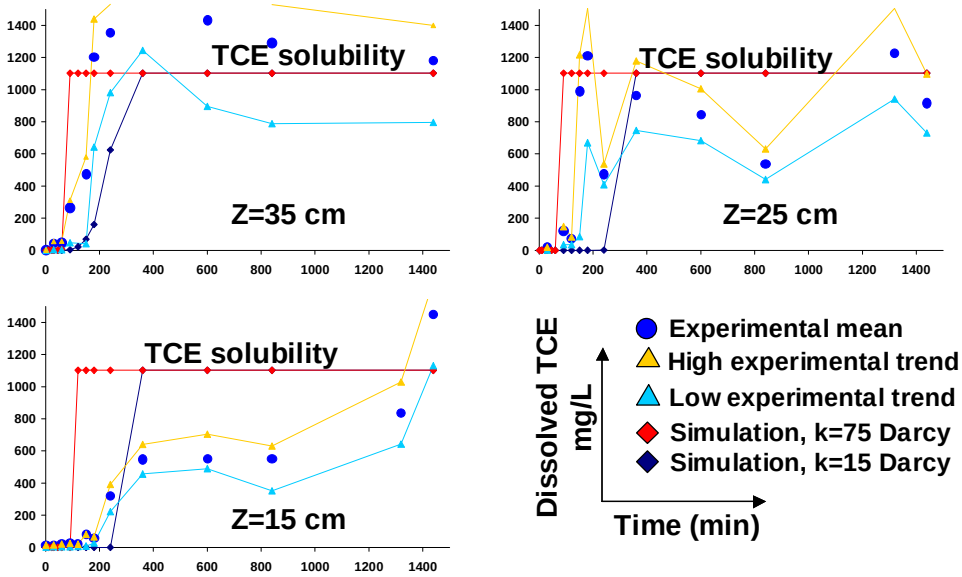

Figure 4: Calculated and experimental evolution of dissolved TCE concentration.

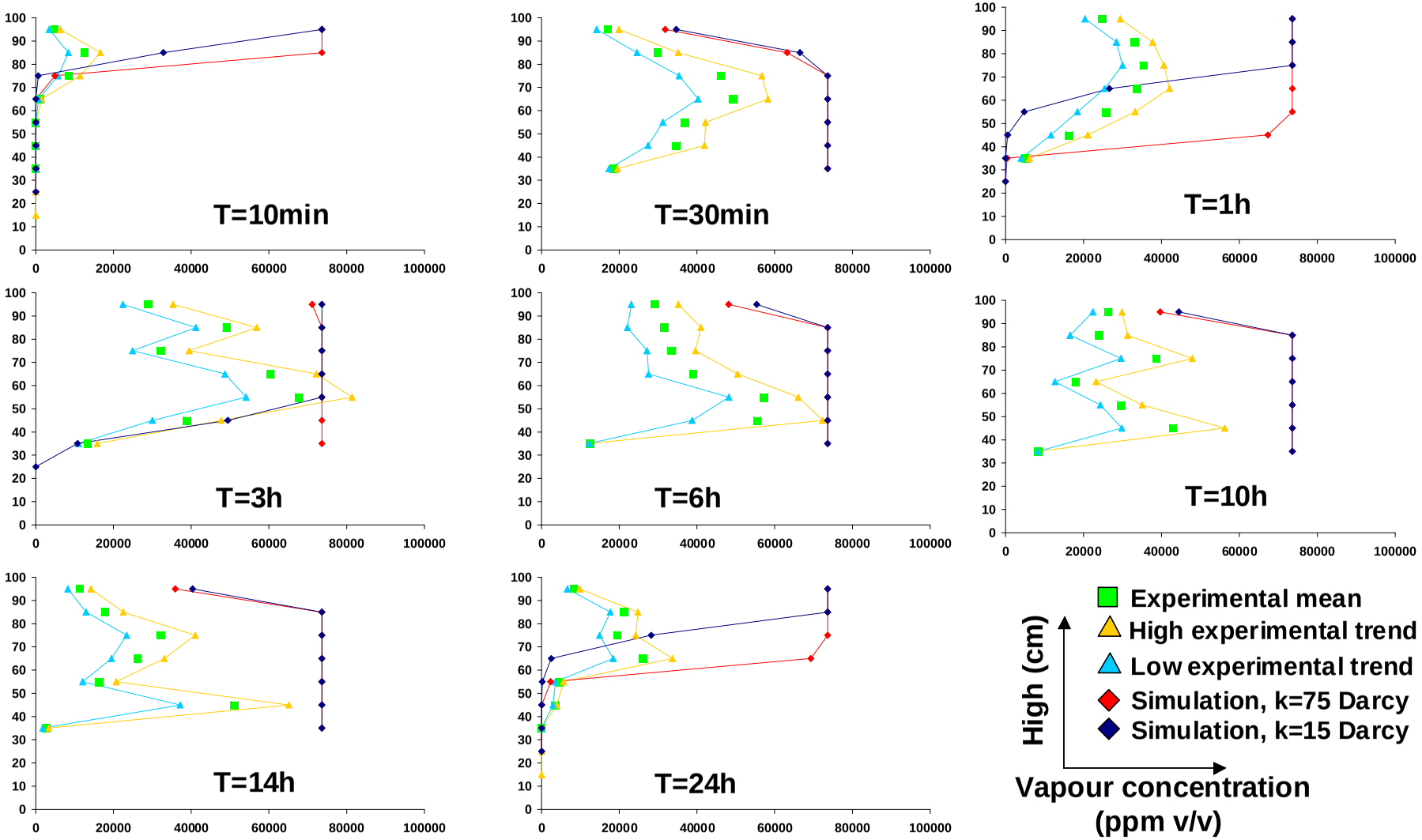

Figure 5: Calculated and experimental evolution of TCE vapours concentration.

For each level, the concentration of dissolved TCE in the water of the column increases with time. The maximum concentration reached corresponds to the solubility of TCE.
For the experiment, at level z=35 cm, this value is quickly reached (3 hours) and even exceeded it. This is due to the fact that during water sampling, some TCE can be taken with water in the syringe and be analysed. For the other levels, concentrations evolve more slowly. For level z=15 cm, the maximum concentration is reached after 14 hours.
The numerical results are different in the first time of the simulation. The simulation with a higher intrinsic permeability reaches the maximum concentration faster (less than 2 hours), for each level. For the other (intrinsic permeability of 15 Darcy), it takes more time (6 hours) to be completely saturated.
And one can notice that the experimental increase of concentration for each level is between the two simulations.

4.3 Discussion

The fact that an equilibrium state is not reached for the vapours and that concentrations in vapours decrease in the upper part of the column may be explained by losses of vapours into the atmosphere. Another explanation can be the evolution (increasing and decreasing of 1° C) of the temperature in the laboratory. Indeed, the physico-chemical properties of the TCE and especially the tension vapour pressure, are very reactive according to temperature. A slight modification of temperature may lead to an increase or decrease of the maximum vapour concentration and may also explain the decreasing of concentration between 4 to 14 hours and the increasing trend around 24 hours.

The experimental evolution of TCE vapours as well as dissolved TCE follows the same trend as the numerical results. However, the simulation with an intrinsic permeability of 75 Darcy seems to be closer to these experimental evolutions (especially for the vapours) than the other simulation, whose data correspond to the experiments. This may be explained, as it was evocated by Pankow and Cherry [1996], by the fact that the hydraulic conductivity is experimentally determined for water in a water saturated porous medium and not according to the physical properties of the TCE (density and dynamic viscosity). These properties may increase the TCE speed migration in the porous medium. That can be a reason why the simulation with a higher intrinsic permeability fits better experimental results than the other one.

5 CONCLUSION

This study presents an experimental device devoted to the study of the migration of a DNAPL in a homogeneous porous medium. This set-up allows to follow the volatilisation and dissolution of TCE in the air or water of the column. These phenomena can be numerically reproduced with SIMUSCOPP. The evolutions of the experimental and numerical results for each phase are similar. But, the simulation that seems to fit better the experimental results, takes into account a higher intrinsic permeability than the experimental value. That brings into relief the fact that the assimilation of the hydraulic conductivity with the intrinsic permeability for a porous medium may be used carefully by taking into account the different fluids involved.
Another noticing results are the development of a sampling procedure for different form of TCE and their analyses by gas chromatography. The method that has been adjusted for these experiments allows to: *(i)* trap vapours of TCE and dissolved TCE in a same solvent (methanol) and *(ii)* determine the level of concentration of TCE in each phase.
This experimental device and the analytical procedure will be used with different porous media and pollutants. After those studies, heterogeneities might be introduced. Another application of this experimental set-up may be the test of different techniques of remediation (injection of surfactant in the medium, injection of air…).
The numerical code is already used at the site scale in order to evaluate the migration of a pollutant and dimension remediation techniques.

6 REFERENCES

ABRIOLA L.M. - Modeling multiphase migration of organic chemicals in groundwater systems. A review and assessment. Environmental Health Perspectives, vol 83, p117-143, 1989.

CHO H.J., JAFFE P.R. and SMITH J.A. - Simulating the volatilisation of solvents in unsaturated soils during laboratory and field infiltration experiments. Water Resources Research, vol 29, N° 10, p 3329-3342, 1993.

GELLER J.T. and HUNT J.R. – Mass transfer from non-aqueous phase organic liquids in water-saturated porous media. Water Resources Research, vol 29, N° 4, p 833-845, 1993.

GRIFFOL J. and COHEN Y. – Contaminant migration in the unsaturated soil zone: the effect of rainfall and evapotranspiration. Journal of Contaminant Hydrology, vol 23, p 185-211, 1996.

JELLALI S., MUNTZER P, RAZAKARISOA O. and SCHÄFER G. – Large scale experiment on transport of Trichloroethylene in a controlled aquifer. Transport in Porous Media. Vol 44, p 145-163, 2001.

MILLER C.T., POIRIER-McNEIL M.M. and MAYER A.S. – Dissolution of trapped non-aqueous phase liquids : mass transfer characteristics. Water Resources Research, vol 26, N° 11, p 2783-2796, 1990.

PANKOW J.F. and CHERRY J.A. – Dense chlorinated solvents and other DNAPLs in groundwater: History, Behavior, and Remediation. Waterloo Press, Ontario, Canada, 260 p, 1996.

PARKER J.C., LENHARD R.J. and KUPPUSAMY T. – A parametric model for constitutive properties governing multiphase flow in porous media. Water Resources Research, Vol 23, N° 4, p 618 – 624, 1987.

POWERS S.E., LOUREIRO C.O., ABRIOLA L.M. and WEBER W.J. – Theoretical study of the significance of non-equilibrium dissolution of non-aqueous phase liquids in subsurface systems. Water Resources Research, vol 27, N° 4, p 463-477, 1991.

POWERS S.E., ABRIOLA L.M and WEBER W.J. – An experimental investigation of non-aqueous phase liquid dissolution in saturated subsurface systems : steady state mass transfer rates. Water Resources Research, vol. 28, N° 10, p 2691-2705, 1992.

POWERS S.E., ABRIOLA L.M and WEBER W.J. – An experimental investigation of non-aqueous phase liquid dissolution in saturated subsurface systems : transient mass transfer rates. Water Resources Research, vol. 30, N° 2, p 321-332, 1994.

SLEEP B.E. and SYKES J.F. – Modelling the transport of volatile organics in variably saturated media. Water Resources Research, vol 25, N° 1, p 81-92, 1989.

TARDY P., QUINTARD M., LE THIEZ P. and SEVA E. – A numerical model of hydrocarbon contaminant flow in soil and aquifers. Development and Application of Computer Techniques to Environmental Studies VI. Ed P. ZANNETTI and C.A. BREBIA, Computational Mechanics Publications, Southampton, 1996.

VAN GENUCHTEN M. Th. – A closed-form equation for predicting the hydraulic conductivity of unsaturated soils. Soil Sci. Soc. Am. J., vol 44, p 892 – 898,1980.

A NEW SPME-BASED CONCEPT FOR STUDYING CHLORINATED HYDROCARBON DEGRADATION IN MICROCOSMS

Katharina Poggel, Roman Breiter, Thomas Neeße

Address: Department of Environmental Process Engineering and Recycling,
University Erlangen-Nuremberg
Paul-Gordan-Straße 3, 91054 Erlangen, Germany
Phone: ++49 9131 85 23176
Fax: ++49 9131 85 23178
Mail: katharina.poggel@uvt.cbi.uni-erlangen.de, roman.breiter@uvt.cbi.uni-erlangen.de

1 Introduction

In their "Technical Protocol for Evaluating Natural Attenuation of Chlorinated Hydrocarbons" (Wiedemeier et al., 1998) the Environmental Protection Agency (EPA) describes the biodegradation as the main process of Natural Attenuation, because only this process leads to a relevant reduction of contaminant concentration and mass in the subsurface. To investigate this process of biodegradation, generally so-called microcosm studies are carried out. For the performance of such a study, however, no standardized methods are available until now. Accordingly, the relevant literature describes a variety of different designs.

In general, there are two basic types of experimental designs (see figure 1). On the one hand, microcosms can be sampled repeatedly (Gao et al., 1997). It is a disadvantage of this design that the system can be altered by the process of sampling from the liquid phase. When sufficiently large microcosms are used, these changes can be neglected, but, especially as far as the handling is concerned, other problems, such as missing space in incubators, may be caused. Microcosm studies "sacrifying" one per sampling event (Barrio-Lage et al., 1986) are far more frequent. It is the main problem of this design that comparable initial conditions cannot be guaranteed, given the heterogeneity of both the soil and the contaminant distribution.

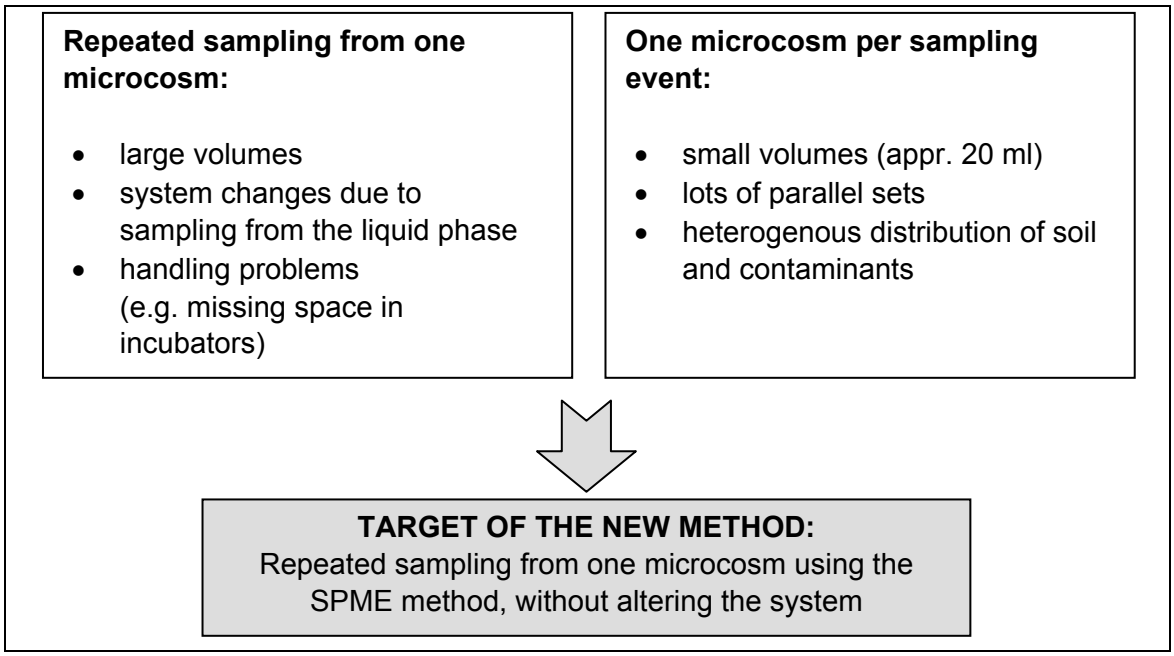

Figure 1: Fundamental designs and disadvantages of microcosm studies and the aim of our own work.

The objective of our work is to develop a method for microcosm studies with chlorinated hydrocarbons, allowing repeated sampling of one microcosm without altering the system inside (Poggel et al., 2001). This aim could be achieved through a combination of a microcosm study and the SPME-analysis (solid phase microextraction). With this new method the naturally occurring biodegradation of chlorinated hydrocarbons in the subsurface of a former landfill site near Lauf an der Pegnitz / Middle Franconia should be investigated under different conditions.

2 Site Characterization

The area to be investigated is located in the region of Nuremberg, near the river Pegnitz. Between 1935 and 1965, the former landfill site was used to deposit (mainly mineral) waste. There is neither a basal liner nor a geological barrier.

Chlorinated hydrocarbons, mainly Trichloroethene (TCE) and cis-1,2-Dichloroethene (cisDCE) as a potential metabolite, were detected in the groundwater in low concentrations (appr. 100µg/L). Apparently it is a matter of diffuse discharge of the contaminants.

Since 1997, the site has been treated with a pump&treat remediation; this approach, however, did not result in any sustainable effect. At the moment, Natural Attenuation processes with the main emphasis on biodegradation are investigated.

3 Material and Methods

3.1 On-site sampling

For getting soil material for the microbial investigations a liner drilling method was used to extract undisturbed soil samples under anaerobic conditions. To minimize contact of oxygen with the soil, directly after the sampling position, the liners were sealed with clay. Subsequently, to enable groundwater monitoring at the site, the liner-boreholes were extended to monitoring wells.

The soil and water samples were further processed under an anaerobic atmosphere (nitrogen/ carbon dioxide). The partial pressure of carbon dioxide in the groundwater was determined by alkaline titration. The mixture of gases was adjusted to a 97% nitrogen / 3% carbon dioxide ratio.

3.2 The New Concept for Microcosm Studies

The microcosms consist of 250 mL Boston bottles, capped with Mininert® valves. The bottles are filled with 60 g of soil and 215 ml of groundwater. The gas phase has a volume of appr. 5 mL and consists of a with 97% nitrogen and 3% carbon dioxide gas mixture (see chapter 3.1).

The abiotic controls contain a solution of sodium acide and an aerobic gas phase (air) but no soil. Additional investigations within the project lead to the assumption that the changes in the described microcosms due to sorption can be neglected.

Previous experiments showed that the microcosms are tight as far as oxygen and the volatile contaminants are concerned. No influence of soil or groundwater components on the SPME-process could be detected.

The microcosms were spiked with definite amounts of pure TCE or cisDCE. The bottles were incubated at 10 or 35°C in the dark. The temperature of the aquifer is appr. 10°C, so that an incubation at this temperature simulates nearly in situ-conditions. With the microcosms that have been incubated at 35°C, a greater activity of microorganisms is expected, resulting in biodegradation to be detected at an early state.

To check the tightness against oxygen, control bottles were prepared consisting of a solution of Resazurin, a redox indicator showing the presence of oxygen by changing from colourless to pink.

For more detailed information about the biodegradation, both the actual and the potential degradation of the chlorinated hydrocarbons were investigated. To that end, different microcosm types, differing in the composition of the liquid phase, were prepared:

- "in situ-microcosms“ → The microcosms contain soil and groundwater from the site without further supplements.
- "enhanced microcosms“ → Beside soil and groundwater from the site, the microcosms contain hydrogen releasing compounds (HRC®).
- "optimized microcosms“ → The soil is suspended in a special media for dechlorinating microorganisms (Dehalospirillum media, DSZM No. 833).

3.3 Analytical Methods

A 100 µm PDMS fibre was used for the solid phase microextraction. Sampling was performed from the gas phase of the microcosms. The SPME was not optimized with regard to the temperature, as the temperature was preset by the temperature of incubation. Extraction time lasted five minutes, which was enough to reach a sorption equilibrium between the gas phase and the fibre.
The desorption took place in the GC-injector (HP 6890+). The GC was equipped with a HP PLOT Q-column (30 m length, 0,32 mm ID) and a FID. The calibration was performed with gas standards in a concentration range between 5 and 100 µg/L.

3.4 Quantification of Dechlorinating Microorganisms

For the quantification of dechlorinating microorganisms the MPN-method was used (most probable number). For the enrichment the medium No. 833 (Dehalospirillum media) from the DSMZ (German: Deutsche Sammlung für Mikroorganismen und Zellkulturen, German Collection of Microorganisms and Cell Cultures) was used. Instead of pyruvate and fumarate we used acetate and formiate. This way, the growth of fermenting microorganisms shall be limited.
Soil samples from four different liner-drillings were used. To 10/ 1/ 0,1/ 0,01 g of soil 10 mL of media was added into 40 mL bottles. Investigations of the particle size distribution did not show significant differences in the initial conditions. The liquid phase was overlayed with a 0,5 molar solution of TCE in hexadecane. The bottles were sealed with Mininert® valves and incubated at 20°C in the dark.
Once per week over a period of six weeks the bottles were sampled for chlorinated hydrocarbons, vinyl chloride and ethene using SPME. The set was rated positive when both a decrease of the TCE-concentration and an increase of possible metabolites could be observed. Evaluation was performed using a MPN table.

3.5 Quantification of Additional Ecophysiological Groups

Beside the dechlorinating microorganisms, additional groups of bacteria were quantified for getting additional information about the redox zonation on site:

- aerobic copiotrophic microorganisms,
- facultatively anaerobic microorganisms,
- nitrate reducing microorganisms,
- sulphate reducing microorganisms.

The aerobic microorganisms were quantified with the spread plate method on R2A-agar. The other groups were enriched in suitable media and quantified with the MPN-method.

4 Results and Discussion

4.1 Suitability of the New Sampling Method

For all chlorinated hydrocarbons linear calibration curves could be observed in the investigated concentration range. Using a level of significance of 95% the following table 1 shows the calculated detection limits. The detection limits in the gas phase (DL_{gas}) were calculated from the calibration functions. Using temperature dependent values of the Henry coefficient (Gossett, 1987) the detection limits were calculated for the liquid phase (DL_{lq}).

Table 1: Detection limits for chlorinated hydrocarbons in the gas and liquid phase.

[µg/L]		11DCE	cisDCE	transDCE	TCE
10°C	**DL_{gas}**	0,9	0,8	0,8	0,9
	DL_{lq}	1,7	11	4,9	5,4
35°C	**DL_{gas}**	1,4	0,7	1,0	1,7
	DL_{lq}	0,9	3,3	1,9	2,7

The values show that with the SPME-sampling even highly chlorinated compounds like TCE can be well detected without using an ECD. Beside the good detection in low concentration ranges the SPME-method is characterized by an easy and fast handling. Sampling the gas phase leads to a minimization of matrix effects. No solvents are necessary. It has to be ensured, however, that constant sampling conditions, especially as far as the temperature is concerned, be kept. Another disadvantage is the fact that the analysis can not be automated and that the liquid concentration can be only quantified indirectly by using Henry coefficients.

4.2 Results of the Microcosm Study

a) "in situ-microcosms"

Over a period of 100 days no biodegradation of TCE could be observed in the in situ-microcosms (see figure 2).

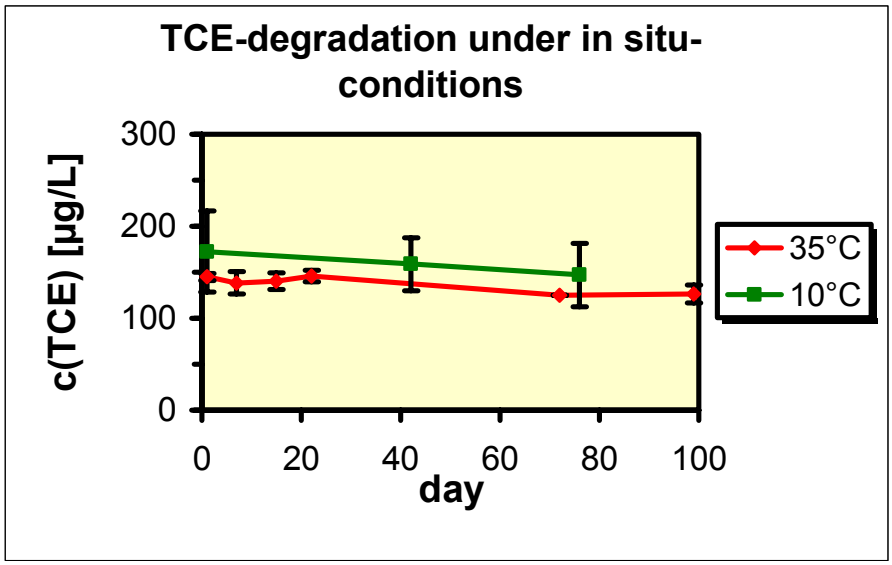

Figure 2: TCE-concentration in the "in situ-microcosms"

A slight decrease of the TCE-concentration has been detected, but this decrease also occurs in the abiotic controls, so it can be attributed to sorption processes at the PTFE of the Mininert® valves.

b) "enhanced microcosms“

Once HRC® has been added, black precipitates could be observed in the microcosms after about 60 days of incubation (see figure 3). A degradation of the added contaminants, however, could not be observed here, either.

Figure 3: Precipitates of iron sulfide in the “enhanced microcosms“ with HRC®.

The analysis of the precipitates showed that they consist mainly of iron sulfide. This result leads to the assumption that the addition of electron donators lowered the redox potential, resulting in a sulphate reduction.

c) "optimized microcosms“

In the microcosms incubated at 10°C a 30% decrease of the TCE-concentration could be observed (see figure 4) but no metabolites of a degradation could be detected. So it is not clear if this observation can be attributed to biotic or abiotic processes. Maybe a dechlorination is catalyzed by components of the enrichment media.

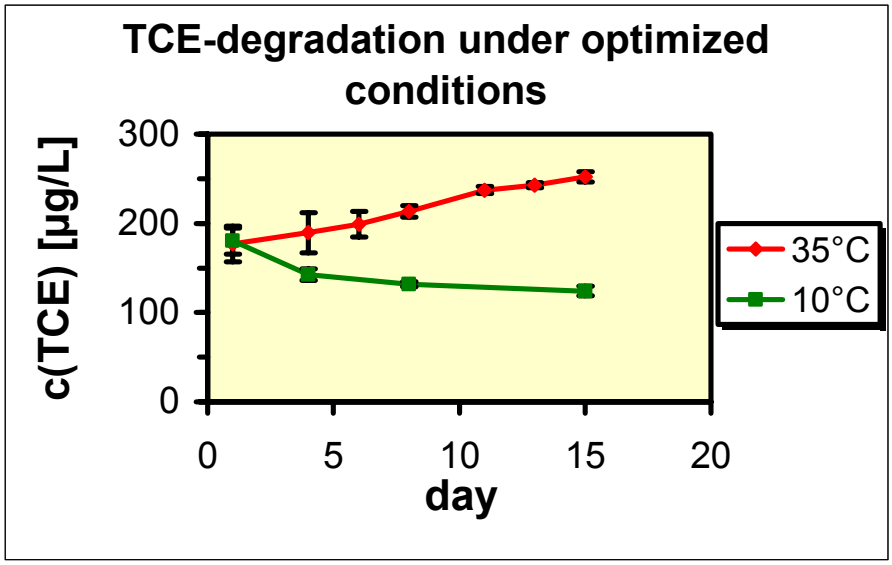

Figure 4: TCE-concentration in the “optimized microcosms“.

The observation of black precipitates in these microcosms again showed a biological reduction of sulphate.
At 35°C the desorption of TCE from the soil leads to an increase of the concentration in the liquid phase and overlayed a probably occurring biodegradation.

4.3 Results of the Quantification Experiments

The quantification of the different micro-organism groups showed that most of the soil bacteria are based on a high redox potential. Only small numbers of sulphate reducing and dechlorinating bacteria were found (see figure 5).

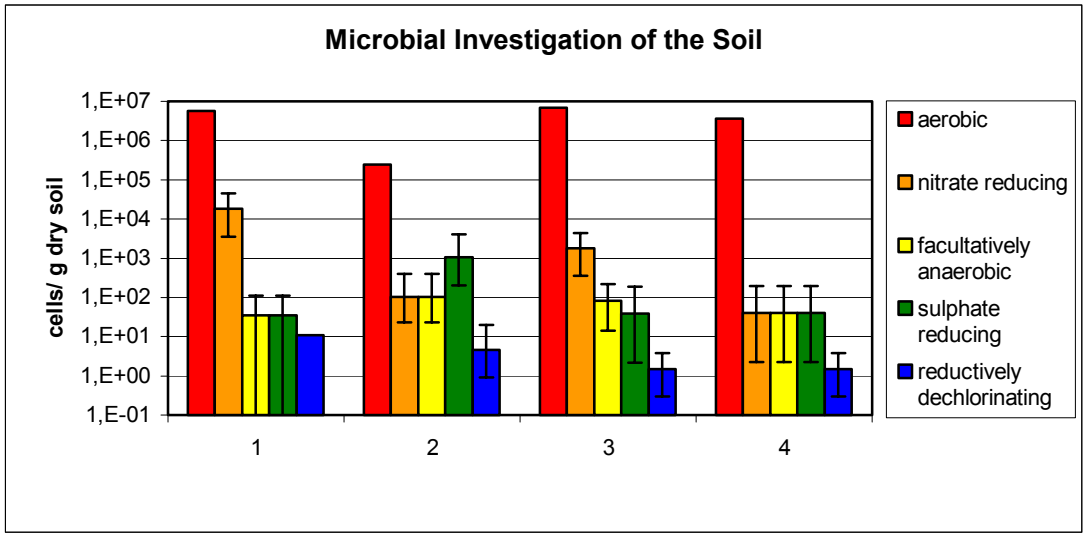

Figure 5: Numbers of different micro-organisms in the four soil samples from the site.

4.4 Conclusions for the Biodegradation on Site

The new concept for microcosm studies based on the SPME has turned out to be suitable to study the biodegradation of chlorinated hydrocarbons in the context of Natural Attenuation. It has many advantages like:

- easy handling,
- simple analytics,
- neglectable sorption of analytes on the PTFE, even at low concentrations.

Generally, one has to assume that there is biological activity on site which is not leading to a degradation of the contamination but of the DOC of the groundwater. Biodegradation will not be an important process for Natural Attenuation on site.
The fact that only after addition of electron donors a sulphate reduction could be observed in the microcosms leads to the conclusion that the redox potential on site and in the "in situ-microcosms“ must be relatively high. This assumption is confirmed by the results of the groundwater monitoring. The aquifer of the landfill site shows mainly nitrate reducing conditions and DOC is comparatively low. A reductive dechlorination of the chlorinated hydrocarbons in situ cannot be expected under these conditions.
By adding electron donors the redox potential can be lowered so that a reductive dechlorination is theoretically possible. But even under optimized conditions a degradation of the contaminants could not be observed. Low numbers of dechlorinating bacteria and perhaps inhibitating substances in the groundwater maybe an explanation.
Only the combination of the three types of microcosms allows for these conclusions about the contribution of biodegradation to Natural Attenuation on the site investigated here.

5 Literature

Barrio-Lage, G.; Parsons, F. Z.; Nassar, R. S.; Lorenzo, P. A. (1986): *Sequential dehalogenation of chlorinated ethenes*. Env. Sci. Tech. 20(1): 96-99.

Gao, J.; Skeen, R. S.; Hooker, B. S.; Quesenberry, R. D. (1997): *Effects of several electron donators on tetrachloroethylene dechlorination in anaerobic soil microcosms*. Wat. Res. 31(10): 2479-2486.

Gossett, J. M. (1987): *Measurement of Henry's Law Constants for C1 and C2 chlorinated hydrocarbons*. Env. Sci. Tech. 21(2): 202-208.

Poggel, K.; Mott, H.; Breiter, R.; Neeße, Th. (2001a): *Entwicklung einer Methode zur Bestimmung von Abbaukonstanten in Mikrokosmen mittels SPME-Analytik*. In: Resümee und Beiträge zum 3. Symposium Natural Attenuation vom 4. bis 5. Dezember 2001 bei der DECHEMA e.V., Frankfurt am Main, S. 57-65..

Wiedemeier, T. D.; Swanson, M. A.; Moutoux, D. E.; Gordon, E. K.; Wilson, J. T.; Wilson, B. H.; Kampbell, D. H.; Haas, P. E.; Miller, R. N.; Hansen, J. E.; Chapelle, F. H. (1998): *Technical protocol for evaluating natural attenuation of chlorinated hydrocarbons in ground water*. US Environmental Protection Agency, Cincinnaty, Ohio.

CHROMIUM, COPPER, AND ARSENIC DISTRIBUTION AND LEACHING FROM SOIL CONTAMINATED WITH TIMBER PRESERVATIVE

Geoffrey LESPAGNOL, Jean Luc BOUCHARDON and Bernard GUY

GENERIC / SPIN / EMSE - 158, Cours Fauriel - 42 023 Saint Etienne Cedex 2 - FRANCE

Phone: +33 (0)4 77 42 02 45 ; Fax: +33 (0)4 77 42 00 66 ; E-mail: lespagnol@emse.fr

Introduction

In several countries (Canada, France, New Zealand, etc.), many timber preservative sites are a source of soil pollution (ADEME, 1998). Copper, Chromium, and Arsenic (CCA), used as an aqueous timber preservative may accumulate in the soil through chronic exposure or accidental spilling. The risk associated with exposure of heavy metals results from their subsequent solubilisation and leaching into groundwater. In addition, soluble metals are potentially bio available and can enter the food chain.
To assess the risk and remediate a contaminated soil, the sampling strategy is an essential and delicate part. Especially due to the heterogeneity of the soil matrix, the conclusion of the sampling results may be erroneous (dilution or nugget effect, not enough sampling point, ...). Moreover, it appears that the pollutant concentration in the soil solution is not always directly correlated to the pollutant content in the soil matrix. Several studies provide essential data for a better understanding of the CCA mobility in the soil. Particularly the laboratory design of soil columns are used to predict the movement of the pollutants down the soil profile. Some examples are given in the literature with the three elements examined one by one [Tevissen et al., 1994] [Montero et al., 1994] [Isenbeck-Shroter et al., 1994] or all together [Carey et al., 1996] [Andersen et al., 1996] [Kelsall et al. 1998]. Nevertheless, no information is available on CCA solubilisation from intact soil contaminated by industrial timber preservative activity and subsequent studies are needed to improve the understanding and prediction of the phenomenon.
The aim of this presentation, concerning the more or less long-term intact (not destructured) soils contaminated by CCA from the timber treatment activity, is twofold :
1- to provide more information about the CCA spatial distribution on surface and in profiles
2- to provide results about the CCA leaching considered closer to the field conditions.

Materials and methods

Sites and sampling areas

In order to get a set of soils with different physicochemical properties and CCA loading, five timber treatment sites were investigated. For reasons of confidentiality, no identification and localisation information will be provided. Upper case letters from A to E designate the five sites. On each site, the first step was to prospect the best-contaminated areas according to the intrinsic nature and the contamination of soils. After hand sampling, the nature of the soil was assessed by field observation (colours, texture, structure and other) and CCA analysis were performed using the 3050B USEPA method. In that way, between 1 to 4 sampling areas were chosen and designated by number following the site letter (ex: B2). Finally, 14 areas were sampled. Most of the sites sampled were closed and abandoned for more or less long-time and no precise source of contamination is known. It can be noticed that the CCA treatment appears in the 30's, developed in the 50's and is still in practice nowadays. In ours sampled areas, the following contamination sources may be split in the following categories (with some reserve):
- The CCA commercial products more or less diluted (B4 and C2),
- The CCA wood ship leachates (C3 and E2)
- The CCA leached from the freshly stored timber (B2, B3, D1, D2 and E1)
- The CCA sources were not directly attributed to the "normal" treatment activity of the sites and may be the consequence of run off or accidental unusual spillage (A1, B1, C1 and C4).
- Two areas are low of CCA contamination (B3 and E3)

Soil sampling and lysimeters preparation

The main sampling procedure was to extract inside a surface of around 800 cm^2, 4 soil cylinders of 10 cm in diameters (78 cm^2) and 10 cm in depth from the surface (except for C3 and C4 where 3 soil cylinders were sampled) (fig.1). The identification of the individual cylinder is done by lower case letters from a to d.

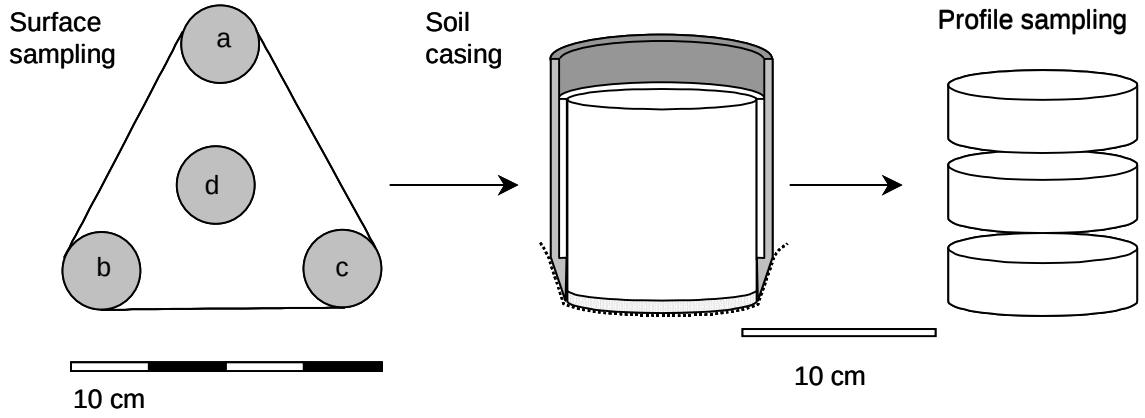

Figure 1: Soil sampling design

For the leaching experiments, soil core samples were removed as undisturbed as possible by a method adapted from Cameron et al. [Cameron et al., 1990].
Briefly, the main features of the method consist of digging a trench around each casing to expose the desired depth of soil below the cutting edge. The lysimeter is then gently pushed down. Lysimeters have an internal cutting ring at the base that allows an annular gap to be produced between the soil monolith and the casing wall. The gap is sealed with warm liquid petrolatum (about 50^oC) to prevent edge-flow effects during the leaching experiments. On sites A and B four lysimeter replicates were used per area and on sites C to E, one lysimeter was used (except for area C3 where we get 2 lysimeters), which give a total of 30 lysimeters.
For each core used for the leaching experiment, the CCA soil contents were analysed as followed: The soil cylinder was removed from its casing, and the surrounding petrolatum cautiously removed. The soil was then split in three equal parts along the profile of 3.3 $\pm$ 0.5 cm.

Soil preparation and analysis

All soil samples were air-dried and handly ground to pass through a 2 mm stainless steel sieve prior to laboratory analysis. The proportion of the fraction > 2 mm was recorded.
Total CCA and Na, K, Ca, Mg, Fe, Al, Mn (designed as major elements) soil content was determined using an HNO_3 / H_2O_2 peroxide digestion method (USEPA method 3050B) for ICP-AES analysis. Along the soil preparation and analysis, a CCA content incertitude was assessed on three soil samples (B1, B2 and E1) with different CCA load by using five aliquots of 2 g.

Leaching procedure

One pore volume of 10^{-3} M of $Ca(NO_3)_2$ solution was leached every 48 hours into each lysimeter. The bulk density and pore volume of the soil were estimated from separate cores collected close to those used for the leaching study. A constant head was maintained with a Mariotte bottle to provide saturated water flow. At the core bottom, a layer of 1 cm acid washed sand and a nylon were added and a funnel was hermetically fitted to collect different leachate volumes. A peristaltic pump has regulated the flow rates. For each area, flow rate value were similar to the one obtained on the field with a percolation test. The flow rate was checked by weighing the fractions collected at a known time from the beginning of each 48h leaching sequence. The pH and conductivity were recorded immediately after each fraction sample was full. Leachate samples were stored at 4^oC with about 1% of concentrated HNO_3 and without filtration (all solutions were clear) before analysis with ICP-AES for CCA and major elements as soon as possible (less than one week). The aqueous concentration uncertainties of the different elements were considered to be 10 % up to a low detection limit of 10 µg/l.

At the end of the leaching experiment, a tracer analysis was carried out. A 500 mg/l NaBr solution was applied on the top of the free drained lysimeters by a step input. Different output fractions were collected and weighed. The Br^- concentrations were measured in each fraction and in the initial input solution using a specific bromide electrode.

CCA soil solution speciation

Less than 4 hours after one leaching cycle, the leaching solutions were analysed to provide CCA aqueous speciation information.
Chromate or Cr(VI) was determined colorimetrically (spectrophotometer, for use at 540 nm, providing a light path of 1 cm) by 1,5-diphenylcarbohydrazyde method.
Arsenate or As(III) was determined using a method adapted from Wilkie et al. [Wilkie et al., 1997]. The solution was passed through an anionic exchange resin (DOWEX 1X8-200, SIGMA) packed in small chromatographic column. This resin retains the As(V) species and let the As(III) in the solution.
The divalent copper cation or Cu^{2+} was determined using a combined ion-selective electrode.

Results and discussion

CCA soil distribution

The Cr, Cu and As contents of the fraction < 2 mm range from 20 – 4 400, 10 – 46 000 and 20 – 16 000 mg/kg respectively. Assuming that the fraction > 2 mm contains a relatively low level of contaminant, the more the fraction > 2mm is important, the more the CCA contents in the bulk soil are lower.
A soil content variation was computed by the ratio of the highest and the lowest CCA content. The variation of five aliquots of a same sample cores is presented for three different areas in figure 2. It corresponds both to the soil sample heterogeneity and the non-controlled soil procedure analysis default (loss, contamination, shift, ...).

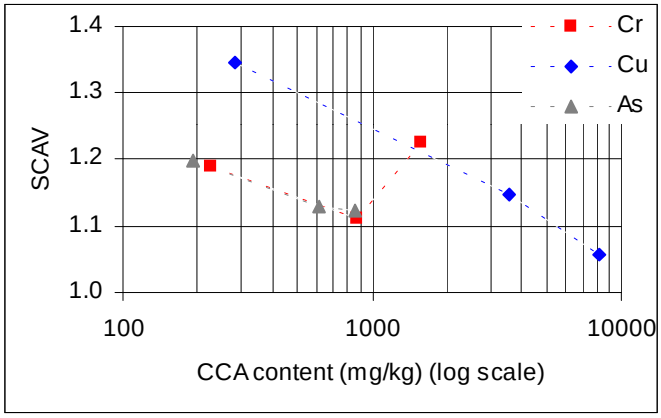

Figure 2: CCA soil content analyses variation

From these observations, it was decided than the intrinsic variations of a sample are 1.20 for Cr and As and Cu > 2000 mg/kg. For Cu < 2000 mg/kg, the variation is 1.35. The intrinsic variation for the major elements of these 3 samples are less than 1.3 (results not shown).
This quantification was done to ensure that the difference observed between CCA content in soil cylinder or part of this cylinder for each area are larger than the intrinsic variation and it is a heterogeneity induced in the field.
The CCA distribution appears to be more or less variable on the 800 cm^2 surface and along the 10 cm profiles. Figure 3 shows a typical example illustrated by the area B2. In this example the source of contamination is supposed to be the CCA leachate from freshly treated wood pieces. The first remarkable point is that the CCA content decreases with depth. This observation confirms the fact than most part of CCA is fixed into the first centimetres of the soil by chemical reactions (precipitation or adsorption). The second point is that the CCA content variability observed is higher in the surface cutting profile. Deeper, the variability comes closest to the intrinsic variability. In the case of the major elements, the content variability among the cores are below 1.75 for any depth.

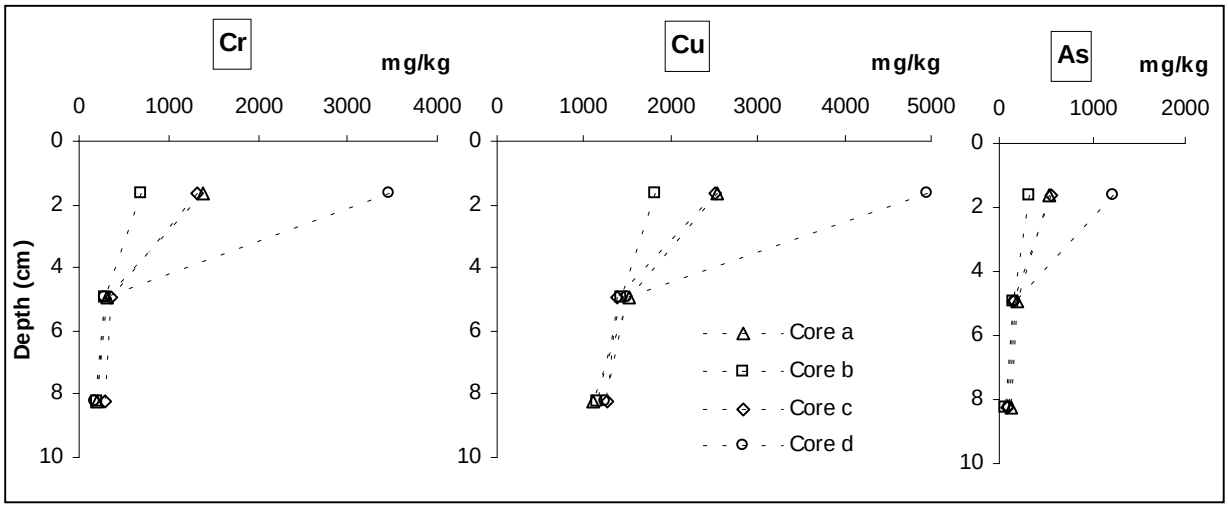

Figure 3: Example (B3) of CCA soil distribution. The CCA variation from results reported on the whole soil give similar trends because the soil texture differences for each area are relatively low

More generally, for each 800 cm^2 area and for a layer of 10 cm, the CCA content variations are given on the figure 4.

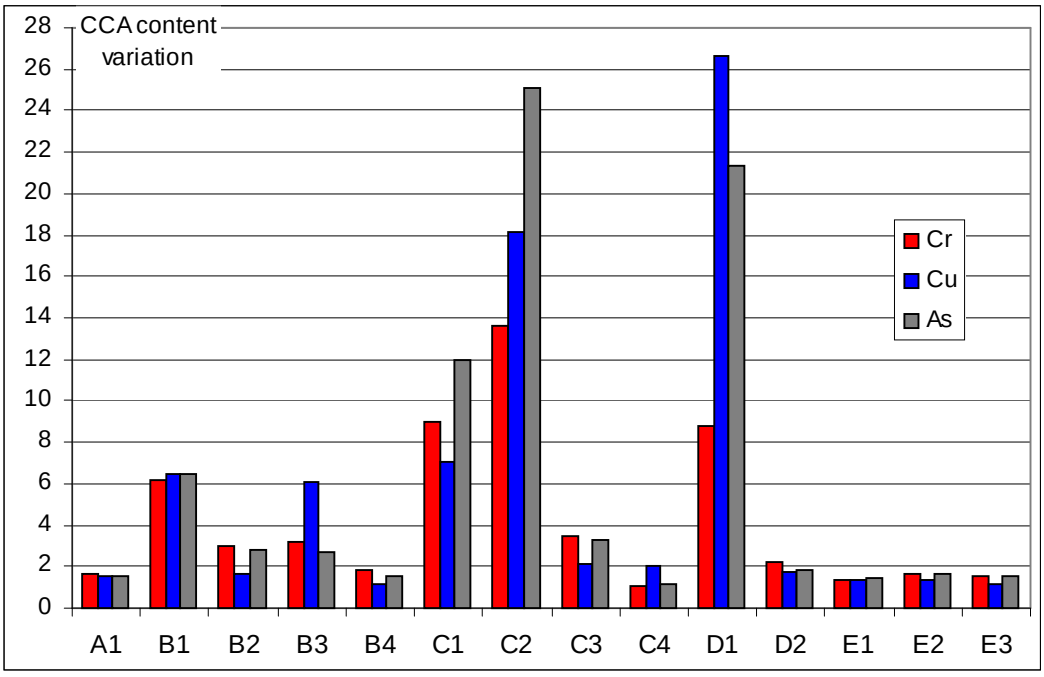

Figure 4: CCA content variations from core samples of each area studied

In 4 areas (B1, C1, C2 and D1), the CCA content variations are higher than 5 and reach a maximum of more than 26 for Cu in D1. At the opposite, CCA content variations are smaller than 2 in 6 areas (A1, B4, C4, E1, E2 and E3). Moreover, the relative Cr, Cu and As variations are different in a given area. At this point of the study, no direct relation was found between the CCA content variations and the soil properties measured (texture > 2mm, effective porosity, major elements, pH and conductivity). The soil micro topography may be an important point to consider with possible accumulation and penetration of CCA solution in the little soil depression (figure 5). Finally, we assume also that the characterisation of the source (initial quantity, CCA concentration and species and time and frequency of occurrence, …) is an important point to consider in the variability of the CCA pollution.

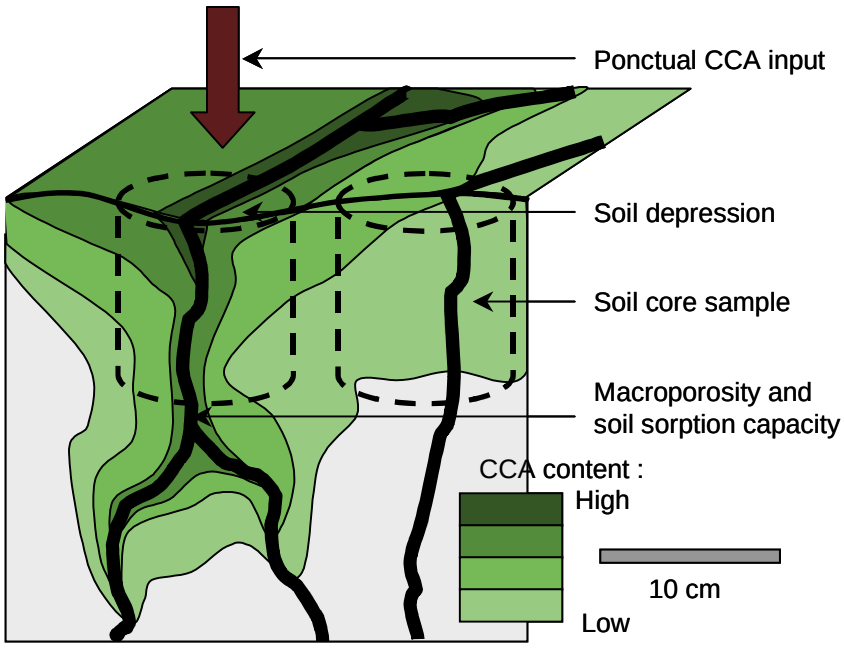

Figure 5: Schematic interpretation of the CCA distribution in the case of a contamination from the surface

CCA Leaching

CCA concentration in soil leachate ranges from 4 – 2250, 3 – 20 000 and 20 – 21 000 µg/l for Cr, Cu and As respectively. The figure 6 illustrates an example of the leaching experiment result (A1-a).

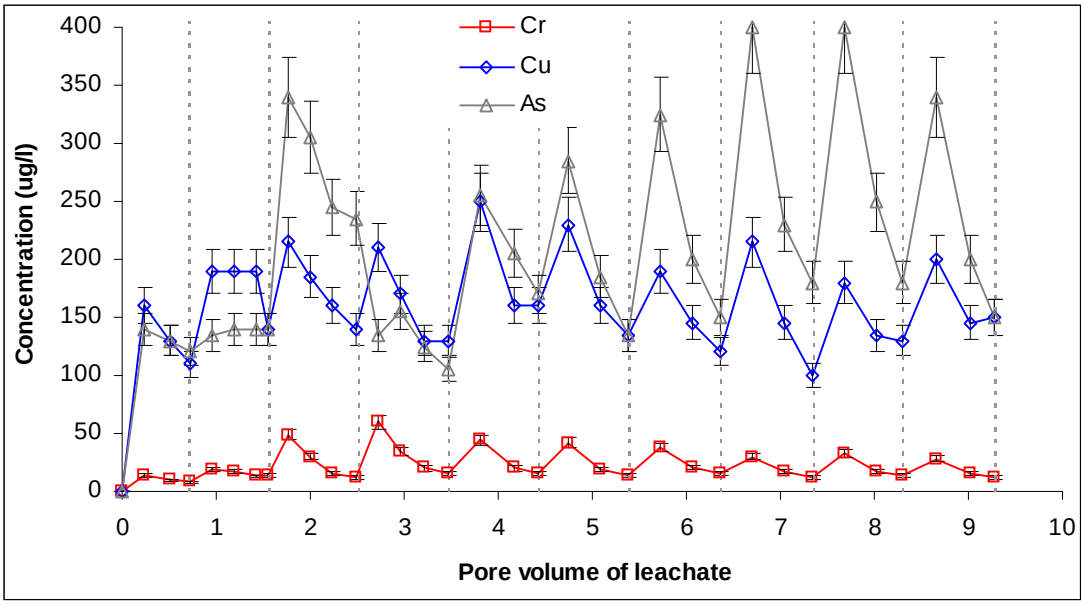

Figure 6: CCA leaching trend from an undisturbed contaminated core (A1a) (the broken line represent the 48 h interleaching periods)

CCA leaching concentrations remain approximately constant from one leaching cycle to the next. For example, in the case of the soil core A1a, about 25 µg/l of Cr, 170 µg/l of Cu and 230 µg/l of As were leached. This point may be explained by the low heavy metals quantity leaching compared to the initial concentrations in the soil. After ten leaching cycles (10 pore volumes), only 0.05 %, 0.2 % and 0.2 %

of the initial content of Cr, Cu and As respectively were leached. Running the experiments with higher leaching volume will certainly decrease the rate of leaching.
We also notice that CCA concentrations are higher in the first leaching fraction at each cycle. This fact may be the combined effect of the diffusion of the CCA into the soil matrix and the convection of the soil solution into preferential flow paths (Beven et al., 1982). The leaching solution moves quicker in the large connected pore volume (created by the roots, earth worms, cracks, etc.) and penetrate slower the soil matrix microporosity as experimented by the Br^- tracer. The Br^- breakthrough occurred before one pore volume was leached. Then, the volume at half Br^- concentration could be a good indicator of the effective pore volume, i.e. the pore volume that is effectively in contact with the moving soil solution. In the A1 core experiment, this volume is estimated between 30 % and 40 % of one pore volume. Then, in a first time, the fresh input solution pushes down the more accessible residual solution enriched in CCA during the interleaching period. Progressively, the fresh solution leaches less CCA, which has not enough time to diffuse from the soil matrix to the connected pores.
Nevertheless, these results are not always so clear. For some soil cores, the leachate concentration is not constant and decreases continuously. Moreover, the higher concentrations in the first leaching fraction at each cycle are not observed in several samples and sometimes the opposite occurs. To relate the CCA concentration in the leachate to some soil properties we have chosen to average a concentration where the leaching sequences were the most stable (i.e. the concentration variability between several cycles was minimal). In that way, the relationship between the CCA solution concentration and the CCA soil content are presented in figure 7.

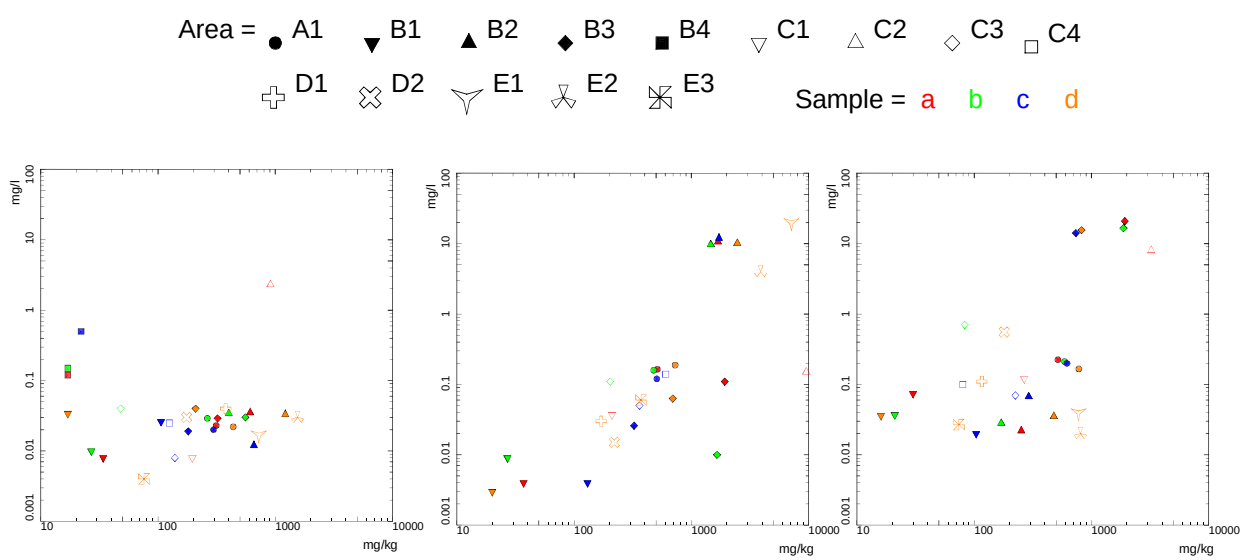

Figure 7: Relationship between CCA in soil matrix and CCA in soil leachate (the axis are in log presentation)

The direct correlation between CCA in the soil solution and in the soil matrix is not so direct, especially for Cr where the majority of the points are below 50 µg/l. Other soil parameters like pH or organic matter may influence the CCA mobility. Statistical study will be performed in further studies to try to link the soil properties and the CCA mobility.

The CCA species measurement reveals that Cr(VI) and As(V) are the dominant redox species, which is coherent with the aerobic conditions of the experiment. In the case of Cu, the trend is different between the samples. The Cu^{2+} proportions are variable among the samples and not correlated to the total Cu concentrations. The highest concentrations of Cu^{2+} recorded reach values as high as 8 mg/l from B2 and 30 mg/l from E1. These concentrations correspond to pH of 5.3 and 4.5, which are the lowest recorded among the lysimeter experiments.

Ternary diagrams are presented to visualise the relative proportion of Cr, Cu and As (fig. 8). On this representation, CCA are expressed in mol/kg to compare stoichiometric proportion. The sum of the contents of the three elements is reported on 100 %.
The diagram of CCA in the soil matrix shows a relative preponderance of Cu for 38 samples, which correspond to 8 sampling areas (B2, C2, C3, C4, D2, E1, E2, E3). It can be noticed that the higher is

the Cu content the higher is its relative content which is not true for Cr and As. The relative Cr contents are the highest for 12 samples and the relative As contents for only 4 samples.

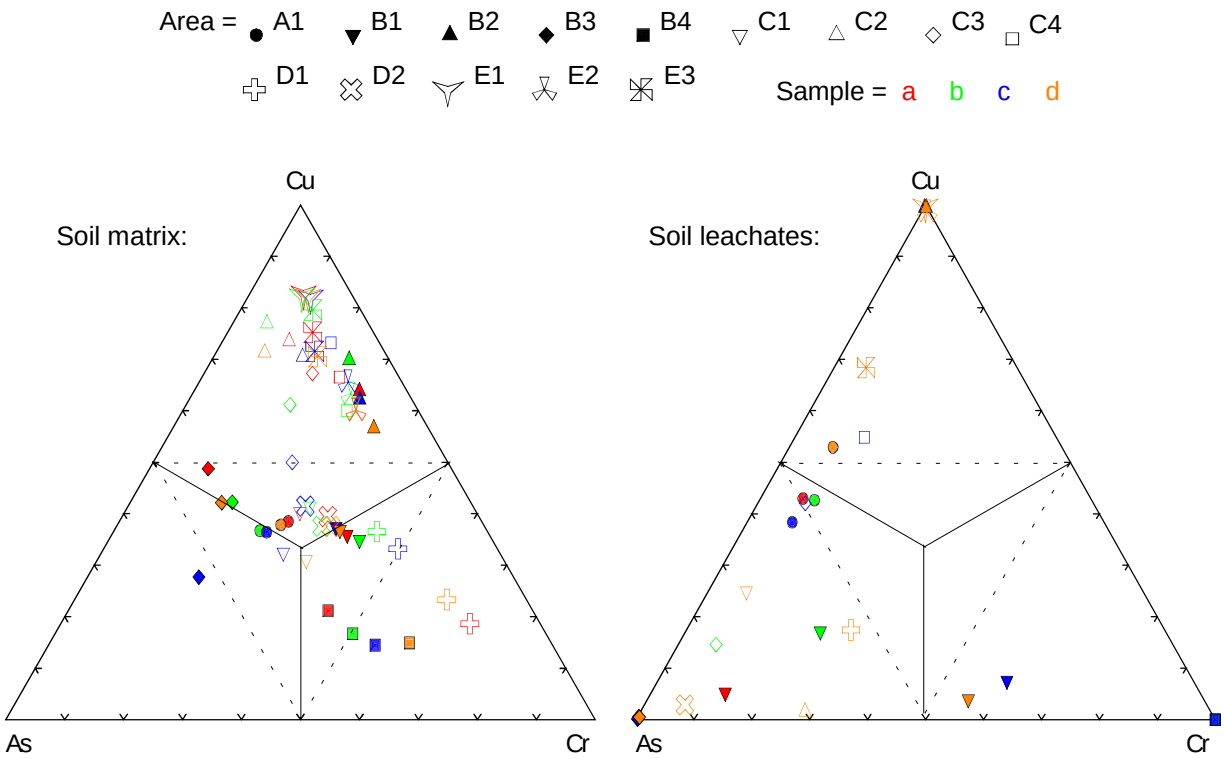

Figure 8: Ternary representation of CCA relative distribution

For some areas, the relative CCA distribution spread largely which get an other aspect of soil contamination heterogeneity. For example the Cu percentage for B2 ranges from 57 to 70 and the As for B4 ranges from 24 to 35 %. In comparison the ternary diagram of CCA in soil leaching reveals a high proportion of As concentration for 6 sampling areas whereas relative concentrations of Cu and Cr are dominant in 4 and 1 areas respectively. A positive correlation can be mentioned between relative Cr and As concentration in the soil leachate and relative Cr and As in the soil matrix.

Conclusion

In some contaminated areas sampled, the CCA distribution can be relatively heterogeneous on a small surface (800 cm^2), belong the depth or in the relative CCA distribution in contaminated soil. This point may be integrated for the sampling procedure to better asses the special representativeness of the pollutant content in the soil matrix. The CCA leaching pattern may be used, with some care, in order to provide a better assessment of CCA risk in contaminated soils. From the results of this study, As is considered as the most hazardous problem of the inorganic compound on the treatment sites.

References

RAYZAL M., DEBROUBAIX G., MOUTON and HEYBERGER A, (1998) - La pollution des sols liée aux activités de préservation du bois (soil pollution from timber treatment sites). ADEME, Guides et cahiers techniques.

ANDERSEN S., RASMUSSEN G., SNILSBERG P., AMUNDSEN C.E. and WESTBY T. (1996) - Assessing toxicity and mobilisation of impregnation salts at a contaminated site. *Fresenius Journal of Analytical Chemistry, Vol. 354, pp. 676-680.*

BEVEN K. and GERMANN P. (1982) - Macropores and water flow in soil. *Water Resources Research, Vol. 18, No. 5, pp. 1311-1325*.

CAMERON K.C., HARRISON D.F., SMITH N.P. and McLAY C.D.A. (1990) - A method to prevent edge-flow in undisturbed soil cores and lysimeters. *Austrialian Journal of Soil Research, Vol. 28, pp. 879-886*.

CAREY P.L., McLAREN R.G., CAMERON K.C. and SEDCOLE J.R. (1994) - Leaching of copper, chromium, and arsenic through some free-draining New Zealand soils. *Australian Journal of Soil Research, Vol. 34, pp. 583-597*.

ISENBECK-SCHROTER M., HAMER K., REITZ F., SCHUBERT J. and SCHULZ H. (1994) - Simulation of arsenic transport in column experiments: Estimation of sorption kinetics of As(III) and As (V) species in simple aquifer systems. *Transport and Reactive Processes in Aquifer, Dracos & Stauffer (eds)*.

KELSALL Y., ALLISON M., ALLISON G., TUROCZY N., STAGNITTI F., NISHIKAW A. and MORITA M. (1998) - Leaching of copper, chromium and arsenic in a soil of south west Victoria, Australia. *Toxicological And Environmental Chemistry, Vol. 70, pp. 375-384.*

MONTERO J.P., MUNOZ J.F., ABELIUK R. and VAUCLIN M. (1994) - A solute transport model for the acid leaching of copper in soil columns. *Soil Science Society of American Journal, Vol. 58, pp. 678-686*.

TEVISSEN E., MARGRITA R., NICOLAS-SIMONNOT M.O., SARDIN M. and SCHWEICH D. (1994) - Transport of chromium (VI) in saturated layer of sediment : column experiment and modelling. *Transport and Reactive Processes in Aquifers, Dracos & Staufer (eds)*.

WILKIE J.A. and HERING J.G. (1997) – Rapid oxidation of geothermal arsenic III in streamwater of the eastern Sierra Nevada. *Environmental Science & Technology, Vol. 32, pp. 657-662*.

USEPA (1996) - method 3050B.

Temporal changes in extractability and mineralization of 2,4-dichlorophenol in plant-amended soil

T. Boucard, R.D. Bardgett, K.C. Jones and K. T. Semple

Full mail address of main author: Department of Environmental Science, Institute of Environmental and Natural Sciences, Lancaster University, Lancaster, LA1 4YQ, UK.

Phone: (+44) 01524 594534
Fax: (+44) 01524 593985

E-mail: k.semple@lancaster.ac.uk

1. Introduction

Chlorinated phenolic compounds are widespread in the pesticide industry, being detected in industrial and domestic wastewaters as well as soils. Chlorinated phenolic compounds are thought to be toxic, relatively persistent and are also being investigated as possible endocrine disrupters and carcinogens. 2,4-Dichlorophenol (2,4-DCP) is an impurity formed during the production of the herbicide 2,4-dichlorophenoxyacetic acid (2,4-D) and is often found in the final product; further, it is also formed as a catabolic intermediate during 2,4-D degradation (Jensen, 1996). When chemicals enter the soil environment, they are subjected to a number of different loss processes: volatilisation, leaching and degradation. However, chemicals may also be retained within the soil, with soil-chemical association strengthening with increased contact time, leading to decreases in availability to solvents and soil biota; a process known as ageing (Hatzinger and Alexander, 1995). Recently, it has been shown that plants may have a role in the extent to which chemicals are retained within soils (Liste and Alexander, 2000). The aim of this study was to investigate the impact of Rye grass (*Lolium perenne*) on the extractability and degradation of 2,4-DCP in soil.

2. Materials and methods

A well characterised soil (Kettering loam, 5% OM) was spiked with ^{14}C-labelled (67 Bq g^{-1} soil) and non-labelled 2,4-DCP (1.4 mg kg^{-1}), in a single-step spiking/re-hydration procedure (adapted from Reid et al, 1998), adjusted to 30 % moisture content with deionised water, and left to equilibrate overnight. Controls were spiked with water only and all treatments were prepared in triplicates. Microcosms consisted of opaque plastic pots (5-cm diameter, 10.5-cm height) with drainage holes, and contained 120 g soil (dry wt). Rye grass (*L. perenne*) seedlings (3) were added to half the soil microcosms, giving planted and non-planted systems. Microcosms were placed randomly in a phytocube with a 16-hour-day cycle at 18-25°C, and destructively sampled after 1, 14, 35 and 57 days incubation. Total ^{14}C-activity was measured by sample oxidation; solvent extractable ^{14}C-2,4-DCP by soxtec distillation (dichloromethane (DCM) for 3 h); and acetonitrile:water (1:1, 24 h shake extraction); mildly extractable ^{14}C-2,4-DCP in an aqueous solution of $CaCl_2$ (20 h shake-extraction); and total bioavailable fraction using 10 d soil-slurry mineralisation assays with an inoculum of known 2,4-DCP degraders (*Burkholderia* sp., ~ 10^6 cells g^{-1}_{soil}).

3. Results and discussion

Table 1 shows the temporal changes in the availability of the ^{14}C-2,4-DCP associated activity to extraction and mineralisation, by a microbial inoculum, in both planted (inoculated with *L. perenne*) and unplanted systems. For DCM and acetonitrile:water extractions, ~100% was available at time 0, where as only 46% was extracted using $CaCl_2$. Over the course of the incubation, the acetonitrile:water extraction was more effective than DCM or $CaCl_2$ at extracting the ^{14}C-2,4-DCP

associated activity from the soils. In all cases, there was a decrease in extractability as soil-2,4-DCP contact time increased. This was also true for the mineralisable fraction of the soil associated ^{14}C-2,4-DCP activity.

In comparing the planted and unplanted soil incubations, it is clear that the presence of *L. perenne* influenced the amount of ^{14}C-2,4-DCP associated activity, which was available for extraction and mineralisation. In the unplanted soils, more ^{14}C-2,4-DCP associated activity was available for extraction or degradation at 35 and 57 days that in the planted microcosms. This suggests that the presence of the plants was enhancing or accelerating the ageing process: there was ~ 20% less ^{14}C-2,4-DCP associated activity available for mineralisation; ~ 30% less ^{14}C-2,4-DCP associated activity available for extraction using acetonitrile water; ~ 10% less ^{14}C-2,4-DCP associated activity available for extraction using $CaCl_2$, and ~ 25% less ^{14}C-2,4-DCP associated activity available for extraction using DCM in the planted systems after 57 days incubation (Table 1).

Table 1. Total ^{14}C-2,4-DCP associated activity (%) mineralised or extracted at each time point, for planted and non-planted soils.

Incubation time (day)	Mineralisation[a] (% ± SD)	Acetonitrile:water extraction[a] (% ± SD)	$CaCl_2$ extraction[a] (% ± SD)	DCM Soxtec extraction[a] (% ± SD)
	Planted			
1	69.58 ± 0.71	105.29 ± 0.49	46.31 ± 1.19	94.72 ± 1.35
14	38.08 ± 2.14	68.72 ± 5.75	11.72 ± 2.35	45.06 ± 3.13
35	15.61 ± 1.58	33.24 ± 5.14	4.37 ± 0.42	24.15 ± 2.37
57	9.94 ± 0.77	17.30 ± 1.05	2.45 ± 0.32	11.04 ± 0.94
	Unplanted			
1	69.58 ± 0.71	105.29 ± 0.49	46.31 ± 1.19	94.72 ± 1.35
14	30.01 ± 3.29	57.02 ± 6.85	13.58 ± 1.74	31.44 ± 3.71
35	29.83 ± 2.64	48.52 ± 8.78	12.66 ± 3.51	41.67 ± 6.04
57	27.00 ± 6.77	48.50 ± 9.59	13.14 ± 3.27	37.91 ± 6.13

[a] Values based on ^{14}C-2,4-DCP associated activity present in the soils at each sample time point as determined by combustion of soils.

It is clear, that the presence of *L. perenne* is influencing the behaviour of 2,4-DCP in the soil. In general, microbial numbers and activity are greater in the rhizosphere than in bulk soils (Killham, 1994). In terms of the behaviour of contaminants in planted soils, increased microbial activity may result in enhanced levels of degradation, uptake into biomass and/or incorporation into soil organic matter of the contaminant carbon; however, the dominant processes have yet to be quantified.

References

Hatzinger, P. B. and Alexander, M. (1995) Effect of ageing chemicals in soil upon their biodegradability and extractability. *Environmental Science and Technology* 29, 537-545.

Jensen J. (1996) Chlorophenols in the terrestrial environment. *Reviews of Environmental Contamination and Toxicology* 146, 25-47.

Killham, K. (1994) Soil Ecology, Cambridge University Press.

Liste, H-H. and Alexander, M. (2000) Plant-promoted pyrene degradation in soil. *Chemosphere* 40, 7-10.

Reid B.J., Northcott G.L., Jones K.C., Semple K.T. (1998) Evaluation of spiking procedures for the introduction of poorly water soluble contaminants into soil. *Environmental Science and Technology* 32, 3224-3227.

IMPACT OF COPPER BASED FUNGICIDES ON THE DEGRADATION OF *p,p´*-DDT TO *p,p´*-DDE IN PIP AND STONEFRUIT ORCHARD SOILS IN THE WAIKATO REGION, NEW ZEALAND.

S.K. Gaw[a,c], G. Palmer[a], N.D. Kim[b] and A.L. Wilkins[a]

[a.] University of Waikato, Private Bag 3105, Hamilton, New Zealand
[b.] Environment Waikato, P.O. Box 4010, Hamilton, New Zealand
[c.] skg3@waikato.ac.nz

Abstract

Orchards (n=7) were sampled as part of a larger survey investigating agrichemical residues (organochlorine pesticides and trace elements) in cropping soils in the Waikato region, New Zealand. ∑DDT concentrations in orchard soils ranged from 0.37 to 34.5 mg kg^{-1}. There was a significant negative correlation (-0.84, $p<0.02$) between Cu concentration (242 to 523 mg kg^{-1}) and the ratio of *p,p´*-DDE to *p,p´*-DDT (0.8 to 3.6) in pip and stonefruit orchard soils. The ratio of soil microbial carbon to soil carbon (% C_{mic}/Org-C) in orchard soils decreased compared to reference soils. The microbial metabolic quotient *q*CO2 increased in orchard soils compared to reference soils. These findings are consistent with the conclusion that elevated soil Cu concentrations in pip and stone fruit orchard soils in the Waikato region may have reduced the ability of the indigenous soil microbial community to degrade DDT to DDE and are in general agreement with those previously published for the Auckland region, New Zealand (Gaw *et al.,* 2003).

Keywords

DDT, DDE, Cu, degradation, microbial biomass, orchards, New Zealand, soil respiration

Introduction

There is growing awareness in New Zealand that horticultural land may have been contaminated by historic applications of agrichemicals (including pesticides, fertilisers and soil amendments). Elevated soil concentrations of trace elements (e.g. As, Cd, Cu, Hg, Pb and Zn) (Giller *et al.,* 1998) and organochlorine pesticides (Harris *et al*, 2001;Wan *et al*., 1989) in intensively cropped soils have also been reported internationally. Trace metal contamination of horticultural soil ecosystems is widely acknowledged as having deleterious effects upon soil microbiological communities (Merrington *et al*., 2002). This has important implications for soil ecosystem function including impacts upon cycling of nutrients and the degradation of organic contaminants (Giller *et al.* 1998). The accumulation of organochlorine pesticides is of significant concern due to their persistence and ability to bioaccumulate (Harris *et al*., 2001; Boul, 1995).

1,1,1-trichloro-2,2-*bis*(*p*-chlorophenyl)ethane (DDT) was used extensively throughout the world from the late 1940s until the 1970s as a pesticide to control chewing insects (Boul, 1995). Until recently the focus in New Zealand has been on soil residues on grazing land, where DDT was widely used to control grassgrub. DDT was also widely used in New Zealand orchards until the mid 1970s to control codlin moth and bronze beetle (Osborne, 1976).

DDT is degraded in soil by both biotic and abiotic processes to form DDD (1,1-dichloro-2,2-*bis*(*p*-chlorophenyl)ethane) and DDE (1,1-dichloro-2,2-*bis*(*p*-chlorophenyl)ethylene) (Foght *et al*., 2001). DDT residues may be lost from the soil through a variety of mechanisms including volatilisation, leaching, loss in solution or suspension, erosion, as well as through biotic and abiotic degradation (Boul 1995). The biodegradation of DDT and its degradation products is co-metabolic. The micro-organisms involved do not gain any nutrients or energy for growth from the process and require an alternate carbon source as a growth substrate (Aislabie *et al*., 1997). The ratio of DDE:DDT can be used as a measure of degradation of the active ingredient and has been used to establish recent illegal use of DDT (Hitch and Day, 1992).

Cu is the active ingredient in a wide range of current and historic fungicides (Giller *et al.*, 1998) and is one of the least mobile trace elements in soil (Kabata-Pendias and Pendias, 2001). Surface soils have a great ability to accumulate Cu where it is strongly bound by soil organic matter and clay minerals (Kabata-Pendias and Pendias, 2001). Elevated levels of copper in horticultural soils have been demonstrated to negatively impact on the soil microbial community (e.g. Merrington *et al.*, 2002; Zelles *et al.*, 1994).

We have recently reported a significant negative correlation between Cu concentrations and the ratio of DDE to DDT in Auckland pip and stonefruit orchard soils and provided evidence that elevated levels of Cu in orchard soils were impacting on microbial activity (Gaw *et al.*,2003). The specific objective of this study was to determine whether the DDE:DDT ratio and Cu were similarly correlated in another fruit growing region of New Zealand, namely the Waikato region.

Methods

The Waikato region is located in the centre of the North Island of New Zealand. The region covers approximately 2,500 km^2 of which 9000 ha are currently used for horticulture. Predominant soil orders under cultivation in the Waikato region include Allophanic (aquands) and Granular (humults) soils (Hewitt, 1998).

Soil Collection
Composite soil samples were collected from a representative hectare of the cropping area on seven orchards in the Waikato region. All of the orchards sampled were established prior to 1975 and several have been active for more than 50 years. The most suitable control for the orchards would have been orchards which had been managed identically apart from the addition of copper. As true controls were not available, soil samples were also collected from 4 grazing paddocks with soils from the same soil series to act as reference sites for the microbial community measurements. It was not possible to identify a suitable reference site for all of the orchards sampled. Seven additional soil samples were collected from soils under native vegetation as background controls for trace elements and organochlorine pesticides. Samples were collected to a nominal depth of 7.5 cm using a stainless steel corer.

All soil samples were mechanically homogenised and a representative subsample dried in a dedicated oven for 5 days at 30° C to ≤ 8% moisture. Soil samples were dried in aluminium trays. The dried subsample was sieved to <2 mm and analysed for trace elements, organochlorine pesticides, total organic carbon and soil pH.

Soil Analyses
Soil pH (1:2.5 soil:water ratio), cation exchange capacity (0.01 M silver thiourea) and total organic carbon (%TOC) were determined following the New Zealand Soil Bureau Methods (Blakemore *et al.* 1987). Particle size was determined by laser analysis using a Malvern Instruments Mastersizer.

Chemical Analyses

Organochlorine Pesticide Analysis
Air dried and ground soil (<2 mm) was pre-wet with phosphoric acid, followed by sonication extraction (Sonorex digital 10P Sonicator) using 1:1 hexane and acetone. Extracts underwent a florisil cleanup and were analysed by GC-ECD (Agilent 6890 plus with micro ECD detector) analysis with internal standard calibration. The GC parameters were as follows: Oven; initial temperature 120 °C, 60 °C/minute ramp to 220 °C, 5 °C/minute ramp to 250 °C, 30 °C/minute ramp to 300 °C, hold for one minute. Inlet: Pulsed splitless 1 μL injection, 250 °C, pulse time 0.5 minutes. Column type: SGE BPX50 GC column, 0.25 mm ID x 0.25 μm film thickness x 30 m column length. A procedural blank was included with each batch of samples. Concentrations of target analytes in all procedural blanks were found to be less than their detection limits. An internal QC sample was also analysed with each batch.

Trace Element Analysis
Trace elements were determined using USEPA Method 200.2 Total Recoverable Metals. The extracts were diluted and determined by ICP-MS (Elan 6000). Four blind duplicates and one certified reference material (CW 7401 Soil, National Research Centre for CRMs, China) sample were also

submitted for trace element analysis. The trace element results for the blind duplicates were within 20% of the certified value with the exception of those trace elements with concentrations close to the detection limit.

Biological Analyses

Respirometry
Respiration was measured by titration with 0.1M HCl after collecting CO_2 in 0.5M KOH traps. Soils (50g) were incubated in gas tight containers for 7 days at 25 °C. Measurements were carried out in triplicate. Respiration is expressed as μg $C0_2$-C g^{-1} soil h^{-1}. The microbial metabolic quotient (*q* CO_2) is reported on a per unit biomass basis, mg $C0_2$-C g^{-1} C_{mic} h^{-1}.

Microbial Biomass
The microbial biomass was determined by a fumigation-extraction method. Triplicates of fumigated ($CHCl_3$ overnight) and non-fumigated soils (5 g oven dry weight equivalent) were extracted with 25 mL of 0.5 M K_2SO_4 for 2 h followed by centrifugation and filtration. The extracts were analysed for organic C using a Shimadzu TOC 5000A fitted with an ASI-5000A autosampler. Soil microbial biomass C (μg C_{mic} g^{-1} soil) was calculated from the equation $C_{mic}=E_c/0.3$ where E_c= [(amount of C extracted by 0.5 M K_2SO_4 from fumigated soil)- (amount of C extracted by 0.5 M K_2SO_4 from non-fumigated soil)].

Results

The median values for arsenic, copper, cadmium, tin and zinc in Waikato orchard soils exceed the median values measured in soils under native vegetation (Table 1). Cu was the trace element most frequently found at elevated concentrations in orchard cropping soils.

Table 1 Concentrations of selected trace elements in soils from Waikato orchards (n=7) compared to soils under native vegetation (n=7). Units are mg kg^{-1} dry weight.

	Orchards			Native vegetation		
Contaminant	**Min**	**Max**	**Median**	**Min**	**Max**	**Median**
Arsenic	4	58	6	3	8	6
Cadmium	0.8	1.5	1	<0.1	0.3	0.1
Copper	242	523	301	8	30	20
Lead	14	251	18	11	45	24
Tin	3	7	5	<1	2	1
Zinc	35	197	121	29	74	43

DDT and/or its degradation products were detected in all of the orchard samples (Table 2). ΣDDT (sum of the *o*,*p´*- and *p*,*p´*- isomers of DDT, DDE and DDD) concentrations in orchard soils ranged from 0.37 to 34.5 mg kg^{-1}. Low levels of lindane (0.01-0.02 mg kg^{-1}) were detected in 3 of the orchard samples and low levels of dieldrin (<0.02 mg kg^{-1}) in 2 of the orchard samples. No other organochlorine pesticides were detected in orchard soils. DDT and/or its degradation products were the only organochlorines detected in grazing soils and ΣDDT concentrations in grazing soils ranged from <0.03 to 0.75 mg kg^{-1} with a median value of 0.07 mg kg^{-1}.

The DDE:DDT ratios (*p*,*p´*--isomers) in pip and stonefruit orchard soils ranged between 0.8 and 3.6 and decreased with increasing Cu concentration. A linear relationship (Figure 1) was observed between the log Cu concentration and the DDE:DDT ratio in Waikato pip and stonefruit orchard soils. The Pearson Correlation Moment for this relationship between Cu concentration and the DDE:DDT ratio was -0.84 $p<0.02$). There was also a significant correlation between ΣDDT and Cu concentrations in orchard soils (0.85, $p<0.02$). No significant relationship was found between the DDE:DDT ratio (*p*,*p´*-isomers) and any other trace metal, pH or % TOC (Table 2).

Figure 1 Relationship between Cu concentration and the DDE:DDT (*p*,*p´*- isomers) ratio for pip and stonefruit orchard soils in the Waikato region, New Zealand.

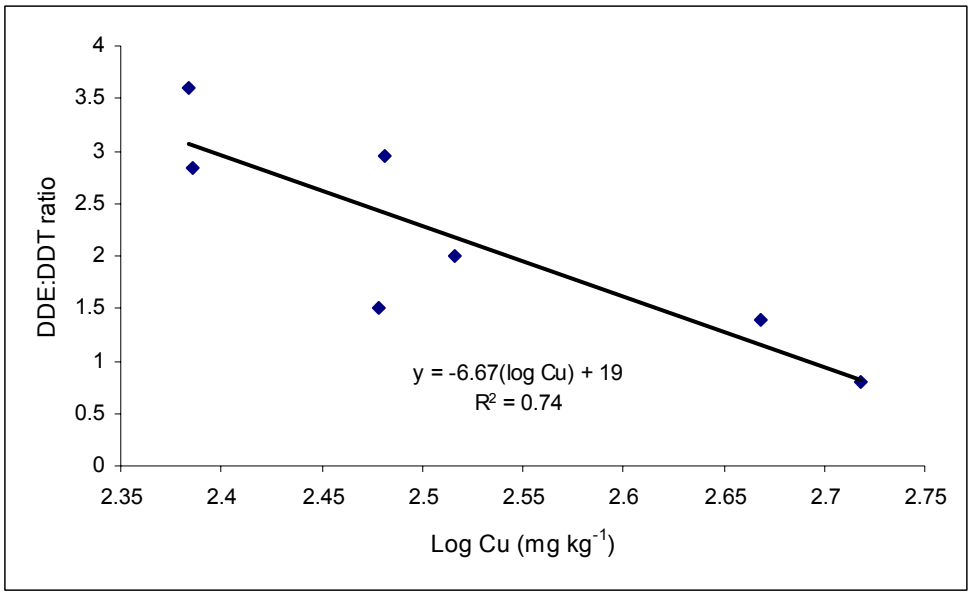

Table 2 Summary of soil characteristics and concentrations of selected contaminants (mg kg^{-1}) for orchards and reference sites. Orchards and their controls have the same letter. Respiration is reported ± the standard error.

Site	% Clay	% Silt	% Sand	As	Cd	Cu	Pb	∑DDT	pH	%TOC	Respiration μg $C0_2$-C g^{-1}soil h^{-1}
Orchard 1[a]	13.3	37.6	49.1	58	1.5	523	251	34.5	5.81	8.4	4.35 ± 0.04
Orchard 2	12.7	51.5	35.8	43	1.0	466	198	9.8	5.97	3.9	2.50 ± 0.05
Orchard 3[b]	11.5	47.2	41.3	6	1.0	328	14	3.2	6.22	6.0	3.19 ± 0.05
Orchard 4[c]	6.0	41.7	52.3	5	1.2	303	17	0.72	6.26	8.1	3.20 ± 0.12
Orchard 5[a]	8.7	47.6	43.8	5	1.0	301	22	8.7	5.97	6.9	3.67 ± 0.03
Orchard 6[c]	6.1	37.4	56.6	4	1.2	243	17	1.4	6.18	8.4	3.15 ± 0.35
Orchard 7[d]	17.5	46.0	36.7	8	0.8	242	18	0.37	5.87	5.3	2.16 ± 0.09
Grazing 1[a]	9.0	39.7	51.3	8	0.7	18	26	0.36	5.76	5.7	1.82 ± 0.04
Grazing 2[b]	6.55	42.4	51.1	8	0.7	17	18	0.75	5.50	8.1	3.11 ± 0.13
Grazing 3[c]	7.4	38.6	54.0	3	1.5	19	12	0.33	6.02	9.4	3.48 ± 0.11
Grazing 4[d]	17.4	42.8	39.8	3	0.6	24	42	<0.03	5.88	5.3	3.33 ± 0.09

The ratio of microbial carbon (μg C_{mic} g^{-1}soil) to soil carbon (mg C g^{-1}soil) (% C_{mic}/Org-C) decreased in orchard soils compared to reference soils from the same soil series (Figure 2). Whilst there was no consistent trend for soil respiration (Table 2), the microbial metabolic quotient qCO_2 increased in orchard soils compared to the reference grazing soils (Figure 2).

Figure 2 Copper concentration (2a), ratio of microbial carbon to soil carbon (% C_{mic}/Org-C) (2b) and the microbial metabolic quotient qCO_2 (2c) in orchard soils compared to reference soils.

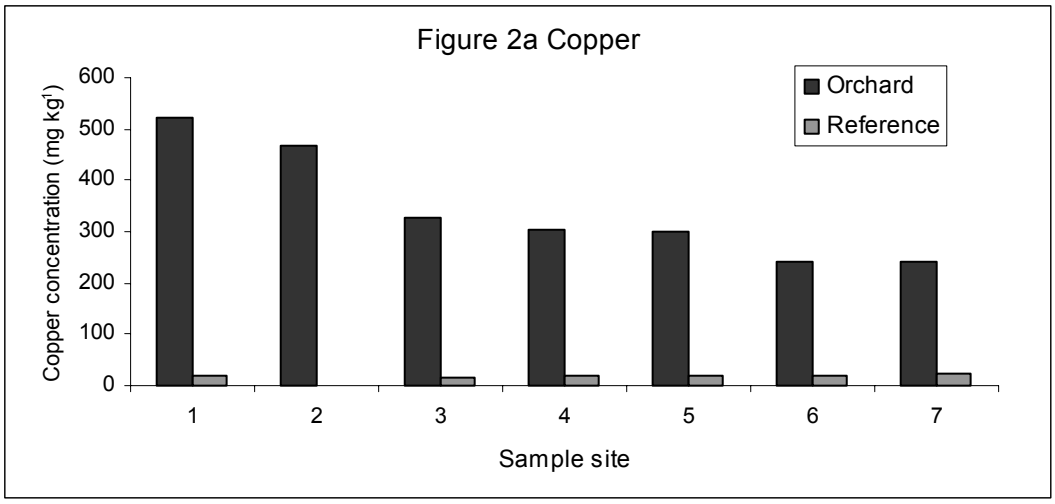

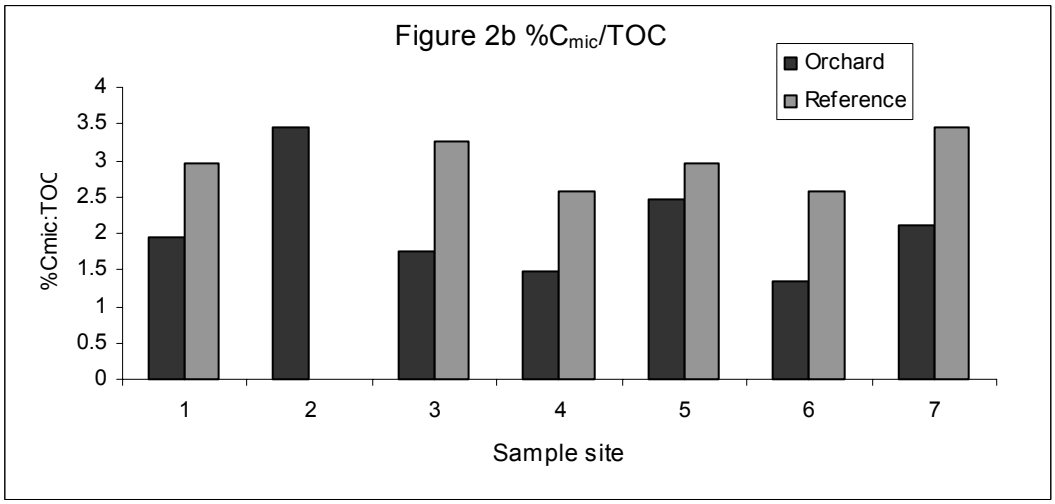

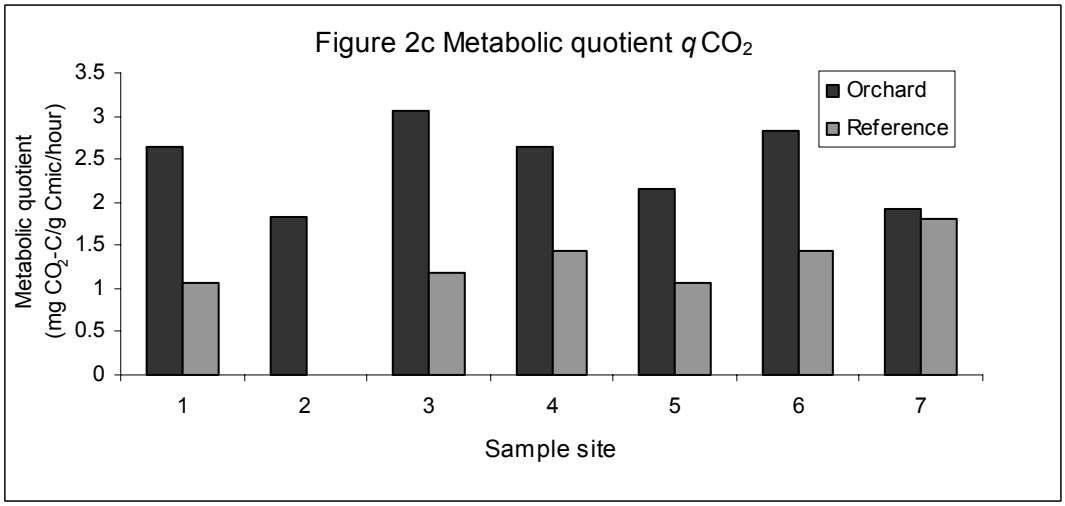

Discussion

The Cu concentrations measured in the Waikato orchard soils are comparable with those reported by Gaw (2002) for orchard soils in the Auckland region, NZ (21 to 490 mg kg^{-1}). Holland and Solomona (1999) reported copper levels of 60 to 480 mg kg^{-1} in 19 New Zealand orchards. Merry *et al.* (1983) measured Cu levels in the range of 11 to 320 mg kg^{-1} in Tasmanian and South Australian orchard soils. The elevated concentrations of Cu found in Waikato orchard soils are most likely due to the long-term use of Cu-based fungicides. Holland and Solomona (1999) also concluded that the elevated soil Cu levels in New Zealand orchard soils were the result of long-term use of Cu based fungicides. As Cu-based formulations are still widely used for horticultural applications in New Zealand, Cu concentrations in soil are likely to increase.

Despite its widespread historical use, there is limited published data on DDT residue levels in New Zealand soils. The elevated ΣDDT concentrations measured in this survey are consistent with those measured in orchards in the Auckland region (<0.03 to 24.4 g kg^{-1}) (Gaw, 2002). ΣDDT concentrations in Waikato region grazing soils ranged from <0.03 to 0.75 mg kg^{-1}. In comparison, the mean value for ΣDDT residues in paddocks on Canterbury farms was 0.27 mg kg^{-1} and only 7% of paddocks sampled had ΣDDT concentrations greater than 1.0 mg kg^{-1} (Roberts *et al.*, 1996). Orchard *et al* (1991) carried out experiments on the degradation of DDT in New Zealand soils using three pastoral soils with ΣDDT levels (top 5 cm) of 2.6, 1.3 and 0.004 mg kg^{-1}. The Ministry for the Environment reported a background concentration of 1.5 μg kg^{-1} for ΣDDT in Hamilton City (Waikato region) soils (MfE, 1998). It was considered unlikely that the elevated concentrations of the active ingredient *p*,*p´*-DDT measured in the Auckland and Waikato orchards were due to recent use. The use of DDT was restricted from 1970 and it was deregistered for use in New Zealand in 1989 (Buckland *et al.*, 1998).

Our ΣDDT results for Waikato orchard soils are in keeping with those of Harris *et al.* (2000). Harris *et al.* (2000) measured ΣDDT concentrations in orchard soils in Canada 20 years after DDT had last been applied and reported mean ΣDDT concentrations of 1.9, 7.1 and 14.4 mg kg^{-1} for the top 10 cm of soil from 3 fruit growing regions.

Elliott *et al.* (1994) estimated that the ratio of DDE:DDT should exceed 20:1 after the use of DDT has been restricted for 15-20 years. However the DDE:DDT ratios in the Waikato orchard soils sampled ranged from 0.8 to 3.6. Similar ratios of DDE:DDT have either been reported or can be calculated from the results reported in the literature for surveys of orchard soils. For example Harris *et al.* (2000) report average DDE:DDT ratios of 1.10, 1.21 and 1.36 in 3 Canadian fruit growing regions. Ratios of DDD:DDT were not calculated for Waikato orchards as DDD was also used as a pesticide on several of the orchards sampled.

There was a significant negative correlation (-0.84 $p<0.02$) between the DDE:DDT ratios (*p*,*p´*-isomers) and the Cu concentration in Waikato pip and stone fruit orchard soils. A significant negative correlation has also been reported between the ratio of DDE:DDT and the Cu concentrations in Auckland orchard soils (Gaw *et al.*, 2003).

One possible explanation for the observed correlation between the DDE:DDT ratios and Cu is that the elevated Cu concentrations on some properties have lead to a change in the functional diversity of the microbial community. Cu tolerant communities may have replaced the soil micro-organisms that were able to co-metabolise DDT. The median Cu concentration for Waikato orchard soils (303 mg kg^{-1}) exceeds the Oak Ridge National Laboratory Ecological Soil Screening Level (microbes) for Cu of 100 mg kg^{-1}. The microbial biomass and metabolic quotient were measured as indicators of microbial activity. The ratio of % C_{mic}/OrgC decreased in orchard soils compared with reference soils; this trend was also observed in Auckland soils (Gaw *et al.*, 2003). These results are also consistent with those of Merrington *et al.* (2002) who found that the ratio of C_{mic}:OrgC was significantly lower in an Australian avocado orchard (Cu residues of 280 and 340 mg kg^{-1}) than in an uncontaminated reference soil. The metabolic quotient increased in orchard soils compared to reference soils. These results indicate that the orchard soil microbial communities are experiencing environmental stressors and support the results of Merrington *et al*. (2002) who reported an increase in soil microbial metabolic quotient with increasing Cu concentration.

Our findings support the conclusion that the soil microbial community was being adversely affected by the presence of elevated concentrations of Cu resulting from the long-term use of copper based fungicides. Under long-term metal stress, the microbial community can undergo a change in genetic structure. (Giller *et al.* 1998). Zelles *et al.* (1994) measured soil microbial biomass, fatty acid pattern and poly-β-hydroxybutyrate content in agriculturally managed soils with different cropping histories: crop rotation, hops and grassland. Cu concentrations were highest in the hop yard soil, which contained a microbial community with markedly different characteristics compared to those of the crop rotation and grassland soils.

DDT has also been shown to be toxic to soil micro-flora (Foght *et al.* 2001). However as a significant correlation ($p<0.02$) was also observed between Cu and ΣDDT concentrations in pip and stonefruit orchard soils, it is more probable that copper rather than ΣDDT is impacting on the soil microbial community. Tate (1974) found that soil concentrations of DDT up to 100 ppm had no significant effect on respiratory activity in a New Zealand pasture soil.

Co-contamination of pip and stonefruit orchard soils with Cu and DDT appears to inhibit the degradation of DDT to DDE in orchard soils in two fruit growing regions of New Zealand. Two mechanisms are implicated in the slow rate of degradation of DDT to DDE in orchard soils: the presence of elevated Cu concentrations inhibiting microbial degradation and the constant grass cover preventing abiotic photochemical reactions. DDT and its degradation products are of environmental concern due to their persistence and ability to bioaccumulate. The implications of the findings presented in this paper are that the use of Cu as a fungicide may have made DDT even more persistent in orchard soils. The results also indicate that the ratio of DDE to DDT in orchard soils should not be used to establish recent (illegal) use of DDT. The findings presented in this paper are of international significance as they demonstrate that co-contamination of trace metals and persistent organic pollutants may have synergistic effects.

Acknowledgements

This project was funded by a grant in aid from Environment Waikato. The landowners are thanked for allowing access to their properties. Hill Laboratories are acknowledged for the trace element and organochlorine pesticide analyses. M Dexter and A Ghani (AgResearch) are acknowledged for their assistance with determining microbial biomass. A Burgess and N Foran (University of Waikato) are thanked for their assistance with sample preparation. SKG thanks the University of Waikato for a Doctoral Scholarship.

References

Aislabie J.M., Richards N.K. and Boul H.L. 1997. Microbial Degradation of DDT and its Residues-A Review. *New Zealand Journal of Agricultural Research* **40**, 269-282.

Blakemore L.C., Searle P.L, and Daly B.K., 1987. *Methods for chemical analysis of soils.* NZ Soil Bureau Scientific Report 80, New Zealand Soil Bureau, DSIR, Lower Hutt, New Zealand.

Boul H.L. 1995. DDT residues in the environment- a review with a New Zealand perspective. *New Zealand Journal of Agricultural Research* **38**, 257-277.

Elliott J.E., Martin P.A., Arnold T.W. and Sinclair P.H. 1994. Organochlorines and reproductive success of birds in orchard and non-orchard areas of central British Columbia, Canada, 1990-91. *Archives of Environmental Contamination and Toxicology* **26**, 435-443.

Foght J., April T., Biggar K. and Aislabie J., 2001. Bioremediation of DDT-contaminated soils: A review. *Bioremediation Journal* **5**, 225-246.

Gaw S.K. 2002. *Pesticide Residues in Horticultural Soils in the Auckland Region.* Auckland Regional Council Working Report No 96.

Gaw S.K, Palmer G., Kim N.D. and Wilkins A.L. 2003. Preliminary evidence that copper inhibits the degradation of DDE to DDT in pip and stonefruit orchard soils in the Auckland region, New Zealand. *Environmental Pollution* **122**, 1-5.

Giller K.E., Witter E. and McGrath S.P. 1998. Toxicity of heavy metals to microorganisms and microbial processes in agricultural soils: A review. *Soil Biology and Biochemistry* **30**, 1389-1414.

Harris M.L., Wilson L.K., Elliott J.E., Bishop C.A., Tomlin A.D. and Henning K.V. (2000) Transfer of DDT and metabolites from fruit orchard soils to american robins (turdus migratorius) twenty years after agricultural use of DDT in Canada. *Archives of Environmental Contamination and Toxicology* **39,** 205-220.

Hewitt A.E. 1998. *New Zealand Soil Classification***.** Manaaki Whenua Press, Canterbury, New Zealand.

Hitch R.K. and Day H.R. 1992. Unusual persistence of DDT in some Western USA soils. *Bulletin of Environmental Contamination and Toxicology* **48**, 259-264.

Holland P. and Solomona S. 1999. Copper status of orchards. *The Orchardist* **May 1999,** 44-45.

Kabata-Pendias A. and Pendias H. 2001. *Trace elements in plants and soils.* CRC Press.

Merry R.H., Tiller K.G. and Alston A.M. 1983. Accumulation of Cu, lead and arsenic in some Australian orchard soils. *Australian Journal of Soil Research* **21**, 549-61.

Merrington G., Rogers S.L. and Van Zwieten L. 2002. The potential impact of long-term copper fungicide usage on soil microbial biomass and microbial activity in an avocado orchard. *Australian Journal of* Soi*l Research* **40**, 749-759.

MfE 1998. *Reporting on persistent organochlorines in New Zealand*. Ministry for the Environment, Wellington.

Orchard V.A., Theng B.K.G., Searle P.L., Burke C.M., Parfitt R.L., Donnell D. and Harper S. 1991. *Interim Report on DDT residues in soil and experiments to enhance their degradation rates*. DSIR Land Resources Technical Record 58, DSIR Land Resources. Department of Scientific and Industrial Research. Lower Hutt, New Zealand.

Osborne G.O. 1976. *Insecticides*. In Ferro DN (Ed) New Zealand Insect Pests, Lincoln University College of Agriculture, Christchurch.

Roberts A.H.C., Cameron K.C., Bolan N.S., Ellis H.K. and Hunt S.D. 1996. *Contaminants and the soil environment in New Zealand*. In Naidu R., (Ed) Proceedings of the First Australasia-Pacific Conference on Contaminants and the Soil Environment in the Australia-Pacific Region held in Adelaide, Australia 18-23 February 1996.

Tate K.R. 1974. Influence of four pesticide formulations on microbial processes in a New Zealand pasture soil. *New Zealand Journal of Agricultural Research* **17**, 1-7.

Wan H., Higginson F.R, Harris C.R. and McDougall K.W. 1989. Organochlorine insecticide residues in soils used for vegetables and tropical fruit production in the Cudgen-Duranbah area of New South Wales. *Bulletin of Environmental Contamination and Toxicology* **42**, 177-180.

Zelles L., Bai Q.Y., Ma R.X, Rackwitz R., Winter K. and Beese F., 1994 Microbial biomass, metabolic activity and nutritional status determined from fatty acid patterns and poly-hydroxybutyrate in agriculturally managed soils. *Soil Biology and Biochemistry* **26**, 439-446.

Data worth analysis in remediation systems planning

Bürger, C., Finkel, M. and Teutsch, G.

Center for Applied Geoscience, University of Tübingen, Sigwartstrasse 10, 72076 Tübingen, Germany

e-mail: claudius.buerger@uni-tuebingen.de

In groundwater clean-up the importance of a proper design of the remediation system cannot be overstated. Due to our incomplete knowledge of the heterogeneous structure of the subsurface the issue of uncertainty plays a major role in the design process. To account for the uncertain spatial distribution of physical and chemical aquifer properties conditioned stochastic aquifer models can be used as a basis for groundwater flow and contaminant transport simulations during technical effectiveness assessments for remediation system designs. The technical effectiveness is then expressed as a level of system reliability. In practice, however, economic effectiveness is another crucial factor regarding the optimal choice of a remediation design. On the one hand, a high level of reliability might demand unfeasably high costs, on the other hand, the most inexpensive solution simply might be highly unlikely to do the job. Decision makers, therefore, are interested in the trade-off between total costs and remediation design reliability.

Obviously, the degree of uncertainty with respect to the significant aquifer properties is strongly related to the extent of site investigation. Therefore, provided that a remediation project has already undergone a first technical site investigation phase, the question whether an additional data collection program is worth the benefit from a reduction of uncertainty is central to the cost-effectiveness of the remediation measure as a whole (investigation, installation and operation). Hereby, it is important to notice that the objective of additional site investigation is not to reduce the uncertainty in the aquifer parameter distributions but to reduce the uncertainty in major cost driving parameters, like the total extraction rate in a pump-and-treat design. That is, a data collection program has to be found, that justifies a higher initial investment in site investigation by decreasing total costs of the remediation project through a reduction in parameter uncertainty. Figure 1 shows a typical example of cost-reliability trade-off curves before and after an additional data collection program.

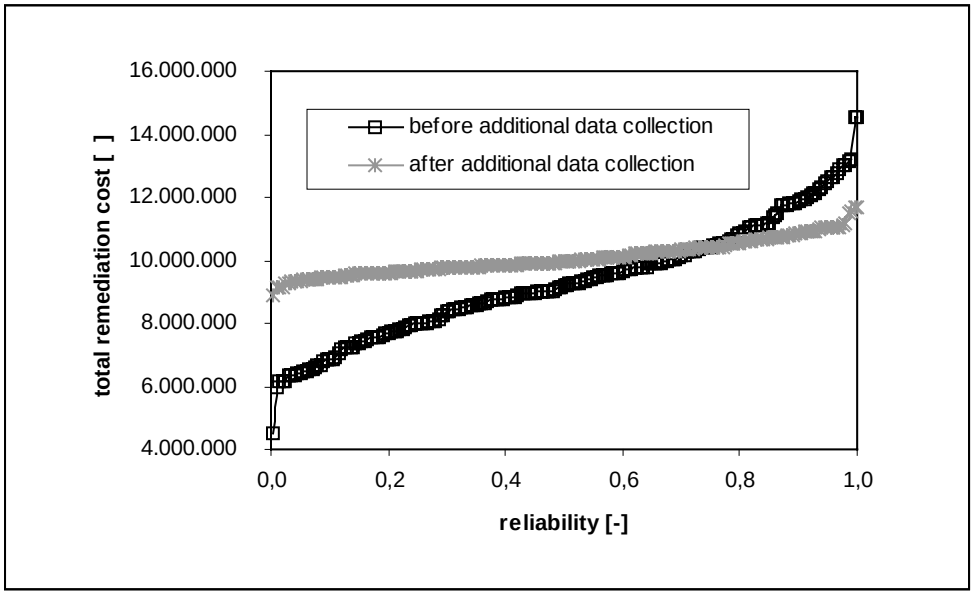

Figure 1: Cost-reliability trade-off curves before and after the completion of an additional data collection program for a single-well pump-and-treat system. It can be seen, that the investment for an additional collection program is cost-effective for required reliability levels higher than 0.75.

The cost-reliability curves are thought to be dependent on the true aquifer conditions, their computer model representation, the amount, the type and the location of collected data points relative to the remediation system. Economical parameters, in particular unit costs for obtaining additional point information and interest rates for discounting operation and maintenance costs, are additional decisive factors. Furthermore the sensitivity to uncertainty may differ between individual remediation technologies.
In this study, in view of the multidimensionality of the problem, we wish to focus on sensitivity analyses regarding the location and the amount of additional data points as well as economic factors. A hypothetical scenario of a single well pump-and-treat system is considered. Aquifer conductivity is represented by a three dimensional multi-Gaussian model with an exponential variogram.
In dependency of correlation length, variance and relative source zone - well geometry, the influence of the extent of a so-called area of interest (data collection area) on the distribution of minimal extraction rates achieving full advective source zone control is determined. The geometric set-up for this procedure is depicted in Figure 2. Additionally the influence of the amount of data collected inside a certain area of interest is investigated for different degrees of heterogeneity.

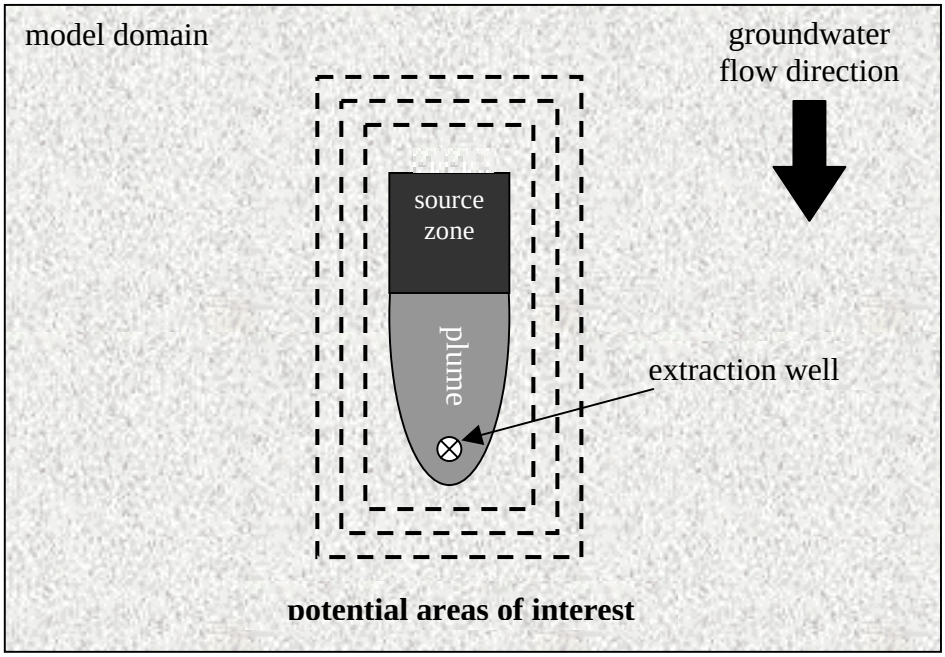

Figure 2: The geometric set-up of a single well pump-and-treat system with potential areas of interest for additional data collection. The heterogeneous aquifer structures (model domain) are shown for the purpose of illustration only and do not represent the correct scale.

The results show that based on the same unit costs certain unfavourable types of aquifer heterogeneity might justify amazingly large amounts of additional data. Especially the cases with a high variance and a very short correlation length demand extensive data collection programs. The results concerning the influence of the area of interest suggest, that depending on the degree of heterogeneity the area of data collection should encompass the whole area from the source zone to the well location. In fact, the area of interest should be sized at least larger than the width of the source zone and in many cases its length should be larger than the distance from the well to the upgradient boundary of the source zone.

Ph.D Flash Presentations:

FpS C
Remediation Technologies and Concepts

STIMULATED BIODEGRADATION OF CHLORINATED HYDROCARBONS IN BIOLOGICAL ACTIVATED CARBON BARRIERS

Misri Gozan*, Axel Müller*, Helmut Lorbeer[#], Peter Werner[#], Andreas Tiehm*
*Water Technology Center, Department Environmental Biotechnology
Karlsruher Str. 84, 76139 Karlsruhe, Germany
Phone +49/(0)721 9678 223; Fax +49/(0) 9678 101; gozan@tzw.de**,** tiehm@tzw.de
[#]Dresden University of Technology, Institute for Waste Management and Contaminated Sites Treatment, Pratzschwitzer Str. 15, 01796 Pirna, Germany

Keywords:
Activated carbon; biobarrier; bioregeneration; chlorobenzene; chloroethenes; dechlorination

SUMMARY

Biodegradation of chlorinated hydrocarbons in activated carbon barriers was studied in order to develop a long lasting subsurface barrier for groundwater remediation, wherein pollutant adsorption and biodegradation occur simultaneously.

Chlorobenzene (CB) was used to study the bioavailability of contaminant adsorbed on granular activated carbon (GAC) in a batch system. In sequential anaerobic/aerobic columns, trichloroethene (TCE) and chlorobenzene were used as model pollutants. The first GAC barrier was operated under anaerobic conditions with sucrose and ethanol as auxiliary substrates. The second barrier was operated with addition of hydrogen peroxide and nitrate.

The results obtained in the batch and continuous systems demonstrated the availability of adsorbed contaminants for biodegradation. A delay in biological activity was observed in batch experiments, related to high amounts of GAC addition. However, this effect did not appear in the column experiment and proved to be insignificant with regard to the time frame of biobarrier operation.

In the sequential anaerobic/aerobic column system, initially elimination of TCE and CB occurred by adsorption. In later periods, a practically complete conversion of TCE to lower chlorinated metabolites, predominantly *cis*-dichloroethene (*cis*-DCE), was obtained. Mass balances validated this reductive dechlorination process. The anaerobic dechlorination was stable, although the concomitant sulphate-reducing and methanogenic processes varied considerably. In the second column operated with oxygen/nitrate addition, dechlorination was limited by oxygen and restricted mainly to CB biodegradation. Increasing oxygen levels led to an almost complete biodegradation of CB.

In conclusion, results demonstrate the feasibility of the sequential anaerobic/aerobic biological activated carbon barrier concept. The pre-sorbed pollutants were available for subsequent biodegradation resulting in a bioregeneration of the activated carbon barriers. The dechlorination processes can be stimulated and controlled by the addition of auxiliary substrates and terminal electron acceptors.

INTRODUCTION

Many abandoned chemical industry areas in the world, such as the large Bitterfeld megasite, Germany, are contaminated with cocktails of chlorinated pollutants. Passive reactive walls represent innovative approaches for the cost-effective remediation of contaminated groundwaters. Driven by the natural groundwater gradient, the groundwater transports the pollutants through reactive zones where elimination occurs. In our concept, the processes of sorption and biodegradation are integrated in order to achieve a longer operation period as compared to elimination by adsorption only.

Adsorption reversibility is a prerequisite for the biodegradation in the activated carbon barriers to occur. The type of activated carbon, the physicochemical properties of the pollutants, and the contact time are important parameters affecting the availability of contaminants to microbial decomposition (DeJonge *et al.*, 1992; Dobrevski and Zvezdova, 1991; Orshansky and Narkis, 1997; Walker and Weatherly, 1998).

TCE is degradable under anaerobic conditions and mostly reported via *cis*-dichloroethene (*cis*-DCE) and vinyl chloride (VC) to ethene. The dechlorination rate of TCE to *cis*-DCE is faster than *cis*-DCE to VC and ethene (Schöllhorn *et al*., 1997; Middeldorp *et al*., 1999). The lower chlorinated metabolites, *cis*-DCE and VC, are biodegradable also under aerobic conditions. Both under anaerobic (Middeldorp *et al*., 1999) and aerobic (Fetzner, 1998) conditions, auxiliary substrates are required for the dechlorination of chloroethenes. H_2 was demonstrated to be the direct electron donor for reductive dechlorination that was observed under sulfidogenic, methanogenic or fermentative conditions (Freedman and Gossett, 1989; Maymó-Gatell *et al*., 1995; Middeldorp *et al*., 1999). Under aerobic conditions, co-metabolic oxidation of *cis*-DCE and VC is catalized by several mono- and dioxygenase systems (Fetzner, 1998). Tiehm *et al*. (2002) demonstrated and discussed various suitable auxiliary substrates for dechlorination of *cis*-DCE and VC, including methane, ethene, toluene, sucrose, ammonium and benzene. CB is degraded without auxiliary substrates, but more rapidly in the presence of molecular oxygen (Nishino *et al*., 1992). Therefore, a sequential anaerobic/aerobic treatment is applied in order to degrade the model pollutant mixture.

This paper focuses on the biodegradation of the model pollutants trichloroethene (TCE) and chlorobenzene (CB), representing important classes of environmental contaminants. The works presented were done to examine (i) the bioavailability of the pollutants pre-sorbed on activated carbon, and (ii) the effect of auxiliary substrates and electron acceptors on dechlorination.

METHODS

Influence of GAC on bioavailability of chlorobenzene under aerobic condition

This experiment was carried out in a Sapromat D12 (Voith), that measures the oxygen utilised by aerobic microorganisms in a closed system. Mineral medium (Tiehm *et al*., 2001) was supplemented into a 1000-ml vial with Hungate seal. The microorganisms were enriched from contaminated groundwater obtained from the Bitterfeld site, and added to the medium as inoculum. Afterwards, 30 µl chlorobenzene were injected as the only carbon source. Beside the active vial set, a sterile set was run as reference (pH reduction was achieved by phosphoric acid addition). Different amounts of granular activated carbon (GAC) were degassed and added to the flasks. Incubation was done at 14°C.

Biobarrier experiments

Anaerobic and aerobic columns were assembled in laboratory (Fig. 1) to study adsorption and biodegradation of the model contaminants. Both columns were filled with Filtrasorb GAC TL 830 (Chemviron Carbon, Belgium). To remove fines, the GAC was washed in demineralised water, followed by drying at 105^{o}C. During the pre-loading period, the flowrate to the column varied from 50 to 90 L/d. Subsequently, the flowrate to the column was adjusted to approx. 4 L per day, followed by injection of bacterial mixed cultures enriched on TCE and CB. To examine the influence on biodegradation of the chlorinated model contaminants, the concentration of auxiliary substrates (1-50 mg/L DOC) added to the anaerobic column, and of H_2O_2 (10-140 mg/L) added to the second column were varied. To study the adsorption-only conditions, a sterile set of columns (continuous NaN_3 additon) was operated.

The mineral medium flowed through a 30 m silicon tube in Na_2SO_3 liquid to eliminate dissolved oxygen before entering a mixing bottle together with the model pollutants. The contaminant mixture of TCE, CB and benzene in volume ratio of 21.8:44.0:34.2 was introduced to the mixing bottle at a rate of 0.03 mL/h. All the contaminants were products of Fluka Co. and had a purity ≥ 99.5%. Ethanol (pa ≥ 99.8%, Merck Co.) and sucrose (microbiology purpose, Merck Co.) were added to favour reductive dechlorination of the chloroethenes in the anaerobic zone. Mixed with the auxiliary substrates, vitamins (Böckle, 1999) were supplied. H_2O_2 and $NaNO_3$ (Merck Co., 30% and ≥ 98% respectively) were added to stimulate biodegradation under aerobic-denitrifying conditions.

Analytical methods

Pollutant and methane analysis was performed by a gas chromatograph from Hewlett Packard (HP Series II 5890) equipped with a head-space autosampler, flame ionisation detector (FID) and electron capture detector (ECD). Separation was accomplished in a 50-m capillary column (PONA id 0.21 mm, methyl silicon film 0.5 µm thickness, Hewlett Packard). Sulphate and chloride concentrations were determined with an ion chromatograph (2010I Dionex) with suppression system and conductivity detector. Measurements of redox potential and pH were done regularly with a multimeter (pH 91 WTW). Determination of dissolved O_2 was carried out with an O_2 electrode and an Oximeter instrument (Oxi 330-WTW). H_2O_2 level was monitored with peroxide test strip (Merck).

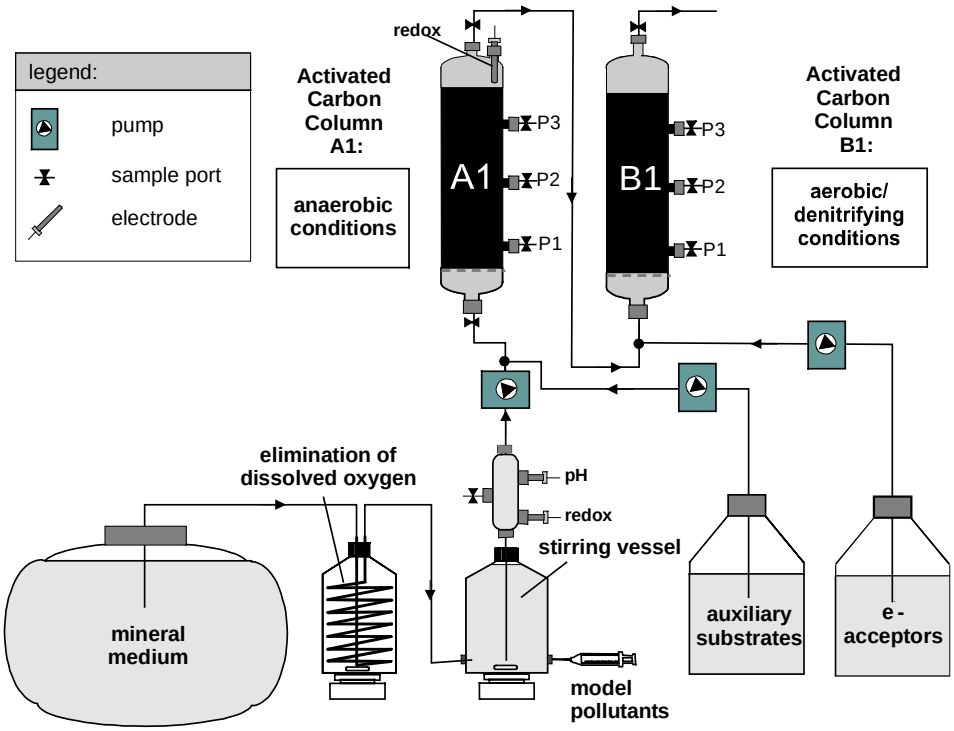

Figure 1. Sequential anaerobic and aerobic GAC biological columns for elimination of chlorinated hydrocarbon. Column dimension: volume 0.164 L, porosity ca. 57%, ϕ 3.5 cm and h 17 cm.

RESULTS AND DISCUSSION

Effect of GAC on Bioavailability

The effect of activated carbon on the bioavailability of chlorobenzene (CB) was investigated in the respirometer. Previous tests by Tiehm et al. (2000) showed no significant effect of adsorption on the bioavailability of chlorobenzene in the presence of low GAC concentrations (0.033 to 0.333 g GAC/L). However, at higher amounts of 1.3 to 13 g/L GAC significantly lower respiration rates were observed (fig. 2). Similar observations have been reported in studies performed with other hydrophobic pollutants (De Jonge *et al*., 1996; Orshansky and Narkis, 1997)

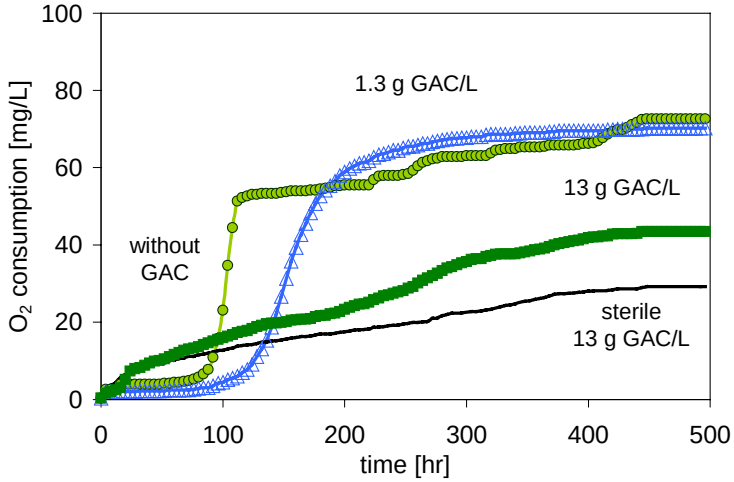

Figure 2. Oxygen consumption of chlorobenzene utilising microorganisms in the presence of granular activated carbon (GAC).

Anaerobic Dechlorination

After elimination of TCE by adsorption in the initial phase (up to 150 l throughput) of the column experiments, biological dechlorination of TCE to cis-DCE started (Fig. 3A). The formation of *cis*-DCE exceeded significantly the TCE influent concentration for about 40 d. Afterwards (100 – 180 d), the mixed culture transformed the influent TCE into *cis*-DCE stoichiometrically.

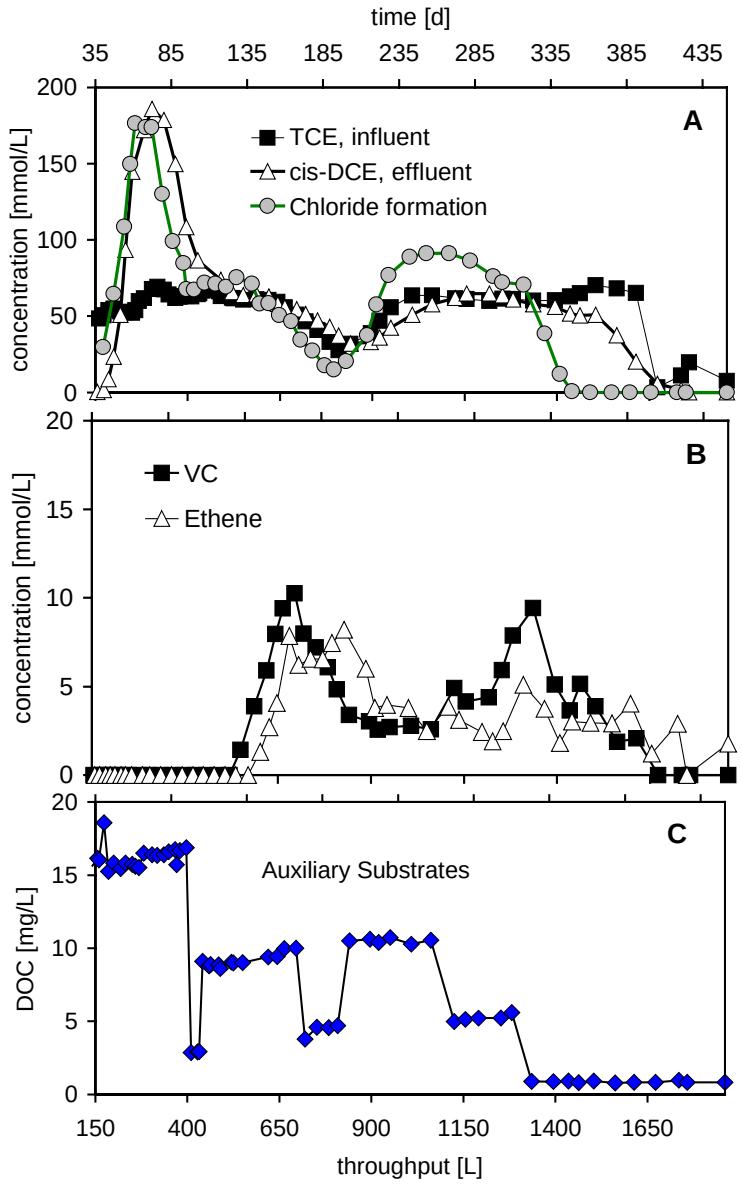

Figure 3. Dechlorination of trichloroethene in the anaerobic column: (A) formation of *cis*-DCE and chloride, (B) further dechlorination to vinyl chloride (VC) and ethene, and (C) addition of auxiliary substrates (ethanol and sucrose).

The chloride peak preceded the *cis*-DCE peak due to a moderate retention of *cis*-DCE on activated carbon (Fig. 3A). This effect was observed again when the contaminant influent concentration was gradually reduced (between 600-800 L throughput) or increased (between 800-960 L throughput), and when reductive dechlorination decreased due to a lack of auxiliary substrates (after 1340 L throughput). Further degradation of *cis*-DCE to VC started after 510 L throughput followed by ethene formation (Fig. 3B). However, the low concentration of VC, about a tenth of *cis*-DCE produced, pointed to a much slower rate of VC formation compared with TCE to *cis*-DCE kinetics. Varying concentrations of sucrose and ethanol (Fig. 3C) in the range of 5-50 mg/L DOC (between 140 and 1340 L throughput) did not affect dechlorination. However, reductive dechlorination decreased after 1340 L throughput as a result of further reduction of the auxiliary substrates to 1 mg/L DOC.

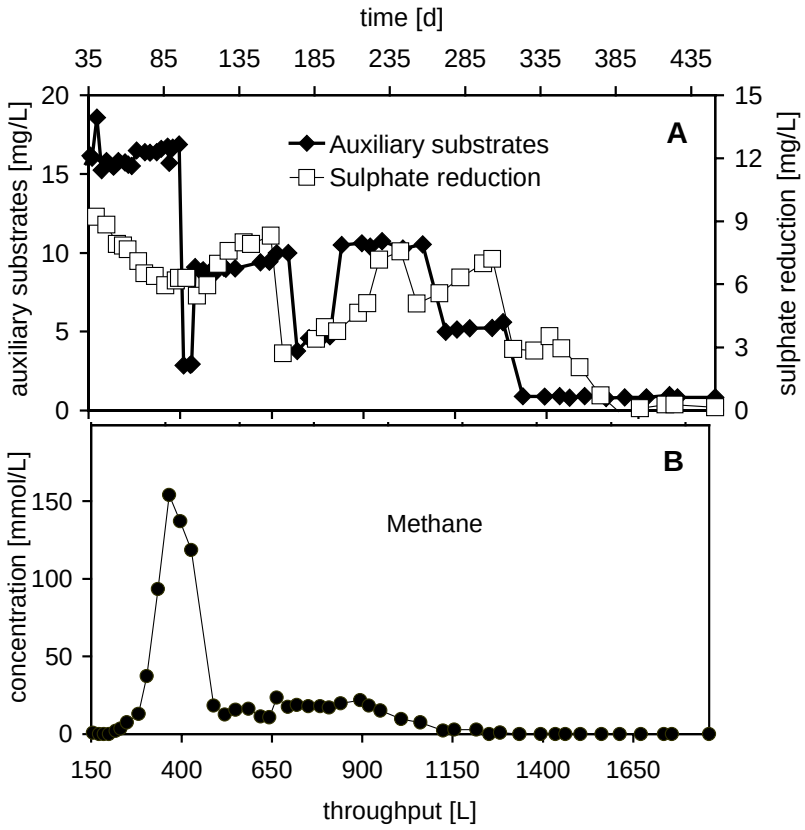

Figure 4. (A) Sulphate reduction and auxiliary substrate (B) methane formation

The redox potential in the anaerobic column was approximately -100 mV. Both methanogenesis and sulphate reduction were observed (Fig. 4A and B). The reduction of sulphate was most pronounced in the initial phase. Later on, sulphate reduction altered, affected by auxiliary substrate reduction, but continued to exist throughout the experiment. On the contrary, the methanogenic activity significantly declined after 425-L throughput and completely ceased after 1100-L throughput. Notably, the reductive dechlorination processes were stable although the microbial community varied significantly.

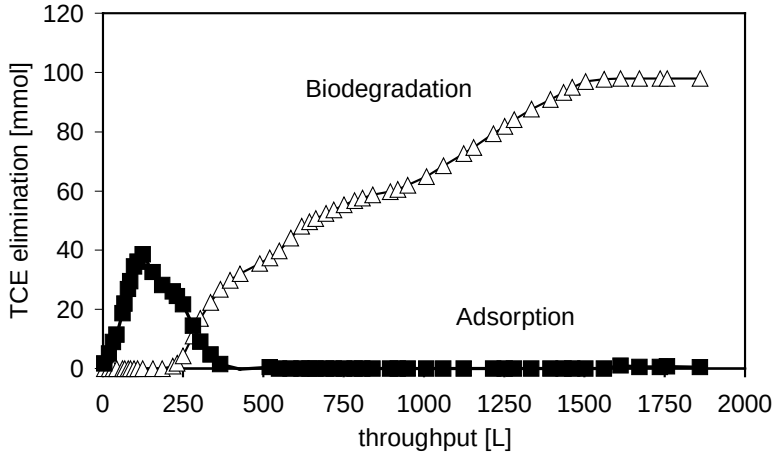

Figure 5. Elimination of trichloroethene in the GAC anaerobic column due to adsorption and biodegradation.

The mass balance revealed a complete bioregeneration of the TCE-loaded GAC, demonstrating a sufficient bioavailability of the pre-sorbed TCE. The curves in figure 5 were prepared based on the mass balance of routine measurements of TCE in the influent and effluent. Initially, TCE was eliminated by adsorption. After the onset of microbial TCE dechlorination, the TCE-loaded GAC was regenerated, and subsequent TCE elimination was due to biodegradation only. Thus, the adsorption capacity available for the elimination of other pollutants was increased.

Aerobic Dechlorination

The aerobic stage is aimed to eliminate CB as well as to further decompose the metabolites from TCE degradation. H_2O_2 and nitrate were added as electron acceptors. In order to avoid toxic effects, the concentration of H_2O_2 was increased gradually from 10 mg/L up to 100 mg/L. At low concentrations of H_2O_2/oxygen, no biodegradation of CB was observed. Obviously, the remaining organic compounds, added in the anaerobic column as auxiliary substrates, consumed most of the available oxygen. Aerobic dechlorination started after increasing the H_2O_2 level to 40 mg/L. Further increments to 100 mg/L H_2O_2 clearly improved dechlorination. The short decrease of hydrogen peroxide after 600-L throughput resulted in an immediate drop of chloride formation (Fig. 6A). On the contrary, a rapid and temporary rise on H_2O_2 supply (140 mg/L) significantly enhanced the chloride release, indicating higher activity of CB-degrading microorganisms.

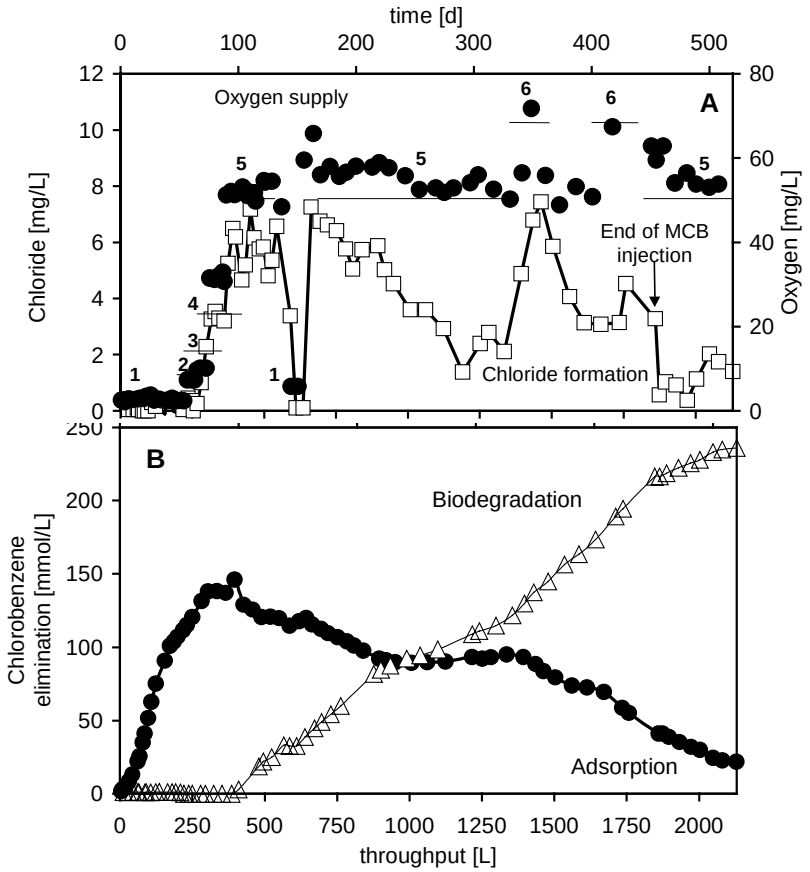

Figure 6. Effect of oxygen supply (A) on chloride released in the activated carbon column and (B) on bioregeneration of the chlorobenzene-loaded activated carbon. The notations 1 to 6 indicate levels of 5, 15, 20, 30, 50, and 70 mg O_2/L, respectively.

Differences between influent and effluent concentrations of *cis*-DCE and VC were first observed after 900-L throughput. However, in the column system the contribution of dechlorination of the TCE daughter products to the overall formation of chloride was low (data not shown) and chloride formation was attributed predominantly to CB degradation.

Most of the oxygen added as H_2O_2 was consumed in front of Port 2 of the column. Nitrate was available also in the upper parts of the column but obviously did not support CB degradation. Therefore, chloride formation decreased after 700-L throughput because the GAC up to Port 2 was already regenerated and bioregeneration beyond Port 2 was limited by oxygen availability. Also after about 700 L throughput, there was a shift in electron acceptor utilisation for the degradation of the remaining auxiliary substrates added in the anaerobic column: nitrate utilisation decreased and oxygen consumption increased. In order to further stimulate aerobic dechlorination, addition of sucrose and ethanol to the anaerobic column was reduced after 1280 L (Fig. 3C) throughput and addition of hydrogen peroxide was increased temporarily. The immediate increase in chloride formation demonstrated the important role of oxygen.

The mass balance with regard to CB is presented in figure 6B. In the initial phase, CB was eliminated by adsorption on GAC. Bioregeneration of the loaded GAC started after 300-L throughput when H_2O_2 addition was increased, thus demonstrating a sufficient bioavailability of the pre-sorbed CB. This result might look contradictory to the batch respirometer test (Fig. 2). But it has to be noted that the time scales of the batch and column experiments are different. The columns were operated for more than one year, rather than hours in batch experiments. Thus, contaminant bioavailability should not be a critical factor for biobarrier application in the field.

CONCLUSION

Results so far demonstrate the feasibility of the sequential anaerobic/aerobic activated carbon barrier concept for the removal of pollutant mixtures such as trichloroethene/chlorobenzene. In general, the integrated activated carbon/microbiological treatment exhibits the following advantages:

- As compared to the aquifer without a reactive wall, groundwater remediation is easier to control and to stimulate since pollutants and microorganisms accumulate in a small volume.
- The activated carbon is continuously or periodically regenerated resulting in a longer operation period as compared to adsorption only.

It has been shown in batch experiments with chlorobenzene that the rate of biodegradation can be reduced in the presence of activated carbon, indicating a reduced bioavailability. However, in the long-term operation a complete bioregeneration of the TCE and CB loaded GAC was achieved in the anaerobic and aerobic columns, respectively.

ACKNOWLEDGEMENT

This study is a part of the SAFIRA research programme, funded by the German Ministry of Education and Research (BMBF No. 02WT9937/7). Misri Gozan gratefully acknowledges a scholarship of the German Academic Exchange Service (DAAD).

REFERENCES

Böckle K. (1999). Praxisorientierte Untersuchungen zur mikrobiellen reduktiven Dechlorierung von leichtflüchtigen chlorierten Kohlenwasserstoffen (LCKW). Reports of the Water Technology Center No. 7, DVGW-TZW, Karlsruhe (in German).

De Jonge, R., Breure, A.M., Van Andel, J.G. (1992) Bioregeneration of powdered activated carbon (PAC) loaded with aromatic compounds. *Wat. Res.* **30**(4): 875-882.

Dobrevski, I., Zvezdova, L. (1991) Biological regeneration of activated carbon. *Appl. Environ. Microbiol.* **57**(8) : 2287-2292.

Fetzner S. (1998). Bacterial dehalogenation. *Appl. Microbiol. Biotechnol.* **50**: 633-657.

Freedman D.L., Gossett J.M. (1989). Biological reductive dechlorination of tetrachloroethylene and trichloroethylene to ethylene under methanogenic conditions. *Appl. Environ. Microbiol.* **55**: 2144-2151.

Maymó-Gatell X., Tandoi V., Gossett J.M., Zinder S.H. (1995). Characterization of an H_2-utilizing enrichment culture that reductively dechlorinates tetrachloroethene to vinyl chloride and ethene in the absence of methanogenesis and acetogenesis. *Appl. Environ. Microbiol.* **61**: 3928-3933.

Middeldorp P.J.M., Luitjen M.L.G.C., van de Pas B.A., van Eekert M.H.A., Kengen S.W.M., Schraa G., Stams A.J.M. (1999). Anaerobic microbial reductive dehalogenation of chlorinated ethenes. *Bioremediation J.* **3**(3): 151-169.

Nishino S.F., Spain J.C., Belcher L.A., Litchfeld C.D. (1992). Chlorobenzene degradation by bacteria isolated from contaminated groundwater. *Appl. Environ. Microbiol.* **58**: 1719-1726.

Orshansky, F., Narkis, N. (1997) Characteristics of organic removal by PACT simultaneous adsorption and biodegradation. *Wat. Res.* **31**(3): 391-398.

Schöllhorn A., Savary C., Stucki G., Hanselmann K.W. (1997). Comparison of different substrates for the fast reductive dechlorination of trichloroethene under groundwater conditions. *Wat. Res.,* **31**(6): 1275-1282.

Tiehm A., Gozan M., Müller A., Böckle K., Lorbeer H., Werner P. (2001). Biological activated carbon barriers for the removal of chloroorganics/BTEX mixtures. *In*: Proceed. of the 6th Int. Symposium In Situ and On-Site Bioremediation, 4-7 June 2001, San Diego, California, pp. 105-112.

Tiehm, A., Gozan, M., Müller, A., Schell, H., Lorbeer, H., Werner, P. (2002) Sequential anaerobic/aerobic biodegradation of chlorinated hydrocarbons in activated carbon barriers. *Water Science and Technology: Water Supply* **2**(2): 51-58.

Tiehm A., Schulze S., Böckle K., Müller A., Lorbeer H., Werner P. (2000). Elimination of chloroorganics in a reactive wall system by biodegradation on activated carbon. *In*: Proceedings of the 7th International FZK/TNO Conference on Contaminated Soil, 18-22 September 2000, Leipzig, Thomas Telford Publ., 924 – 931.

Walker, G.M. and Weatherley, L.R. (1998) Bacterial Regeneration in Biological Activated Carbon Systems, *Trans IChemE*, Vol **76**(B), 177-182.

PHOTOCATALYTIC REMEDIATION OF MTBE IN GROUNDWATER

[1]CHAN, May S.M. and [2]LYNCH, Rod J.

[1]&[2]Cambridge University Engineering Department, Trumpington Street, Cambridge, CB2 1PZ, UK

[1]Tel: +44 (01223) 766683 [2]Tel: +44 (01223) 766683 [1]&[2]Fax: +44 (01223) 339713

[1]msmc3@eng.cam.ac.uk [2]rjl1@eng.cam.ac.uk

Abstract

Contamination of groundwater by MTBE poses serious environmental problems and economical losses to water companies. Remediation methods of MTBE, such as air-stripping and biodegradation, have been proven inefficient. Photocatalysis is an advanced technology for remediation of MTBE.

This paper investigates the feasibility of using a supported-catalyst reactor for photocatalytic degradation of MTBE in water. Titanium dioxide (Degussa P25) was used as catalyst in experiments and it was supported onto the internal wall of the reactor (glass) by coating and heating to high temperature (400^{o}C). The reactor is cylindrical in shape, in which uniform light illumination onto catalyst surface can be achieved. The results show that photocatalytic degradation of MTBE follows first-order kinetics. In batch experiments, the rate constants (k) of reactors of different diameters were found and used to predict photocatalytic degradation efficiency in flow experiments.

Some flow experiments were also conducted. The efficiency of MTBE degradation has been investigated with cylindrical reactors of different sizes and various flow rates. The ratio between the outlet and inlet concentrations (C_{out}/C_{in}) was found to approach a constant when there is a constant flow (Q) through the photocatalytic reactor. The log of this ratio, $\ln(C_{out}/C_{in})$, was proportional to V*k/Q, where Q is the flow rate, k is the batch rate constant of the reactor and V is the volume of the reactor. The results were also compared to the ideal values deduced from $C_{out}/C_{in} = e^{-V*k/Q}$. It was found that the MTBE concentration reduction obtained at the reactor outlet in flow experiments are always less then the ideal values predicted from batch experiments. $\ln(C_{out}/C_{in})$ roughly equals 0.77 of V*k/Q.

In general, the photocatalytic degradation efficiency was convincing. As much as 99% of degradation of MTBE was achieved in 40 hr with a UVA light intensity input of 4.5 mW/cm^2 in a batch experiment of reactor volume 292 ml. With the same reactor and input light intensity, the MTBE concentration of outlet to inlet was measured as 61% in a circulation flow of 40 ml/hr. Complete degradation of MTBE, in which no intermediates were observed, was achieved with excess supply of oxygen.

Keywords: photocatalysis, MTBE, supported-catalyst reactor

Introduction

Methyl tert-butyl ether (MTBE) has been used as a replacement of anti-knocking agent of leaded compounds in petroleum since 1970s. MTBE possesses a distinct odor which can be easily detected by humans even at trace quantities (sub ppb levels). It is believed that the legislation on controls of the groundwater pollutants, particularly MTBE, will be tightened in the future. However, the production and consumption of MTBE are still increasing in Europe [1,2]. These are likely to result in more contaminated sites that require remediation in the future.

The Henry's law constant is relatively low, compared to other common organic pollutants, like BTEX (benzene, toluene, ethylbenzene and xylenes). This indicates low extractability by air-stripping. MTBE is also characterized by its high solubility and low retardation. When MTBE enters groundwater, it usually migrates at the same speed as the water flow and partitions weakly to the organic fraction in soil. The chemical stability and resistance to biodegradation of MTBE are also

responsible for its persistence in the environment. Once released from an underground source, MTBE has a high potential to leach extensively and rapidly into the groundwater [3,4].

Photocatalysis is a chemical process in which MTBE and other organic pollutants can be broken down to simpler compounds [5,6]. Recent studies suggested that it is a promising remediation technology for a wide range of organics, including aromatics and chlorinated compounds [5,6,7]. Photocatalytic oxidation of organics occurs in the presence of the catalyst, light and oxygen. Titanium dioxide (TiO_2) is the most widely used catalyst in photocatalysis as it is safe, economical and easily available. TiO_2 has a band gap energy of 3.2 eV and only ultra-violet light of 387 nm or shorter wavelength will has sufficient energy to promote the reaction [5]. In photocatalysis, organic pollutants are actually degraded, whereas in other traditional methods, such as air-stripping and carbon adsorption, the organics pollutants are only transferred from groundwater to another medium [3,4].

There are two main types of photocatalytic reactors for degradation of organics in water: slurry-catalyst reactors and supported-catalyst reactors [8]. In slurry-catalyst reactors, the catalyst, TiO_2, is mixed with the contaminated water to form a slurry. TiO_2 has to be separated from the decontaminated water, usually by filtration, after photocatalytic reactions. In supported-catalyst reactors, TiO_2 is fixed onto a structural surface, such as glass mesh or optical fibre, which eliminates the need for recovery of catalyst by filtration or other methods after treatment [9]. Moreover, it is difficult to achieve a uniform light intensity on all catalyst surfaces in a slurry-catalyst reactor and the white TiO_2 itself is a shielding to the light. This is suspected to be the reason that photocatalytic degradation efficiency falls when the catalyst loading excesses an optimum. One example of a supported-catalyst reactor is one containing optical fibres coated with catalyst, in which the light is also transmitted by the optical fibres. The pollutants must diffuse through the catalyst coating to the fibre surface to receive the light. In this case, the reaction rate is controlled by diffusion, which is a slow process compared to photocatalytic degradation [10,11,12].

The photocatalytic reactor described in this paper is a supported-catalyst reactor with cylindrical shape. In this reactor, both the light and the pollutants approach the catalyst from the same direction which avoids the reaction rate being controlled by diffusion through the catalyst layer. TiO_2, is coated on the internal wall of the reactor and the ultra-violet light source is place in the centre, which results in uniform light intensity at all catalyst surfaces.

The photocatalytic degradation efficiency will be governed by both the disappearing rate of MTBE and also the completeness of reaction (i.e. the amount of intermediates generated).

Experimental and Analytical Methods

The layout of the reactor is shown in Figure 1. The reaction vessel is a glass cylinder. In batch experiments, the inlets were for feeding in water before experiments and draining samples out during experiments. The experimental set-up is illustrated in Figure 2. The air inlet was connected to a compressor, via a pressure regulator, for continuous supply of excess air (oxygen) to the solution. The air outlet avoids building up of high pressure within the reactor. The flow of air also generates some bubbling effect to facilitate stirring inside the reactor. The air outlet was connected to fume cupboard exhaust. The reservoir was only used in flow experiments but not batch experiments. In flow experiments, water was continuously circulated between the reservoir and the reactor. The flow rate was controlled by the pump between the reservoir and the inlet of the reactor.

A fluorescent tube (Philips CLEO Compact 15W) was used as the UV light source for photocatalytic reaction. The spectrum of this light source is shown in Figure 3. The lamp was placed in the center of the cylindrical section to achieve uniform radiation on the catalyst surface. The source of light is mainly between wavelength 320 to 380 nm (UVA), which provides sufficient energy to overcome the band gap energy of TiO_2. There is no UV light below 300 nm and photolysis cannot happen. Therefore, all the degradation of pollutants should be resulted from photocatalysis rather than photolysis. An in-house designed UV sensor, which was calibrated against standard light source, was used for measuring light intensity to ensure it is constant throughout an experiment. The intensity of UV light (with UV light between 300 to 400 nm, excluding the visible light above 400 nm) of a new lamp is about 4.5mW/cm^2 on the lamp surface, which was the same in all experiments. Depreciation of UV light with lamp lifetime was often reported by previous reserchers. The lifetime of full output of

each lamp is about 100 hr as recommended by the manufacturer and the lamp was replaced every two experiments. Depreciation of the power output of the lamp was not observed during experiments.

The inner wall of the cylinder was coated with catalyst, TiO_2. TiO_2 (Degussa P25) was obtained from Degussa in the form of fine powder. A thin slurry suspension of TiO_2 in water, with 20% weight of TiO_2 forms the coating. Lumps of TiO_2 can be eliminated by grinding the slurry in mortar and pestle and adding several droplets of dilute nitric acid to the mixture. The slurry was deposited onto the inner wall of the cylinder and spread evenly with a glass rod. The coated cylinder was left on an electrical roller for drying. The continuous rolling of the cylinder can help to avoid the TiO_2 sliding to the bottom so that a more even thickness of the coating can be formed. After drying, the coated cylinder was heated to 400 ^oC for 30 min in a furnace and cooled naturally to ambient temperature. The coating and heating processes were repeated once before the coated cylinder can be used for the experiment. A new TiO_2 coating was used in each experiment.

All the MTBE solution used in experiments was prepared by mixing pure MTBE with deionised water (laboratory standard) and left for 12 hr for complete and uniform solution. During the experiments, samples of 1 ml were taken and stored in 2 ml vials. This created a 1 ml head space and the samples were left for several hours before analysis to ensure that equilibrium between the vapor phase and the liquid phase has been reached. Analysis of MTBE was done by a gas chromatograph with flame ionization detector (GC/FID). Vapor injection of 50µl of the 1ml head space was used. The GC system is an Agilent Model 6850. The retention time of MTBE is 0.915 min in a 2 min run at temperature 70 ^oC. In batch experiments, samples were drained out from the reactor. For flow experiments, in which circulation of water between the reactor and the reservoir continues, samples were always taken at both the inlet and outlet of the reactor.

Each experiment consists of two stages. In the first stage (light-off stage), the UV light was not turned on. The light-off stage allows adsorption of MTBE solution onto the catalyst surface and this stage is indicated by the gradual decrease in concentration in the reaction vessel. When the adsorption of MTBE had saturated, the second stage (light-on stage) began. The UV light was turned on and air was continuously supplied to the reactor. In flow experiments, the pump was only turned on in the light-on stage.

Results and Discussions

The result of a batch experiment using a reactor of 48.2 mm in diameter and 180 mm in length is shown in Figure 4. It shows the change of MTBE concentration, normalized by the initial concentration 100 ppm, with time. In the light-off stage, the MTBE concentration falls from initially 100 ppm to about 69 ppm in 7 hr. In the light-on stage, the MTBE concentration decreases to less than 1% in 40 hr. First order kinetics ($C = C_o * e^{-k*t}$ where C is the instantaneous concentration, C_o is the initial concentrations, k is the rate constant and t is time after light-on) was observed in photocatalytic degradation of MTBE in the presence of UV light and catalyst with rate constant of 0.1144 hr^{-1}. The results of two control experiments are also presented in Figure 4. In one control (no catalyst / no light), the reactor was not coated with catalyst and the lamp was covered with foil to deliver only heat but no UV light to the MTBE solution. About 17 ppm of MTBE was lost in the in the light-off stage and a further 15 ppm was lost in the light-on stage due to evaporation to the airflow. Another control (catalyst / no light) was done with the reactor coated with catalyst but again, the lamp is covered to avoid illumination of light to the catalyst. About 34 ppm was lost in the light-off stage, and a further 13 ppm in the light-on stage. Comparing the photocatalytic experiment and the two controls, it is clear that the reduction of MTBE concentration in a photocatalytic experiment is a resultant of photocatalytic reaction, adsorption to the catalyst and loss to the airflow. The effect of photocatalytic reaction is the most significant among the three.

Figure 5 shows the results of three batch experiments, using exactly the same reactor (48.2 mm diameter) and light intensity but different initial concentrations of MTBE. For initial concentrations of 10 ppm, 100 ppm and 1000 ppm, the adsorption of MTBE to the catalyst in the light-on stage were 35%, 31% and 36%, respectively. The adsorption of MTBE is a certain proportion of the initial concentration instead of a certain amount. Three straight lines on a log(concentration)-time scale indicates they all obey the first order kinetics in this range of concentration. They have very similar reaction rate constants, 0.114 hr^{-1}, 0.114 hr^{-1} and 0.115 hr^{-1}.

Using the same UV lamp as light source, the effect on photocatalytic reaction rate for different reactor diameters was also investigated. The plots in Figure 6 suggest that the reaction rate, k, decreases with increasing diameter of the reactor, D. The effects of light intensity and reactor diameter on reaction rate are further investigated and discussed in [16]. The reaction rate constants of all batch experiments are summarized in Table 1. These batch rate constants, k, for reactors of different diameters, D, will be used in the discussion of the flow experiments below.

The result of a flow experiment is shown in Figure 7. The reactor (48.2 mm in diameter, 180 mm in length and a 16 mm diameter UV lamp in the center) has a volume of 292 ml and the total volume of the whole system (reactor plus reservoir) was 1000 ml flow. Figure 7 shows the change of MTBE concentration, normalized by the initial concentration 100 ppm, with time at inlet and outlet of the reactor. Sample represents the system with photo catalytic reaction and Control represents another set-up in which the UV lamp was covered. In the light-off stage, there was no circulation between the reactor and the reservoir. The Sample outlet and Control outlet data represent the concentration of solution inside the reactor. In the light-on stage, constant circulation of 40 ml/hr occurred and the inlet and outlet of the reactor had different concentrations. It can be seen in Figure 8 that this ratio, C_{out}/C_{in}, in the Sample approaches a constant of 0.61.

When a different size reactor was used, the reservoir volume was changed to keep the total volume of the reactor and reservoir was the same, i.e. 1000 ml in all flow experiments. In a photocatalytic reaction with constant flow, it was found that the ratio between outlet and inlet concentrations, C_{out}/C_{in}, approaches a constant value. Table 2 is a summary of the C_{out}/C_{in}, the volume of the reactor (V), the batch rate constant of the reactor (k) and the flow rate (Q) values of different experiments. The value of V/Q represents the average time the MTBE solution would stay in the reactor in each pass through the reactor. As we have already shown that photocatalytic degradation of MTBE follows the first order kinetics ($C = C_o*e^{-k*t}$), it can be deduced that $C_{out}/C_{in} = e^{-V*k/Q}$ or $\ln(C_{out}/C_{in}) = -V*k/Q$ in an ideal case. Figure 9 plots C_{out}/C_{in} against V*k/Q as listed in table 2 and the data fit into an exponential trend. However, it was found that $\ln(C_{out}/C_{in})$ roughly equals -0.77*V*k/Q, which indicates a less efficient reduction of MTBE concentration than predicted from the batch experiments. A possible explanation to this observation would be that the mixing within the reactor are different in batch experiments and flow experiments. In batch experiments, mixing of MTBE solution within the reactor relies on stirring due the airflow as well as diffusion between solution at the reactor center and at the reactor surface. In flow experiments, apart from stirring and diffusion between solution at center and at surface, there is also diffusion between solution at the inlet and inside the reactor.

Conclusions

Photocatalytic reaction using a supported-catalyst reactor is a promising remediation method for degradation of MTBE in water.

Complete degradation of MTBE was achieved with excess supply of oxygen.

The effect of photocatalytic reaction is the much more significant than adsorption to the catalyst or loss to the airflow in remediation of MTBE in water using a supported-catalyst reactor.

Photocatalytic degradation follows the first-order kinetics in the range of initial concentration 10 ppm to 1000 ppm.

In a photocatalytic reactions with constant flow, it was found that the ratio between outlet and inlet concentrations, C_{out}/C_{in}, approaches constant and $\ln(C_{out}/C_{in})$ roughly equals -0.77*V*k/Q, where V is the volume of the reactor, k is the batch rate constant of the reactor and Q is the flow rate.

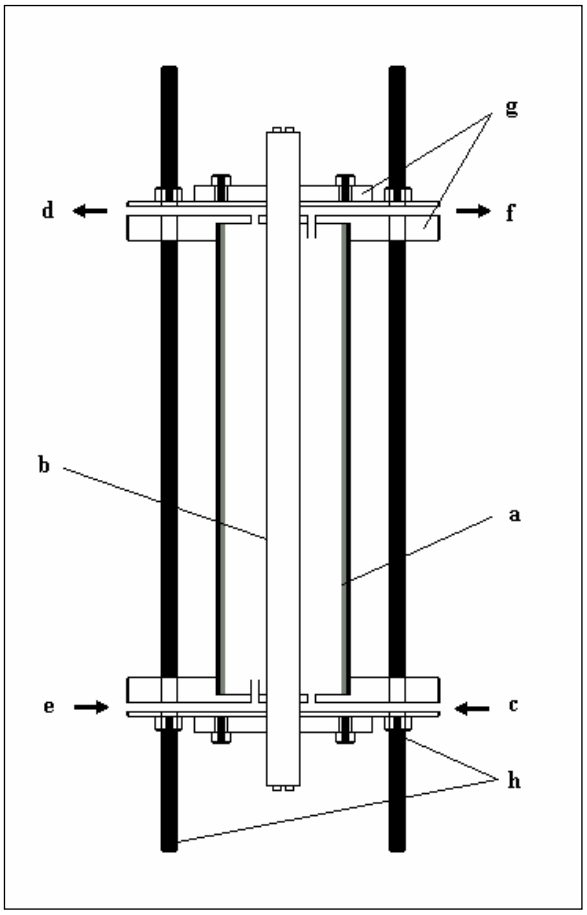

Figure 1: Layout of supported-catalyst reactor.
(a) glass cylinder 28.2-58.2mm dia., 60-180mm len. (b) UV lamp
(c) water inlet to reservoir via pump in flow expt.
(d) water outlet to reservoir in flow expt.
(e) air inlet from compressor via pressure regulator (f) air outlet to exhaust
(g) plastic mountings (h) steel stands

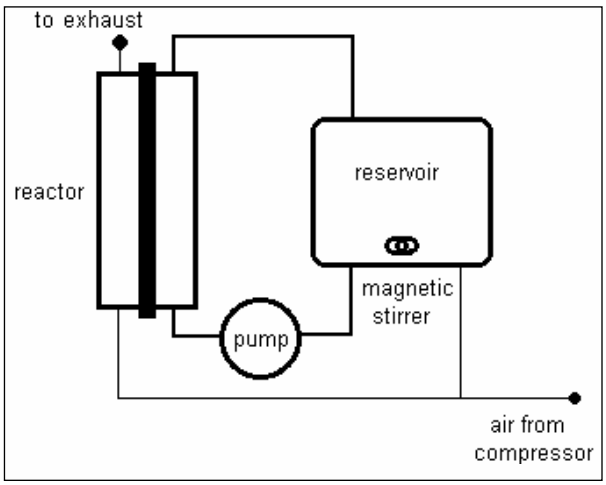

Figure 2: Schematic diagram of set-up.

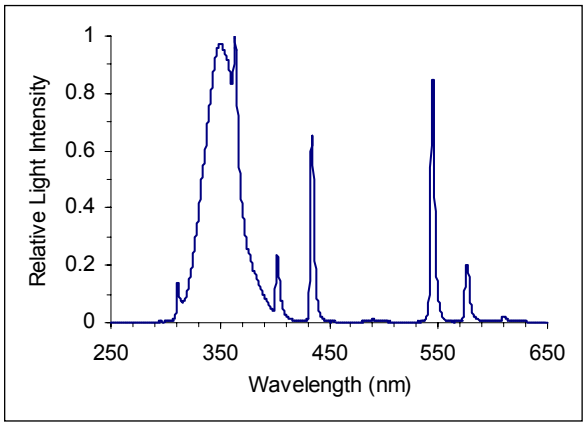

Figure 3: Power spectrum of UV lamp.

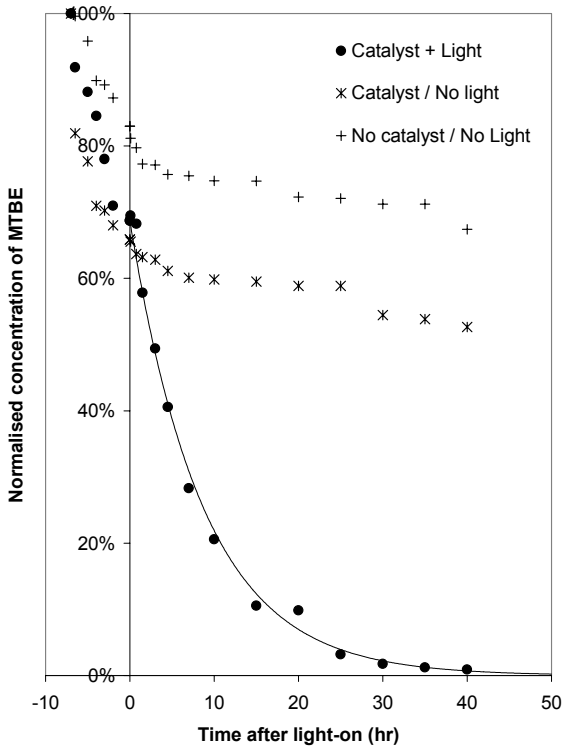

Figure 4: Reduction of [MTBE] in batch expt. using reactor of 48.2mm dia. and 180mm leng. with initial conc.100ppm.

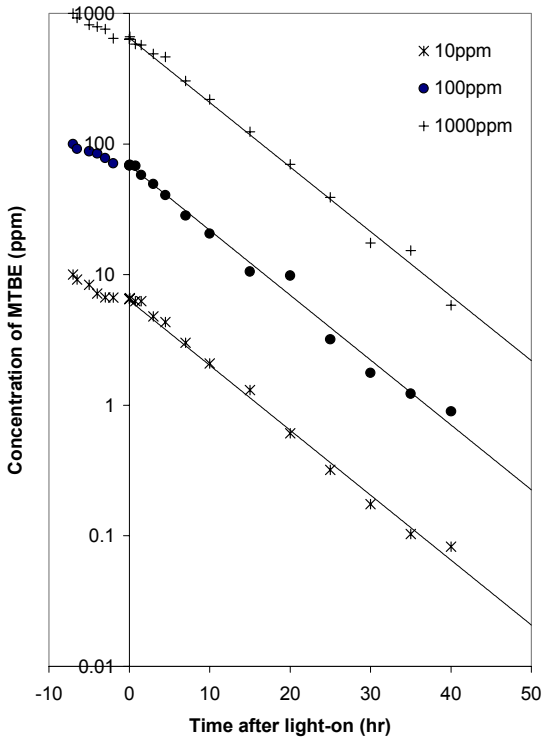

Figure 5: Reduction of [MTBE] in batch expt. using reactor of 48.2mm dia. and 180mm leng. with different initial concentrations.

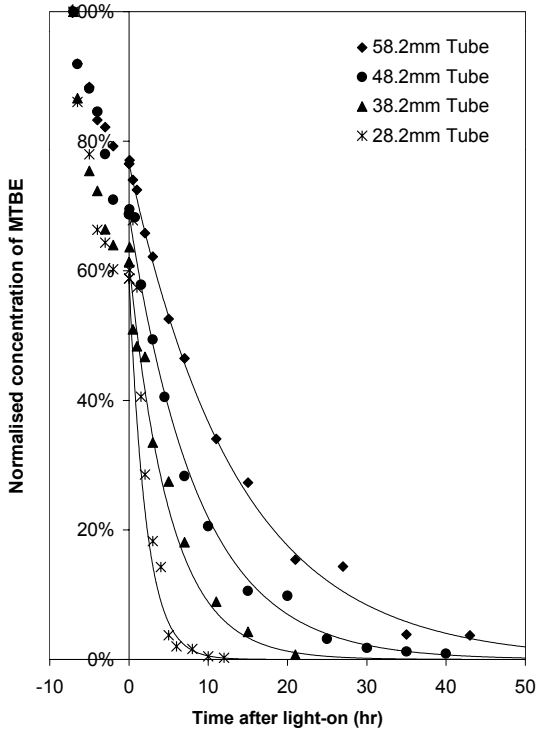

Figure 6: Reduction of [MTBE] in batch expt. using reactor of 180mm in leng. and different dia. with initial conc 100ppm.

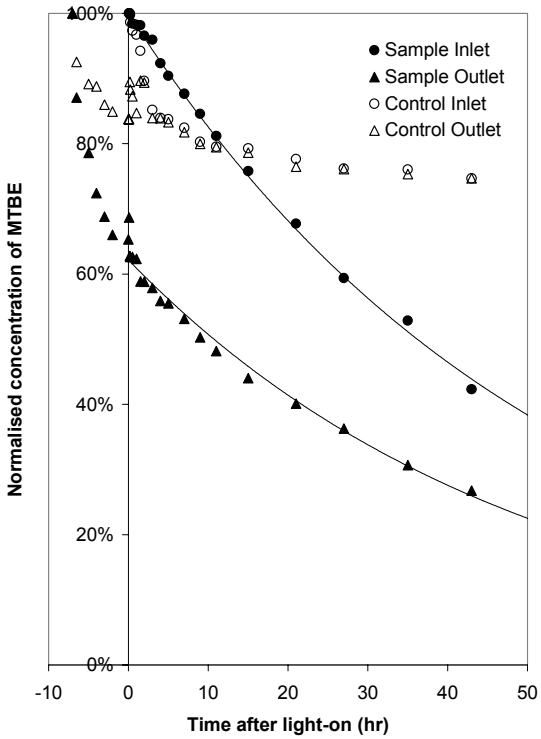

Figure 7: Reduction of [MTBE] in flow expt. using reactor of 48.2mm in dia. and 180mm in leng. with initial conc. 100ppm and flow rate 40ml/hr.

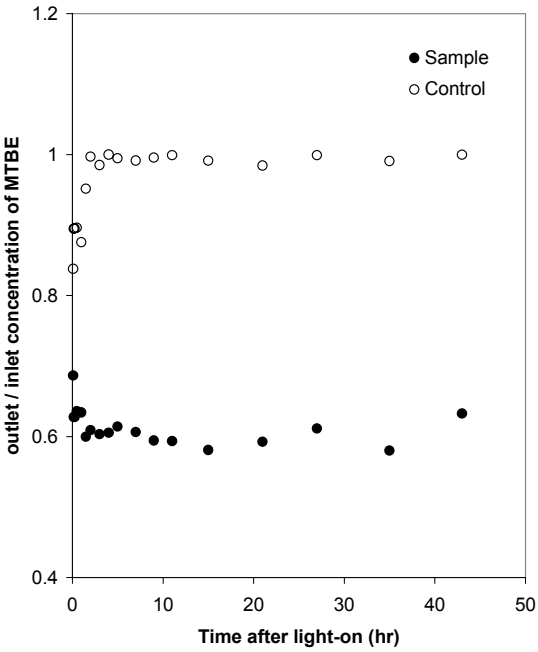

Figure 8: Outlet/inlet concentration of MTBE in flow expt. using reactor of 48.2mm dia. and 180mm leng. with initial conc. 100ppm and flow rate 40ml/hr.

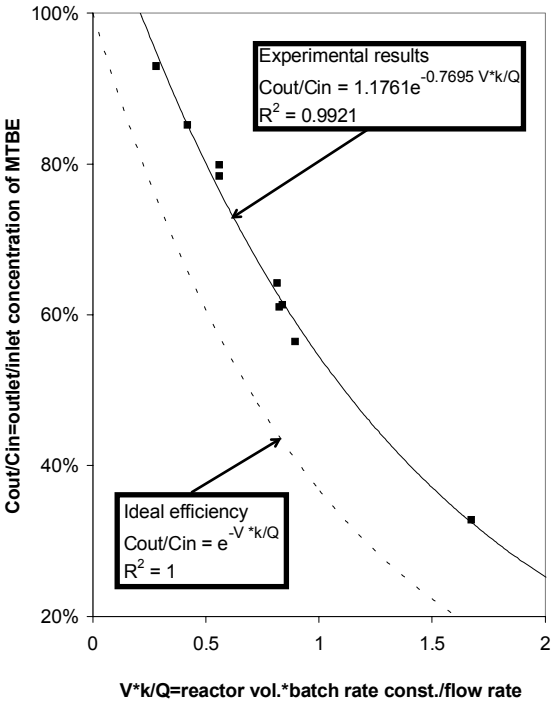

Figure 9: Outlet/inlet concentration of MTBE (Cout/Cin) in flow expt. using reactor of different vol. (V) and batch rate constant (k) and flow rate (Q) with initial conc.100ppm.

Table 1: Summary of data in batch experiments.

D mm	C_o ppm	C_1 ppm	k hr^{-1}
48.2	1000	649	0.115
48.2	100	68.7	0.114
48.2	10	6.35	0.114
58.2	100	76.5	0.074
38.2	100	61.3	0.140
28.2	100	58.8	0.469

D = diameter of reactor
C_o = initial MTBE conc. as light-off stage starts
C_1 = MTBE conc. as light-on stage starts
k = batch rate constant of reactor

Table 2: Summary of data in flow experiments.

D mm	L mm	Q ml/hr	V*k/Q	C_{out}/C_{in}
48.2	180	20	1.67	0.33
48.2	180	40	0.84	0.61
48.2	180	60	0.56	0.80
48.2	180	80	0.42	0.85
48.2	120	40	0.56	0.78
48.2	60	40	0.28	0.93
58.2	180	40	0.81	0.64
38.2	180	40	0.82	0.61
28.2	180	40	0.89	0.57

D = diameter of reactor
L = length of reactor
V = volume of reactor
k = batch rate constant of reactor
Q = flow rate
C_{in},C_{out}: MTBE conc. at reactor inlet,outlet

References

1. The European Fuel Oxygenates Association (EFOA), MTBE Resource Guide, **2000**, *The European Fuel Oxygenates Association (EFOA)*.
2. Fernandez, L.F., Keller A.A., **2000**, Cost Benefit Analysis of MTBE and Alternative Gasoline Formulations, *Environmental Science and Policy*, 3, 173-188.
3. Keller, A.A., Sandall, O.C., Rinker R.G., Mitani, M.M., Bierwagen, B., Snodgrass, M.J., **2000**, An Evaluation of Physicochemical Treatment Technologies for Water Contaminated with MTBE, *Ground Water Monitoring and Remediation*, 20 (3), 114-134.
4. Keller, A.A., Sirivithayapakorn, S., Kram, M., **1999**, Remediation of MTBE Contaminated Water and Soil, *Remediation Journal,* 10 (1), 55-68.
5. Mills, A., Davies, R.H., and Worsley, D., **1993**, Water Purification by Semiconductor Photocatalysis, *Chemical Society Reviews*, 22, 417-425.
6. Hoffmann, M.R., Martin, S.T., Choi, W. and Bahnemann, D.W., **1995**, Environmental Applications of Semiconductor Photocatalysis, *Chemical Review*, 95, 69-96.
7. Choi, W. Y. and Hoffmann, M.R., **1997**, Novel Photocatalytic Mechanisms for $CHCl_3$, $CHBr_3$, and CCl_3CO_2 - Degradation and the Fate of Photogenerated Trihalomethyl Radicals on TiO_2, *Environmental Science and Technology*, 31 (1), 89-95.

8. Feitz, A.J., Boyden, B.H., Waite, T.D., **2000**, Evaluation of Two Solar Pilot Scale Fixed-Bed Photocatalytic Reactors, *Water Research*, 34 (16), 3927-3932.
9. Choi, W., Hong, S.J., Chang, Y.S. and Cho, Y., **2000**, Photocatalytic Degradation of Polychlorinated Dibenzo-p-dioxins on TiO2 Film under UV or Solar Light Irradiation**,** *Environmental Science and Technology*, 34 (22), 4810-4815.
10. Peill, N.J. and Hoffmann, M.R., **1995**, Development and Optimization of a TiO_2-Coated Fiber Optic Cable Reactor: Photocatalytic Degradation of 4-Chlorophenol, *Environmental Science and Technology*, 29 (12), 2974-2981.
11. Peill, N.J. and Hoffmann, M.R., **1998**, Mathematical Model of Photocatalytic Fiber-Optic Cable Reactor for Heterogeneous Photocatalysis, *Environmental Science and Technology*, 32 (3), 398-404.
12. Miller, L.W., Tejedor-Tejedor, M. I. and Anderson, M.A., **1999**, Titanium Dioxide-Coated Silica Waveguides for the Photocatalytic Oxidation of Formic Acid in Water, *Environmental Science and Technology*, 33 (12), 2070 –2075.
13. Davydov, L., Pratsinis, S.E. and Smirniotis, P.G., **2000**, The Intrinsic Catalytic Activity in Photoreactors, *Environmental Science and Technology*, 34 (16), 3435-3442.
14. Serrano, B. and de Lasa, H., **1997**, Photocatalytic Degradation of Water Organic Pollutants. Kinetic Modeling and Energy Efficiency, *Ind. Eng. Chem. Res.*, 36, 4705-4711.
15. Serrano, B., de Lasa, H., **1999**, Photocatalytic Degradation of Water Organic Pollutants: Pollutant Reactivity and Kinetic Modeling, *Chemical Engineering Science*, 54, 3063-3069.
16. Chan, M.S.M. and Lynch, R.J., **2002**, Photocatalytic Degradation of Aqueous MTBE in a Supported-Catalyst Reactor, Conference Proceeding of 3rd European Meeting of Environmental Chemistry, Geneva, Switzerland.

STUDY ON THE APPLICABILITY OF THE THERMAL DESORPTION PROCESS TO ALKYL-LEAD CONTAMINATED SOILS

Mentore Vaccari, Roberto Bellini**, Carlo Collivignarelli*, Pio Forzatti°, Luca Lietti°, Vincenzo Riganti+*

* University of Brescia, Department of Civil Engineering ,Via Branze 38, 25123 Brescia (I), phone: +39 030375421, fax: +39 0303715503, e-mail: vaccari@ing.unibs.it
** Studio Associato Professione Ambiente, Via G. B. Cacciamali 61/I, 25125 Brescia (I), phone: +39 0303533699, fax: +39 0303546800, e-mail: roby.bell@libero.it
° Politecnico di Milano, Department of Chemistry, Materials and Chemical Engineering, P.zza L. da Vinci, 32, 20123 Milano (I), phone: +39 0223993272, fax: +39 0270638173, e-mail: luca.lietti@polimi.it
+ University of Pavia, Department of General Chemistry, Via Taramelli 12, 27100 Pavia (I), phone: +39 0382507345, fax: +39 0382528544, e-mail: riganti@unipv.it

1 INTRODUCTION

Nowadays, brownfields remediation represents a priority environmental aim, because of the need of either reducing the surrounding population sanitary risk, or restoring degraded areas and giving them back to the community.
Since brownfields contamination is usually characterised by great heterogeneity, it is not possible to identify the remediation technology without carrying out previous laboratory/pilot tests in order to verify the effectiveness of the process and to define the best operating conditions (Riganti et al., 2001; Bertanza et al., 2002).

The aim of this work was to verify the applicability of the ex situ thermal desorption process in the case of soils (collected in a brownfield situated in a town of the North of Italy) contaminated with alkyl-lead compounds (in particular tetraethyllead) and other odorigenous species. In particular, aim of this experimentation, carried out at laboratory scale, was to determine the treatment temperature at which the removal of the organic compounds and of the odorigenous pollutants occurred, in order to allow the application of the following removal/stabilization treatments of the residual inorganic lead.

2 EX-SITU THERMAL DESORPTION

Thermal desorption is a physical separation process, in which contaminated soils are heated to volatilize water and organic contaminants. A carrier gas or vacuum system transports volatilized water and organics to the gas treatment system. The bed temperatures and residence times are typically designed in order to volatilize the contaminants without achieving oxidation of the contaminants themselves.
Based on the operating temperature of the desorber, thermal desorption processes can be divided into two groups (USEPA, 2002):
- low temperature thermal desorption (LTTD), in which wastes are heated in the range 90 - 320 °C;
- high temperature thermal desorption (HTTD), in which wastes are heated in the range 320 - 560 °C.

Thermal desorption systems have varying degrees of effectiveness against the full spectrum of organic contaminants. The target contaminant groups for LTTD systems are non-halogenated volatile organic compounds (VOCs) and fuels. The technology can also be used to treat semi-volatile organic compounds (SVOCs) at reduced effectiveness.
The target contaminants for HTTD are SVOCs, PAHs, PCBs, and pesticides; however, VOCs and fuels also may be treated, but treatment may be less cost-effective. Moreover, volatile metals may be removed by HTTD systems.

Lighty et al. (1988, 1989, 1990) carried out several researches which are considered up-to-date studies on thermal desorption of organic compounds contaminated soils (Ayen et al., 1995). In these studies, performed with several contaminants including cyclohexane, n-heptane, toluene and naphthalene, Lighty et al. demonstrated that the desorption rate mainly depends on the chemical

structure of the organic substance, and that temperature is the most important operating parameter. These considerations were further confirmed by Szabo et al. (1988).
The comparison of Lighty et al.'s and Szabo et al.'s studies shows that a good SVOCs removal can be achieved reaching at least treatment temperature of 300°C. Obviously, the required temperature varies also according to other parameters, such as treatment time, soil texture, kind of treatment plant (Ayen et al., 1995).

3 THE ALKYL-LEAD COMPOUNDS

Alkyl-lead are a particular class of organolead compounds, characterized by a direct link between the lead atom and one or more alkyls. Tetraalkyllead compounds, such as tetraethyllead (TEL, Et_4Pb) and tetramethyllead are the most common alkyl-lead compounds used in the past and still in use as a fuel additive to reduce "knock" in combustion engines (Irwin et al., 1997), although they are now prohibited by legislation in most industrialised Countries.
This use of tetraalkyllead has deeply contributed to the spread of a great quantity of lead in the environment (Chiodo et al., 2000), equal to 95% of total lead present in the air of the main cities of the Earth (USEPA, 1998).

Alkyl-lead is released to the environment primarily through evaporative emissions from unburned gasoline retained in an engine's carburetor or fuel tanks and through evaporative losses during the filling of gasoline tanks, accidental spillages and releases during production. However, alkyl-lead compounds combine with other compounds during the combustion process to form inorganic lead halogenides that are subsequently emitted as microparticulates in exhaust.
Alkyl-lead in the atmosphere degrades rapidly by direct photolysis, reaction with ozone, and by reaction with hydroxyl compounds. The half-life of Et_4Pb in the atmosphere vary from about two hours in summer to some days in winter. In water and soil, alkyl-lead compounds are degraded to other forms of lead, eventually forming stable inorganic lead compounds.

The usual human exposure pathways for alkyl-lead include inhalation of leaded gasoline vapours and dermal exposure to leaded gasoline. Unlike metallic forms of lead, alkyl-lead is easily absorbed through the skin (Bress & Bidanset, 1991; Moore et al., 1980). Additionally, through the combustion process, alkyl-lead in gasoline is converted to lead halogenides which are exhausted into the air where they can be inhaled. Subsequent deposition of these lead halogenides contributes to exposure to lead through ingestion of lead contaminated soil or dust, and ingestion of lead-contaminated food or water. Moreover, the toxicity of alkyl-lead compounds varies with the degree of alkylation: tetraalkyllead compounds are considered to be more toxic than trialkyllead or dialkyllead compounds (USEPA & EC, 1999).

4 THE CONTAMINATED SITE

The brownfield, 5.5 ha extended, is situated in an industrial area of a town of the North of Italy. Previous hydrogeologic investigations showed that the most superficial soil layer (till –6 m deep) mainly consists of silt and clay, and groundwater table is 2 m deep.
The presence of pollutants in the area derives from the plant previous industrial activity, devoted to the production of alkyl-lead compounds.

At the moment, contamination interests both the superficial and the deeper soil layers and has reached the main aquifer, causing the closing of several surrounding agricultural and industrial wells. In particular, superficial soil and subsoil present high concentration of TEL and inorganic lead, because of their low mobility. TEL degradation, moreover, gave origin to triethyllead and diethyllead, in part adsorbed to soil and in part transported to aquifer.
Moreover, the release of residual industrial products in the near superficial irrigation channels has caused the contamination of the neighbouring area, as well.

5 EXPERIMENTAL SECTION

During this study, carried out at a laboratory scale, several thermal desorption tests were conducted with samples of contaminated soil either with an inert gas or air. Experiments were performed by placing the soil at room temperature in an oven with indirect heating; the oven temperature was then linearly increased up to 650 °C under flow of either the inert gas or air. Two different types of experiments have been performed: in the first case (in-line FID tests), the gases effluent from the reactor were continuously analysed by means of a flame ionisation detector (FID), whereas in the other case the desorbed compounds were collected (either through condensation or GAC adsorption) and analysed by GC-MS. Accordingly, the quali-quantitative characteristics of the pollutants and their desorption temperature could be obtained.
Finally, chemical analysis were also performed on the soil treated at different temperatures and discharged from the oven in order to establish, by comparison with the original contaminated soil, the efficiency of the treatment.
The experimental plant, shown in Figure 1, was composed by three main parts: i) the gas flow regulation section; ii) the thermal treatment section; iii) the analysis/collection section of desorbed compounds.

Figure 1: *The experimental plant.*

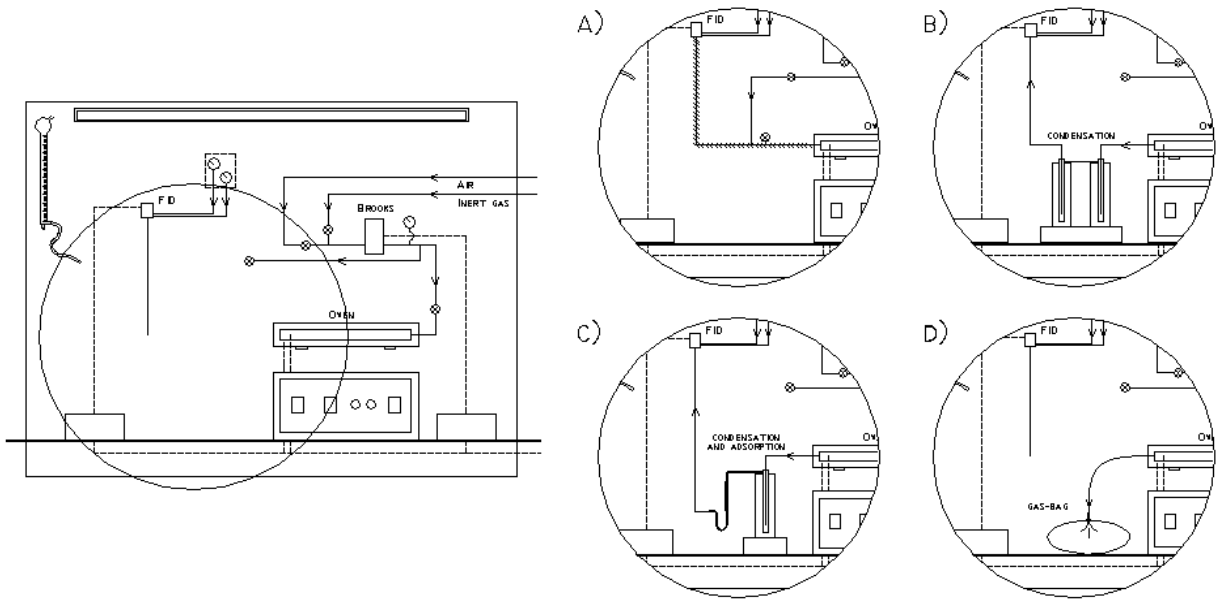

The Pb, VOCs and SVOCs content of the soil, before and after the thermal treatment, was determined by chemical analysis. In particular, Pb concentration was determined as follows: a portion of the soil was dried at 40°C and mixed. Then a sample of 0.5-1 g was mixed with 10 mL HNO_3 for two hours at room temperature. The suspension was then heated for two hours and, after cooling down, 10 mL HNO_3 and 2 mL $HClO_4$ were added. The mineralization lasted until the complete removal of organic material was achieved; then 1 mL HNO_3 and 20 mL of deionized water were added and the mixture was heated up to boiling point. At the end, the mixture was filtered and brought to 100 mL by addition of deionized water. The resulting solution was analysed by means of atomic absorption spectrophotometry.
VOCs were measured as follows: 2 g of soil were dried using anhydrous sodium sulfate, then 10 mL n-pentane were added (also carbon disulfide and methanol were tested as extraction compounds, but they did not give good results). The resulting slurry was mixed at room temperature for 60 minutes, and then 1 μL of 4-heptanone was added as internal standard. After sedimentation, the liquid phase was separated and analysed by means of gas chromatography - mass spectrometry (GC/MS).

SVOCs were misuread as follows: 2 g of soil were dried using anhydrous sodium sulfate and extracted for 24 hours at 50°C in a 100 mL Soxhlet extractor with 90 mL methylene chloride. The extracted was concentrated by evaporation (reaching about 1 mL volume), then 50 mL n-hexane were added and the whole was concentrated again to 1 mL volume. After addiction of 1 μL of 4-heptanone as internal standard, the mixture was analysed by GC/MS.

6 RESULTS AND DISCUSSION

The experiments were performed on three samples of soil drown inside the contaminated brownfield. The samples were kept off from direct light contact and stored in air-tight closed glass containers in order to keep the original in-situ soil characteristics.

6.1 Soil characterisation before treatment

The main chemical-physical characteristics of the three samples are summarised in Table 1.

Table 1: *Samples characterisation.*

Parameter	Sample A	Sample B	Sample C
Sampling depth	from 0 to –0.5 m	from –0.5 to –1.0 m	from –1.0 to –1.5 m
Colour	brown	brown	brown
Odour	+	+ + +	+ + +
Texture	silt-clay	silt-clay	silt-clay
Moisture	~ 30%	~ 30%	~ 25%
pH	7.3	6.8	7.3
Pb_{tot}	13,25 mg/Kg	5,49 mg/Kg	5,93 mg/Kg
$(C_2H_5)_4Pb$	40 mg/Kg	450 mg/Kg	absent

Data show a significant difference in lead concentration between the surface and the deeper samples. Lead concentration in sample A is more than double of samples B and C. Sample B, extracted from the intermediate layer, contains highest quantity of Et_4Pb and organic compounds as well, as confirmed by the desorption tests reported below.

6.2 Thermal desorption tests

These tests were carried out on sample B, which presents the highest Et_4Pb concentration and, moreover, which was very malodorous.

6.2.1 In-line FID tests

Tests were performed with the in-line FID device with either inert gas or air as process gas. Figure 2 shows the comparison between the desorption profiles obtained with air or with the inert gas as a function of the desorption temperature.

Figure 2: *Comparison between air and inert gas desorption profile. FID signal vs. temperature.*

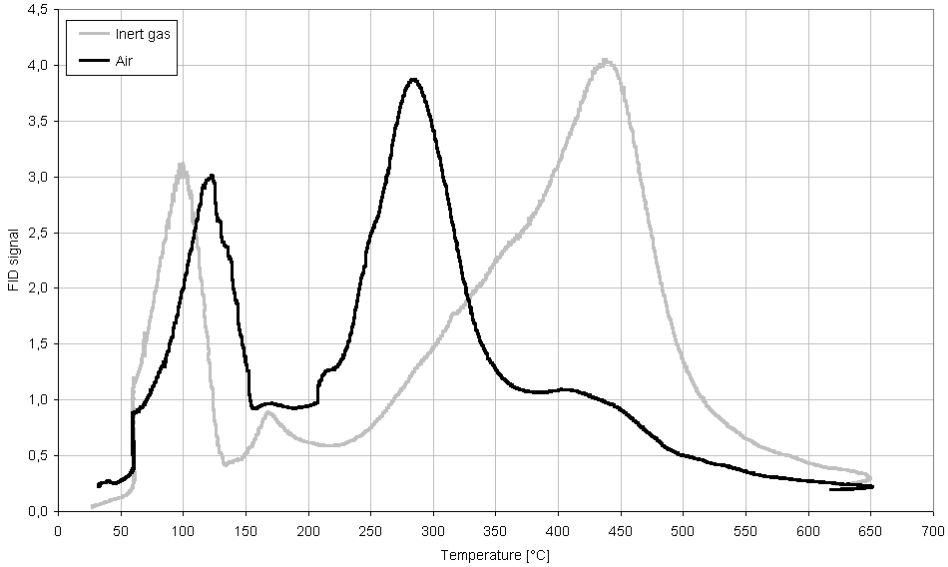

Both curves present two separate desorption peaks, the first in the low temperature region, near 100°C, and the second at higher temperatures. In particular, in the case of the inert gas the peaks are evident at 100 and 430°C, whereas at 120 and 280°C with air. Therefore, the use of air as process gas decreases by 150°C the temperature needed for maximum desorption at the high-temperature peak. On the other hand, at lowest peak, an increase of (only) 20°C is produced.
The temperature needed for the complete desorption of the two main peaks (excluding the long desorption tail) is 550°C and 450°C for process with the inert gas or air, respectively.

Figure 3 shows the integrated concentration-time profiles of the two desorption curves shown in Figure 2 (setting the integration value at 99% with a temperature of 650°C). The integrated values do not show significant difference until 200°C (Figure 3). At higher temperatures, the integrated values grow differently: indeed already at 350°C the value related to air is 79% versus 55% for the inert gas. At 400°C values are 85% and 65% for air and inert gas, respectively, whereas at 450°C values are 90% and 77%.

Figure 3: *Air and inert gas desorption integral values vs. temperature.*

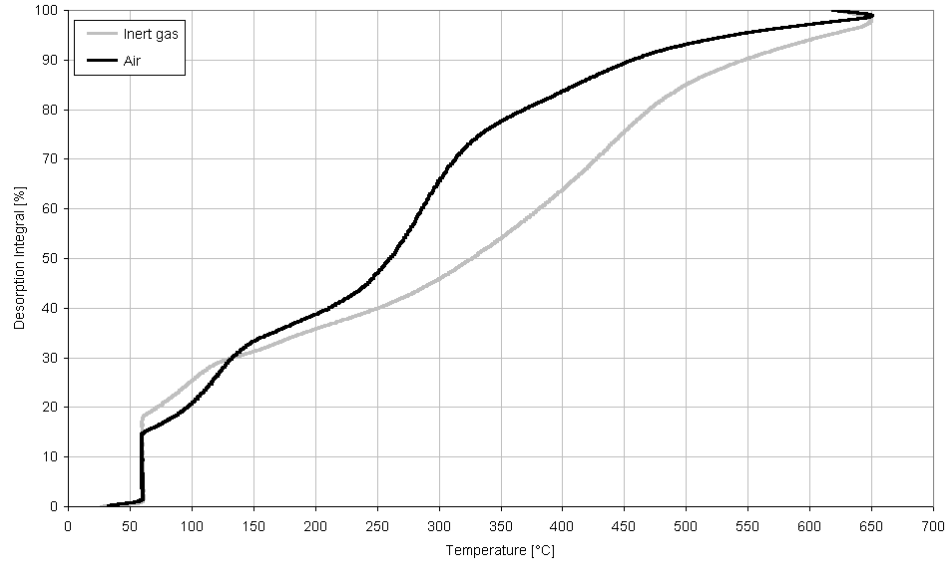

6.2.2 Tests with condensation/adsorption of desorbed compounds

Based on data gathered with in-line FID tests, several further sets of experiments were carried out with the aim of:

- identify and quantify the desorbed compounds related to the thermal range of the two peaks separately;
- identify and quantify the desorbed compounds, specially referring to Et_4Pb, for different process temperatures.

Tests with inert gas

Two tests were performed in order to evaluate the quantity of Et_4Pb desorbed in two temperature ranges: 20-160°C and 160-650°C. The gases exiting from the desorber were passed through a liquid-nitrogen condensation step followed by GAC adsorption. In both cases, only Et_4Pb was found in the desorbed products. Figure 4 reports the amounts of Et_4Pb recovered during the two runs: values near 200 mg/kg have been obtained in both cases.

Figure 4: *Et_4Pb collected during tests with inert gas.*

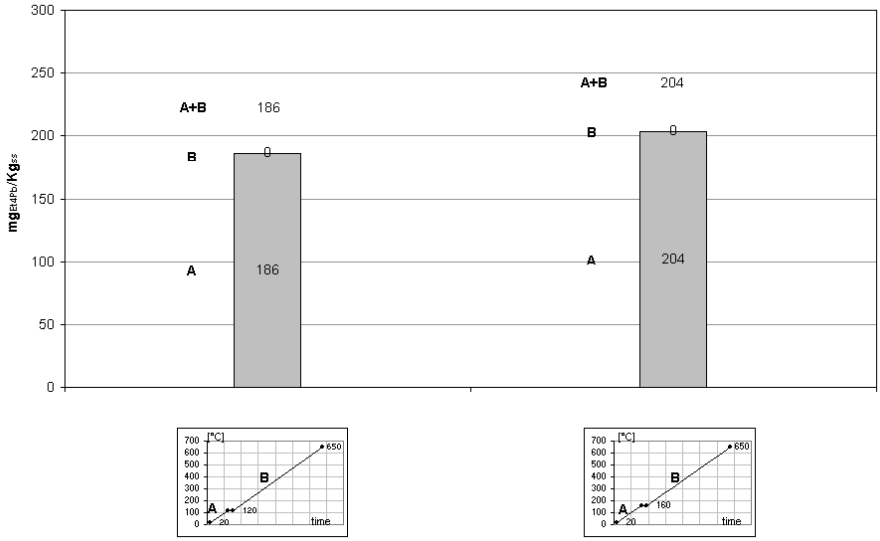

Tests with air

Initially the desorbed compounds were collected in three distinct ranges of temperature (20-105°C; 105-350°C; 350-650°C). Also in this case the desorption of Et_4Pb took place at the lowest temperature, as shown in Figure 5.

Figure 5: *Et_4Pb collected during tests with air.*

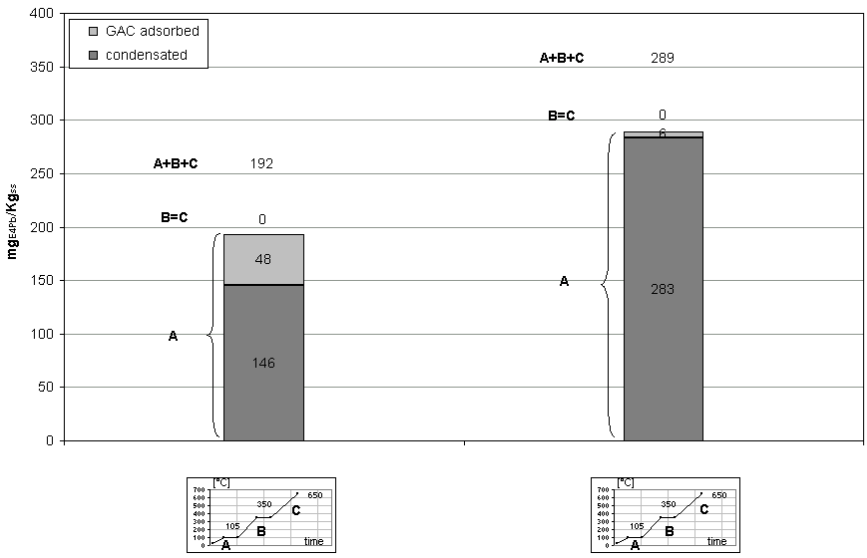

A closer analysis of the products desorbed in the lowest temperature range showed the presence of three additional compounds, beside the Et_4Pb, along with many others with very low concentrations. These three major compounds, as shown in Figure 6, have been identified by GC/MS as diethyl sulfide ($C_4H_{10}S$), diethyl disulfide ($C_4H_{10}S_2$), diethyl trisulfide ($C_4H_{10}S_3$).

Figure 6: *Chromatographic analysis of compounds desorbed at 20-105°C.*

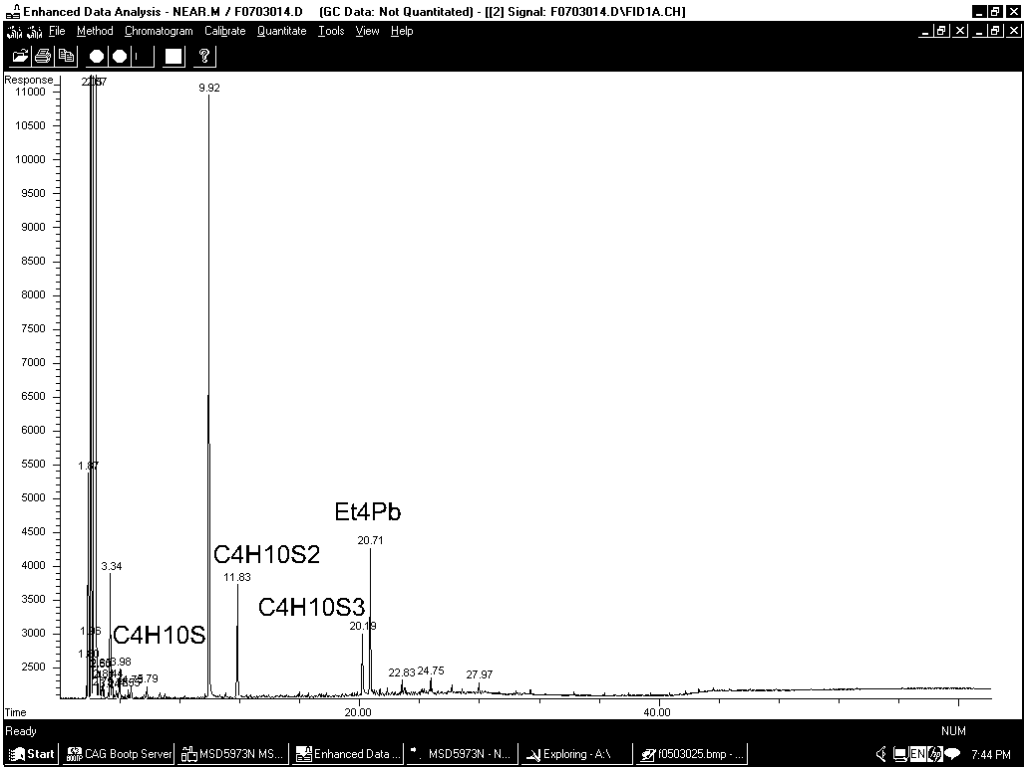

Later on, a set of experiments were performed by stopping the heating at different maximum desorption temperature (40, 105, 200, 350, 500°C), in order to evaluate the efficiency of Et_4Pb desorption at these different temperatures. Aim of this investigation was to identify the minimum desorption temperature that guarantees the complete desorption of Et_4Pb from soil. Figure 7 illustrates the Et_4Pb quantity collected during the various experiments.

Figure 7: Et_4Pb collected during the isothermal tests.

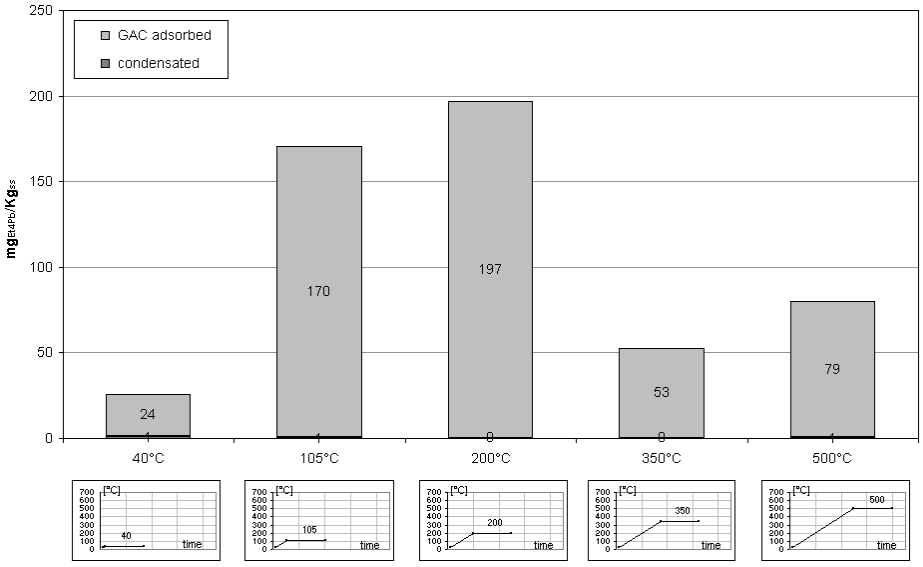

It is clear that the maximum quantity of Et_4Pb (197 mg/kg, which is 50% of total Et_4Pb initially in the soil) was extracted at 200°C. Moreover, for higher temperature, the quantity of Et_4Pb collected decreased because of its degradation both in soil and collection system.
The same behaviour was observed for desorbed sulfide compounds, too.

Finally, some tests were carried out to identify the desorbed compounds in the temperature range 200-400°C. The gaseous flow exiting the oven was stored in a gas-bag and directly analysed by means of GC/MS. In the chromatogram, several unidentified peaks appeared at very low retention times, indicating the presence of a large number of volatile compounds.

6.3 Soil characterisation after treatment

The samples treated at constant temperature were submitted to characterisation. First of all, it was possible to state that malodours compounds disappeared in samples treated above 200°C. With regard to lead, Figure 8 shows that thermal desorption is not efficient towards inorganic lead, that must be removed or immobilised by means of other techniques (i.e. soil washing or stabilization/solidification).

Figure 8: Pb concentration in treated soils.

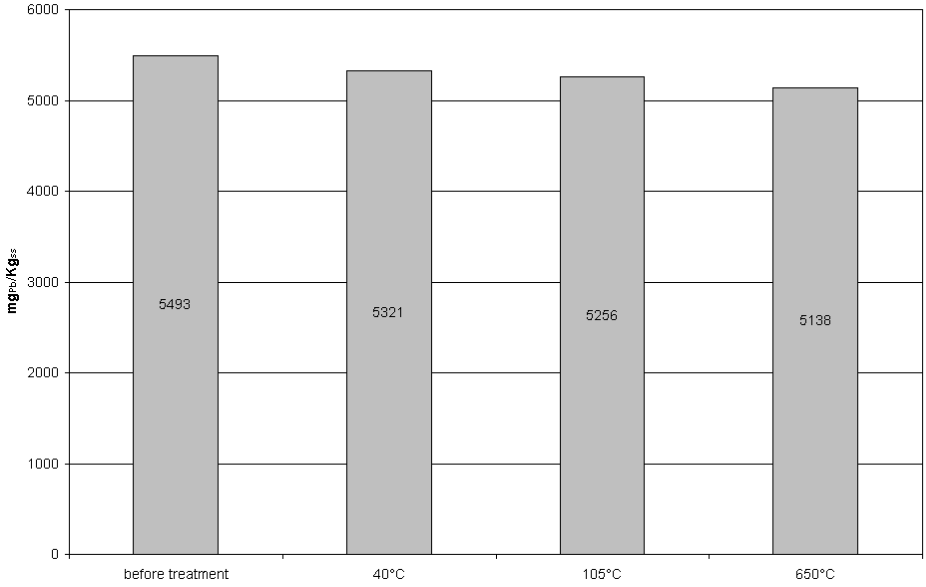

With regard to Et_4Pb, the analysis pointed out that its concentration decreased to 24 mg/kg in 40°C treated soil and that already in 105°C treated-soil Et_4Pb disappeared.

7 CONCLUSIONS

The experimentation, as a whole, led to the following main considerations:

- soil characterisation and desorbed compounds analysis confirmed the mean presence of Et_4Pb among the soil organic compounds;
- the presence of sulphurous malodorous compounds was confirmed by the chromatograms of the desorbed compounds;
- the maximum quantity of desorbed Et_4Pb, equals to about 50% of total Et_4Pb initially in the soil, was reached at 200°C;
- the compounds desorbed at 200-400°C are volatile and, partially, derive from Et_4Pb degradation;
- thermal treatment of soil at 200°C allows the complete removal/degradation of Et_4Pb and the removal of malodorous substances, in addition to the reduction of soil weight, which later needs to be treated to remove/immobilise the residual inorganic lead;
- extending the treatment up to 400-450°C allows the desorption of residual organic fraction from soil.

In conclusion, it is possible to state that the thermal desorption process represents a good solution for the treatment of alkyllead contaminated soils, because it allows:

- the removal of the volatile organic compounds, and in particular of the tetraethyllead;
- the complete removal of malodorous species;
- the weight reduction of soil, that has to be treated in the following remediation phases.

8 REFERENCES

Ayen R.J., Hoeffner S.L., Navratil J.D. (1995). *Trattamenti termici*. In "Siti Contaminati, Tecniche Ottimali di Risanamento", C.I.P.A. Editore, Milano

Bertanza G., Collivignarelli C., Riganti V., Vaccari M. (2002). *The use of BATNEECs in landfills remediation*. Proceedings of the 6th Simpòsio Italo Brasileiro de Engenharia Sanitària e Ambiental, Vitòria – ES, Brasil, 1-5 September, III-080, pp. 1-10

Bress W.C., Bidanset J.H. (1991). *Percutanous in vivo and in vitro adsorption of lead.* Vet. Hum. Toxicol., 33: 212-214

Chiodo et al. (2000). *Health Effects of Eleven Hazardous Air Contaminants and Recommended Evaluation Criteria. Final Report*. Ministry for the Environment's Review of the Ambient Air Quality Guidelines, New Zealand. Available on http://mfe.govt.nz/monitoring/epi/13hazardousair.pdf

Irwin R.J., Van Moouwerik M., Stevens L., Seese M.D., Basham W. (1997). *Gasoline Additives.* In Environmental Contaminants Enc., National Park Servica, W.S.D., Fort Collins, Colorado

Lighty J.S., Pershing D.W., Cundy V.A., Linz D.G. (1988). *Characterization of thermal desorption phenomena for the cleanup of contaminated soil*. Nucl. Chem. Waste Manage, 8 (22), 225-237

Lighty J.S., Silcox G.D., Pershing D.W., Cundy V.A., Linz D.G. (1989). *Fundamental experiments on thermal desorption of contaminants from soils*. Environ. Prog., 8 (1), 57-61

Lighty J.S., Silcox G.D., Pershing D.W. (1990). *Investigation of rate process in the thermal treatment of contaminated soils*. Gas Research Institute, March 1990, GRI-90/0112

Moore M.R., Meredith P.A., Watson W.S., Sumner D.J., Taylor M.K., Goldberg A. (1980). *The Percutanous Absorption of Lead-203 in Humans from Cosmetic Preparations Containing Lead Acetate as Assessed by Whole-Body Counting and Other Techniques.* Food and Cosmetic Toxicology, 18: 399-405

Riganti V., Collivignarelli C., Vaccari M. (2001). *Decision making process in the management of remediation interventions*. Proceedings of the 13th IGWT Symposium "Commodity Science in Global Quality Perspective. Products – Technology, Quality and Environment", Maribor, Slovenia, 2-8 September, pp. 1207-1212

Szabo M.F., Fox R.D., Thurnau R.C. (1988). *Application of Low Temperature Thermal Treatment Technology to CERCLA Soils*. EPA 600-9-88-021

USEPA (1998). *Reducing Health Risks Worldwide: EPA's International Lead Risk Reduction Program*. EPA 160-K-98-001

USEPA & EC (1999). *Great Lakes Binational Toxics Strategy. Alkyl-lead: Sources, Regulations and Options*. Draft Report, October

USEPA (2002). *Remediation Technologies Screening Matrix.* 4th Edition, April. Available on http://www.frtr.gov/matrix2/top_page.html

TECHNICAL SCALE INVESTIGATIONS FOR THE IN SITU REMEDIATION OF LOW VOLATILE CONTAMINANTS BY THERMAL WELLS

Uwe Hiester, Tilman Theurer, Angela Winkler, Hans-Peter Koschitzky, Arne Färber
Institute of Hydraulic Engineering, *VEGAS* – Research Facility for Subsurface Remediation,
University of Stuttgart, Pfaffenwaldring 61, 70550 Stuttgart, BRD
phone: +49 – (0)711 – 685 – 4720, fax: +49 – (0)711 – 685 – 7020
uwe.hiester@iws.uni-stuttgart.de

1. INTRODUCTION

The 'cold' soil vapour extraction (SVE) is a common method to extract volatile non-aqueous phase liquids (NAPL) in the gaseous phase from the unsaturated zone. Limitations in remediation efficiency arise due to low vapour pressure of contaminants at natural soil temperature of 10°C. Due to their low evaporation rates, the remediation with cold SVE often takes several years.

To overcome the vaporisation limitations, thermal enhancement is efficient. Therefore various techniques, e.g. steam injection (Fig. 1) have been developed and applied successfully on field sites [KOSCHITZKY ET AL. 2000, SCHMIDT ET AL. 2000, THEURER ET AL. 2000, HERON ET AL. 2002]. Although energy is needed to heat the subsurface, environmental balancing proves, that the impacts of thermally enhanced SVE are smaller compared to cold SVE due to shorter remediation times which extend from several weeks to months [HIESTER ET AL. 2003].

However, steam injection is limited by soil permeability and, furthermore, by the vaporisation rates of low volatile contaminants such as kerosene. For these substances, the volatility can be increased significantly by the high-temperature technology 'thermal wells'. Each well contains one or more heating elements (HE), which operate at several hundred °C (Fig. 1). Aim of this project is the development of the thermal in-situ remediation scheme THERIS using thermal wells.

To understand the complex interrelated heat and mass transport processes in detail, comprehensive experimental and numerical work was conducted before transferring the technology from lab scale to a field site application. One interim step are technical scale experiments under controlled boundary conditions, which are conducted at the Research Facility for Groundwater and Subsurface Remediation *(VEGAS)* at the Institute of Hydraulic Engineering, University of Stuttgart, Germany.

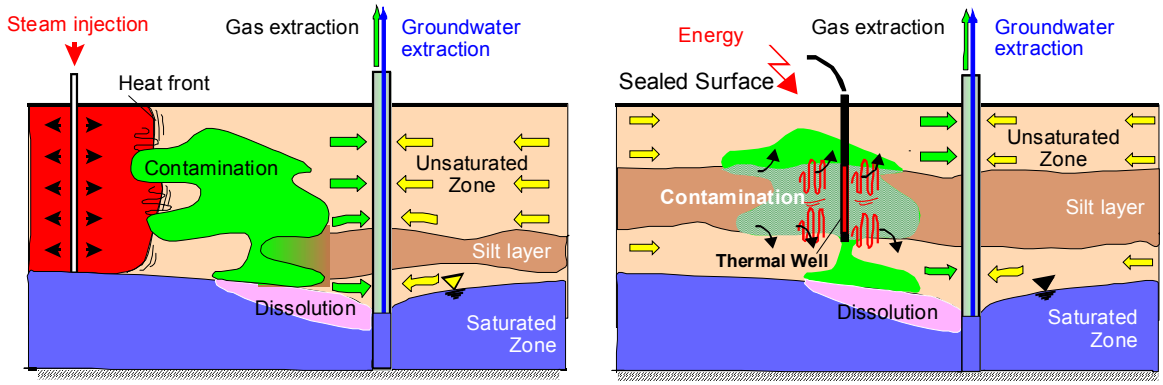

Fig. 1: Principles of steam injection (left) and thermal wells (right))

2. NEED FOR TECHNICAL SCALE INVESTIGATIONS

The technical feasibility of the THERIS scheme is to be proven by experiments and numerical modelling. Batch and small-scale experiments in columns and flumes combined with two-dimensional numerical modelling provide a basic understanding of the processes [WINKLER ET AL. 2002]. To overcome the unavoidable boundary conditions of small scale investigations, experimental research under controlled, natural-similar conditions are necessary. Thus, experiments in the VEGAS technical scale container are conducted to transfer the technology from laboratory to field scale.

In order to evaluate the highly complex non-isothermal, three-dimensional flow in all phases (water, NAPL and air), defined properties as well as impacts on the subsurface such as layering, position of groundwater table and volume of the contamination are indispensable. Hence experiments are run in a stainless steel tank with a soil volume of about 150 m³ with almost natural layering of the subsurface. Heating elements (HE) heat a low permeable layer and remove a contamination known in mass of injected NAPL, location, etc. Soil vapour is extracted. Subsurface temperature and water saturation are measured, while contaminant mass output is monitored in both extracted soil vapour and aqueous phase. So a mass balance can be achieved under controlled conditions unlike experiments carried out in the field. The measurement equipment allows temperatures up to 500°C to be monitored, such that different temperatures and operation schemes can be tested to ensure maximum remediation efficiency for the contaminants under regard.

The container with an inner sealing of high-density polyethylene was equipped for experiments on technical scale. With its dimensions of approx. 6 m x 6 m and a height of 4.5 m (Fig. 2), energy losses across the container boundaries are almost avoided. To simulate the mass flow and heat transport processes in different soils, a three-layer system with a fine grain layer of 1 m thickness was placed in the middle of the container, surrounded by coarse sand material (Fig. 2). The permeability of the fine grain layer is 100 times less compared to the surrounding coarse sand.

Numerical modelling, together with batch- and small-scale experiments [WINKLER ET AL. 2002, THEURER ET AL. 2003] were a first approach to design parts of the technical scale experiments such as the spacing of the thermal wells, their distance to the tank boundaries etc. [THEURER ET AL. 2002]. It is also used to forecast the spatial-temporal temperature distribution and progression of the remediation process of experiments and, later on, field site application.

In total, more than 300 temperature sensors and 35 highly temperature resistant Time Domain Reflectometry (TDR-) Sensors are used to detect the change of moisture in the subsurface (Fig. 2).

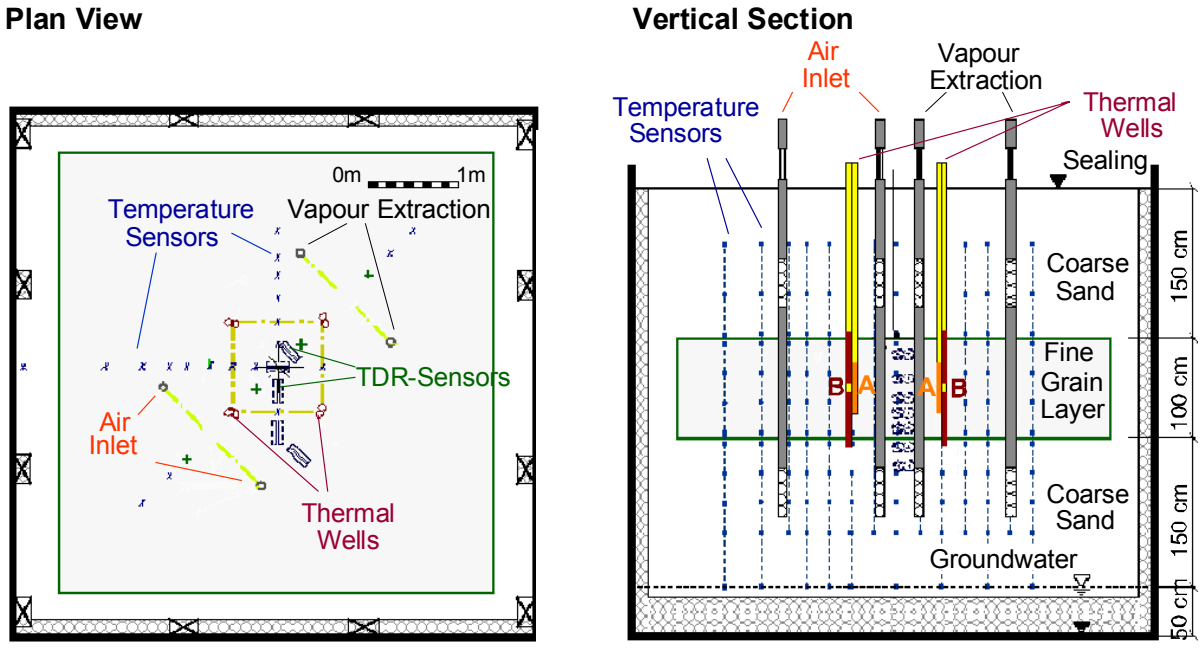

Fig. 2: VEGAS Technical Scale Container: Plan View and Vertical Section

Several physical and technical effects are to be explained by the results from technical scale experiments. Therefore, some experiments were planned, where the investigation of processes is divided into two transport parts: heat (without NAPL) and contamination. For efficiency reasons, the

questions to be solved for the heat transport were combined in one long-term heat transport experiment. The results from this experiment, allowing the identification of the dominating processes on technical scale and the development of preliminary System Operation Rules (SOR) are presented in the following.

A three-dimensional remediation experiment will start in the beginning of 2003 to proof the feasibility of a remediation by thermal wells on technical scale and to allow estimation of the economical feasibility for field sites.

3. HEAT TRANSPORT EXPERIMENT – DESCRIPTION AND RESULTS

The heating elements of the thermal wells in the technical scale experiments operate at a constant temperature of 500°C. The heat transport depends on two major components: conduction and convection. Thermal radiation is negligible.

Aim of the heat transport experiment was to prove, that thermal wells allow the heating of a low permeable soil volume of about 1 m³ to a minimum of 150 °C in the centre. This 'central cube' (Fig. 3) is defined for the top view in the middle of the container and for the side view over the complete height of the fine layer.

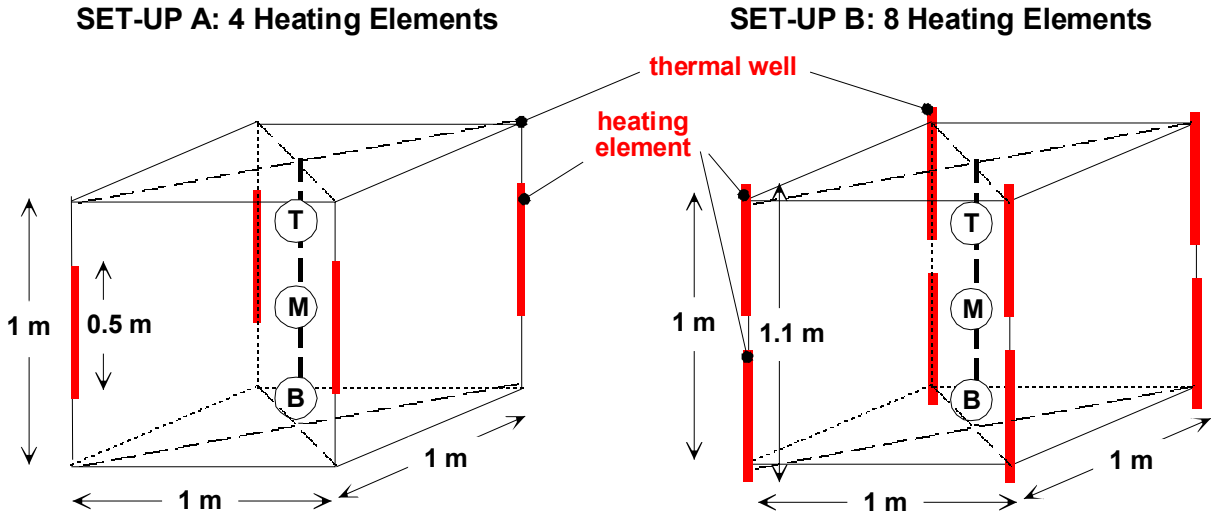

Fig. 3: Sketch of the 'central cube' in the fine grain layer with vertical HE configuration in set-up A (right) and set-up B (left) and the characteristic points in the centre profile [bottom (B), middle (M) and top (T)].

To achieve realistic soil moisture contents equivalent to natural conditions in the container, it was flooded and afterwards drained for several weeks. From additional small-scale experiments and measurements by TDR-sensors in the container, steady-state saturation can be assumed in the beginning of the experiment.

The experiment is split up in two set-ups of HE configuration with in total nine phases. Starting with a 4 HE configuration, the HE were placed in a square of 1m by 1m in the middle of the fine grain layer with a thickness of 1m. Each HE has a length of 0.5m and operates at constant temperature of 500°C (Fig. 3, left figure).

PHASE I: HEATING PHASE A

The first heating phase is characterised by fast increase in temperature and drying of the fine grain layer by mobilisation and evaporation of water (Fig. 4). However, there are only low or moderate temperature gradients in the container. This indicates the convective heat transport to be dominant in most parts of the soil expect of course in the vicinity of the heating elements, where the pore water is vaporised immediately at the very beginning of the experiment and conduction is dominant.

PHASE II: HEAT PIPE

In this phase, the further heating process becomes quasi-stagnant. Boundary losses of the 'central cube' caused more or less constant temperatures despite a constant energy input. Water saturation decreases much slower than in phase I. Only directly at the bottom of the fine layer, no difference in drying is detected (Fig. 4). This is caused by the so-called heat pipe effect. Hereby, vaporised water is transported in direction of the temperature gradient and condenses while reaching colder regions. Capillary forces provide a reversal mass transfer: liquid water is sucked back into the already heated area driven by saturation gradients. This causes a distribution to energy and prevents the central area from heating over 100 °C. Details will be explained in chapter 4.

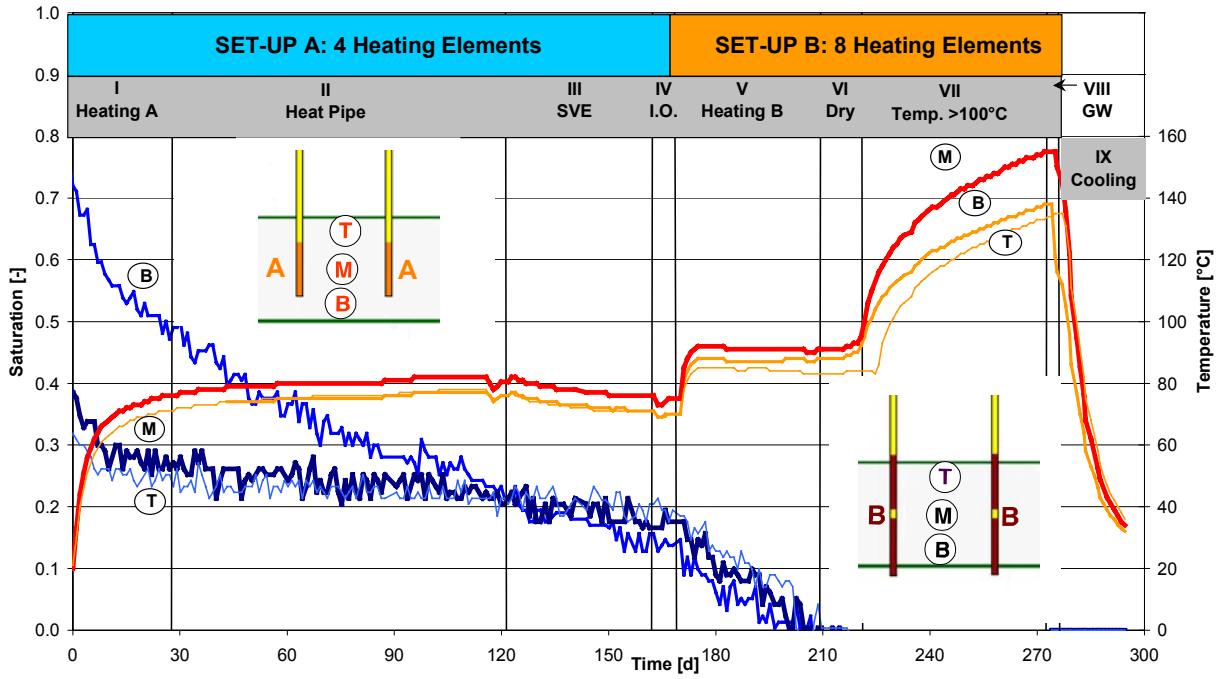

Fig. 4: Development of saturation and temperature in characteristic points in the centre profile

PHASE III: SOIL VAPOUR EXTRACTION

To reduce the impact of the heat pipe effect, saturation has to be lessened in the central area to obtain a higher temperature. The pore water has to be vaporised or drained completely, until a temperature above 100°C can be achieved. Therefore, soil vapour extraction was operated additionally to enable drying of the soil. The extraction horizons of the SVE wells are at about 1 m horizontal distance from the central area and located in the middle of the coarse sand. The influence of the SVE on the drying in the fine grain layer is marginal (Fig. 4). However, energy is extracted from the container, which can be seen from decreasing temperatures even in the middle of the low permeable layer.

PHASE IV: INTERMITTING OPERATION

An intermitting operation of the HE was tested to evaluate its effects on heat transport and drying. The HE cool down to surrounding temperature within some hours. Afterwards, a fast temperature decrease of the already heated subsurface, following the temperature gradient to the boundary can be detected. On the other hand, the influence on the saturation is low in case of a power cut of some hours. It might become of interest in case of a shutdown for several days, due to imbibitions in the cooling area (Fig. 5, phase IX, profile 1).

After restarting the heating, higher energy transfer is achieved only for a short period. With reaching the regular operating temperature of 500 °C, the energy consumption is as before.

PHASE V: HEATING PHASE B

To enlarge the energy input, the HE configuration was changed to set-up B (Fig. 3, right figure). Operating eight HE such that heating was provided over the total height of the fine grain layer doubled the heated length of the four thermal wells. The horizontal distance between the HE remained.

Right after starting, a higher temperature in the 'central cube' was observed (Fig. 4). The drying in the middle and the top heights of the fine grain layer changed rapidly in the 'central cube'. A similar drying behaviour can be observed now at all heights in the centre (Fig. 4).

Regarding a water balance for horizontal sections, the situation looks different. For this calculation, the data from the TDR-sensors are used. Over the height of the fine grain layer, five TDR-sensors per profile are installed. From these data, an average saturation per profile over the height of the fine grain layer is calculated (Fig. 5 top). Hereby, the profiles 1 and 2 are located outside the central area, the profiles 3 and 4 are located in the central area. Profile 2 and 3 are in symmetrical distance to the boundary of the 'central cube'.

During the operation of set-up A, no significant differences between the profiles are found. A differencing influence of the heat pipe effect or SVE-operation is not reflected by the average saturation. The situation changes clearly after changing the set-up: now the profiles 3 and 4 in the central area dry much faster compared to the profiles outside.

The analyse of the drying processes enables an assessment of the possibility to achieve 'heating over 100 °C'. They are calculated as an average drying per profile and experimental phase (Fig. 5, bottom). The heating phase A is characterised by a strong drying process in the centre and a moderate in the boundary region. While the heat pipe is dominant, the drying process decreases in all profiles. A significant effect of the SVE-operation on the drying in the fine grain layer cannot be found.

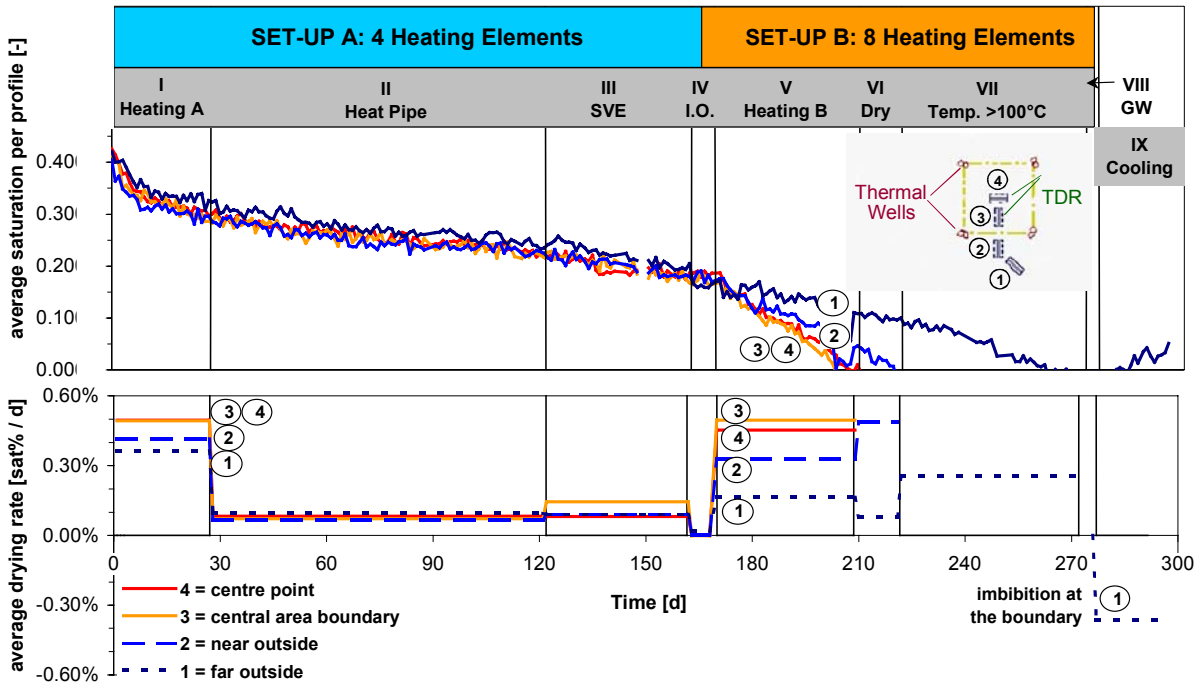

Fig. 5:Average saturation of vertical profiles in the fine grain layer (top) and average drying rate for each experimental phase (bottom)

With the change of the set-up, drying is enhanced at all profiles. Mostly affected is the central area. Here the efficiency increases by a factor of four compared to phases before and becomes equivalent to heating phase A. In contrast to that, a difference in the drying behaviour between the profiles inside and outside the central area can be seen.

A significant mean spatial saturation gradient from outside (profile 1) to the 'centre cube' (profile 3 and 4) is detected.

PHASE VI: DRYING IN THE CENTRE

Within six weeks, the 'central cube' is dried completely which enables to obtain a temperature higher than 100°C. It ensures an interruption of the 'central cube' with respect to liquid flow. Consequently the convective heat transport vanishes and only conduction dominates the heat transfer.

The complete drying in one profile enhances the drying in the neighbouring profiles. Hereby, the profiles 3 and 4 in the central area are characterised by an even drying behaviour (Fig. 5, phase V). The completed drying in these profiles provokes an acceleration of the drying in profile 2 (Fig. 5, phase VI) and analogous in profile 1 (Fig. 5, phase VII) after the drying of profile 2. This is caused by the reduction of the area where the heat pipe is dominant.

PHASE VII: Temperatures >> 100°C in the central area

A strongly rising temperature in the central area over the total height of the fine grain layer is characterising this phase. Higher spatial temperature gradients indicate that conduction is dominating the heat transport. A temperature of more than 150 °C in the middle of the fine grain layer and about nearly 140°C at its boundaries is achieved, when this phase is terminated.

This shows, that thermal wells can be successfully used for the heating of the subsurface to a temperature of 150 °C and more (Fig. 6). The further development of this in-situ remediation technology will be done with a remediation experiment in 2003.

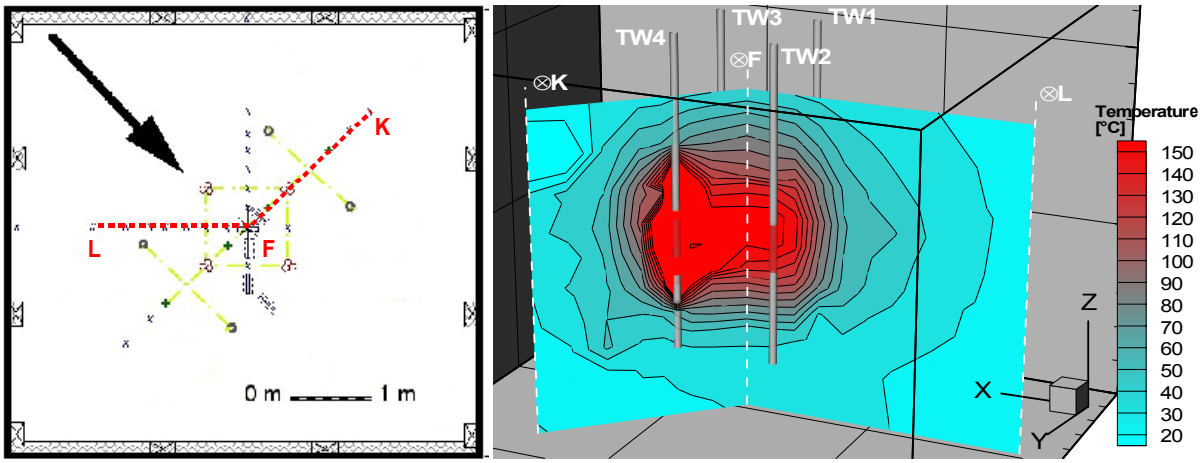

Fig. 6: Temperature profiles in the VEGAS technical scale container at the end of phase VII

PHASE VIII: RISING GROUNDWATER LEVEL

Seasonally fluctuating groundwater level might affect the remediation of a field site. To quantify this influence, the groundwater level is raised from 0.5 to 1.7 m, which is 30 cm below the low permeable layer, while keeping the HE under operation.

Capillary forces in the coarse sand suck water from the capillary fringe close to the hot and still dry boundary of the fine grain layer. Energy has to be transferred from the centre to this boundary of the fine grain layer to vaporise this water, which evokes a sudden temperature decrease at the bottom and in the middle of the fine grain layer (Fig. 4). The average saturation in the fine layer is not influenced yet (Fig. 5, all locations remaining dry).

The phase VIII shows clearly the great sensitivity of the heating process for the effect of adding water to the system: if the distance between the 'target zone' for the remediation and the capillary fringe is not sufficient, heating and thus efficiency of the remediation can be reduced. The influence of natural conditions must be carefully considered and surveyed individually for each site.

PHASE IX: COOLING PHASE

Fast cooling of the body of soil in the technical scale container occurs after shutting down the energy supply for the HE at the end of phase VIII. At the end of the cooling phase, remaining water from the fine grain layer boundaries is sucked in the former high temperature zone (Fig. 5).

4. CAPILLARITY AND HEAT PIPE

As described, the heat pipe develops in the fine grain layer causing a horizontal counter current flow of both liquid and water vapour [UDELL and FITCH 1985]. This results in a stagnation of temperatures.

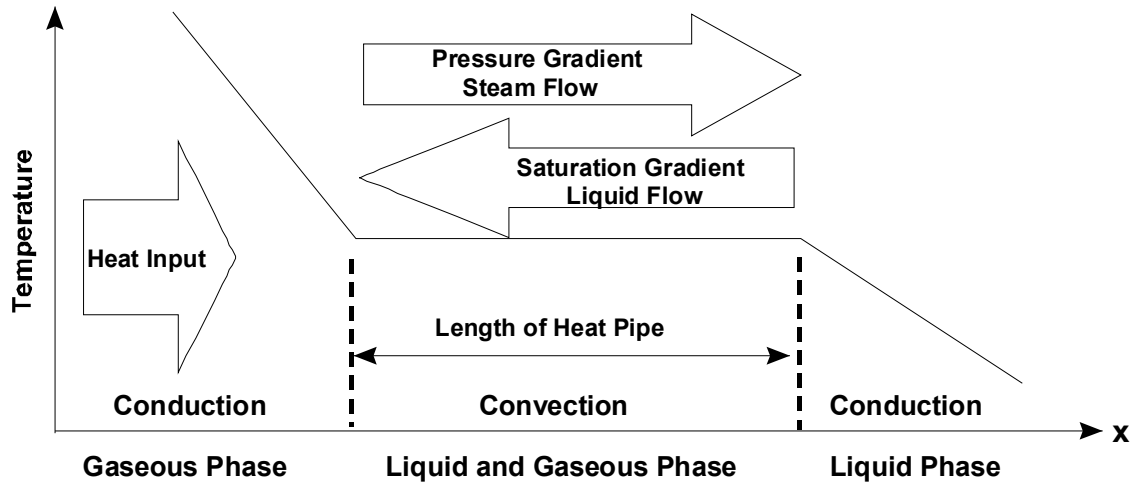

Fig. 7: Principle of the heat pipe

The heat pipe effect dominates the heat transport in the central area from phase II to phase V. This arises from two reasons: large capillary forces in the fine grain layer and large thermal well spacing compared to their length. These principles have to be transferred on the three-dimensional technical scale situation.

Therefore, the two set-ups of HE configurations must be distinguished. In set-up A with 4 HE, the horizontal distance between the HE (1 m) is twice the length (0.5 m) of the HE. The HE in set-up A operate more like 'single HE' (Fig. 8). In difference to that, the HE is extended to the total height of the fine grain layer in the set-up B. The relation distance of the HE to length of the HE is now about 1. Hereby, the 'permeable area for the heat pipe' (Fig. 8, grey areas) is significantly reduced. An immediate increase in temperature is observed (Fig. 4). In parallel, the saturation decreases much faster compared to the previous phases even in the centre profile.

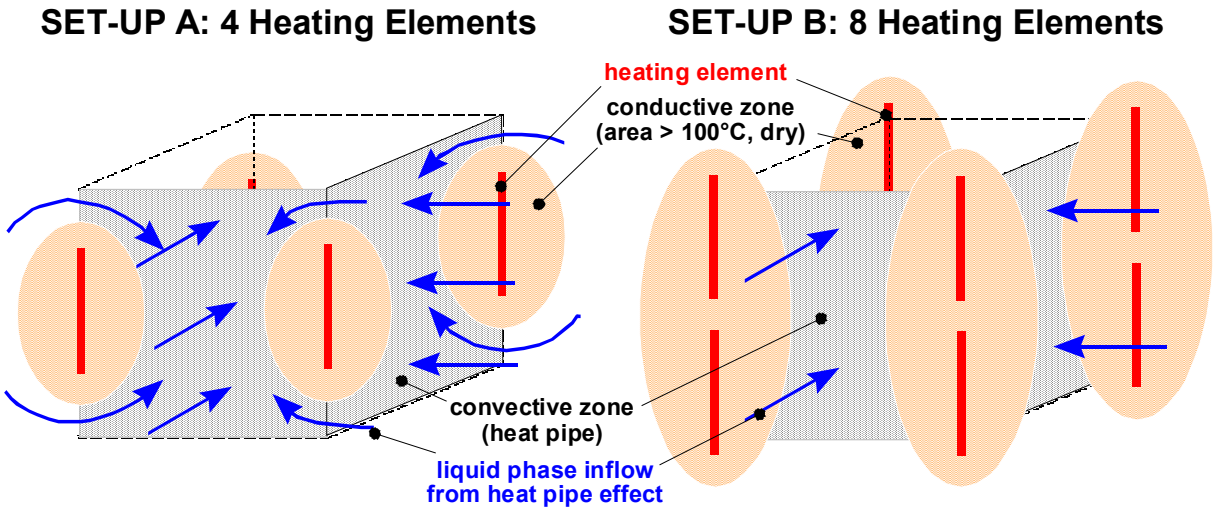

Fig. 8: Scheme of liquid flow into the central area in set-up A (4 HE) and set-up B (8 HE)

To illustrate the development of both temperature and saturation, cross-sectional profiles at the bottom and in the middle of the fine grain layer are presented (Fig. 9). Over the x-axis, the temperature section starts at the left side at the boundary point Tb, enters the central area between the thermal wells (Tc) and ends in the centre C. Directly next to it, the saturation section begins in the centre C, exits the central area between the thermal wells (Sc) and ends at boundary point Sb. Over the y-axis, the operation time of the experiment is shown.

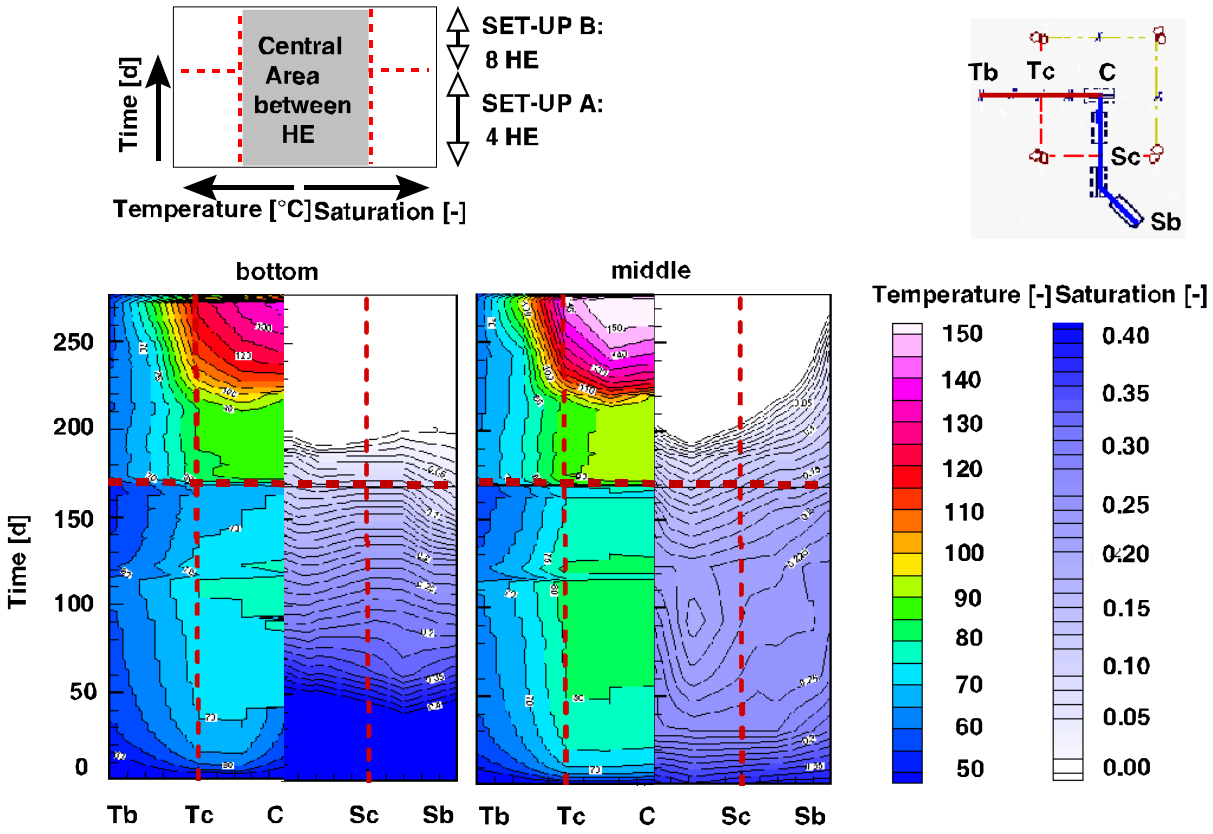

Fig. 9: Temperature and saturation over time along the section Tb – C – Sb at two heights in the fine grain layer

For set-up A, in the complete central area, temperature becomes stagnant, while outside still temperature gradients exist (phase II). Subsequently, temperature decreases due to the energy sink by SVE. On the other hand, differences in the drying progress are seen. At the bottom of the fine grain layer, drying over the complete length of this section is detected. It seems to be unaffected by the heat pipe. Nevertheless, while interpreting such data, it should be noticed, that the underlying processes of coupled heat and mass transfer are highly non-linear and complex. The middle of the fine grain layer shows a fast drying in the beginning (phase I) and later a quasi-stagnant saturation with a slow drying (phase II).

With the beginning of operation of set-up B, the temperature increases immediately. The influence of the still operating SVE is not noticeable anymore. The drying, especially in the central area, increases. As expected, this area dries at first. At the bottom of the fine grain layer, homogeneous drying along the complete section occurs.

5. CRITICAL OPERATION CONDITIONS

Aim of this experiment was not only to proof the technical feasibility of thermal wells on technical scale. Of interest are rather conditions, which have negative impact on the system even under otherwise positive conditions.

One of the critical factors is the failure of a HE or its temperature regulation. During the experiment, both cases happened causing each with the shutdown of one HE. This influenced the

whole temperature field. The breakdown was compensated by changing HE or regulating module, respectively. Therefore, standby regulators and heating elements are recommended for field sites.

The cooling even in the centre profile (Phase IV and IX) is much faster according to the heating. Dependent on the situation on a field sites, a stable power supply over the complete remediation time is important.

Even the groundwater level raised (phase VIII) near to the dry and very hot central area, led to a temperature decrease at the bottom of the fine grain layer. For field sites, a sufficient distance between the 'remediation zone' and the capillary fringe should be ensured to ease the remediation success.

6. PRELIMINARY SYSTEM OPERATION RULES FOR THERMAL WELLS

Despite a temperature of 150 °C in the 'central cube' was reached, the technical scale heat transport experiment shows some boundaries and limitations for this heating method.

Concluding numerical calculations [THEURER ET AL. 2003], laboratory [WINKLER 2003] and technical scale investigations, some preliminary design criteria for the use of thermal wells as a remediation technology in the unsaturated zone are deduced:

1. The 'target temperature' as criteria to ensure an almost complete remediation of the unsaturated zone depends on the type of contaminant.
2. The energy needed for heating depends on the soil type, characterised by its capillary forces, and the soil moisture.
3. Soil type and soil moisture determine the sustainability of the heat pipe effect.
4. The length of the operating heating elements per thermal well affects the required horizontal distance between the wells. This crucial aspect for the economic feasibility will be investigated in the further research.
5. The time required to reach the 'target temperature' depends on the heating temperature of the HE, the thermal well spacing and the ratio of well length to well spacing.
6. Thermal wells should allow the fast replacement of HE and their regulator assembly for maintenance works and quick replacement of damaged HE.
7. The vertical distance of the 'remediation zone' and the capillary fringe must be sufficient to ensure that the remediation success is not endangered due by temperature degradation.

7. CONCLUSIONS

The technical feasibility of the subsurface heating method 'thermal wells' is shown by technical scale experiment. More than 150°C is achieved in the centre of the 'central cube'. Depending on capillary forces and soil moisture, the heat pipe effect may dominate the heating process temporarily. Nevertheless, the efficiency of the heating process can be qualified by detecting the drying rate of the technical system.

From the current experiment and the results from numerical calculations and small-scale laboratory investigations, preliminary system operation rules are developed. These are needed for the conduction of the technical scale remediation experiment in 2003 at *VEGAS*.

The economical efficiency of the technology depends amongst others on the well spacing in the field and the heating time. The equations for an economical design will be developed during the technical scale remediation experiment.

ACKNOLEDEGEMENTS

Funding of this study is cooperatively provided by the Federal Ministry of Education and Research *bmb+f* and the research program *BWPLUS* of the federal state of Baden-Württemberg.

REFERENCES

HELMIG, R.; 1997: Multiphase Flow and Transport Processes in the Subsurface, Springer-Verlag, ISBN 3-540-62703-0.

HERON, T., HAUGAARD HERON, B., HERON, G. 2002: Full-scale clean-up of PCE and terpentine under buildings by steam injection, Proceedings of the 3rd International Conference on Remediation of Chlorinated and Recalcitrant Compounds, Monterey, May 20-26, 2002.

HIESTER, U.; THEURER, T.; WINKLER, A.; KOSCHITZKY, H.-P. 2002: Large-scale Experiments to develop a thermally enhanced Remediation Technology, Proceedings of the 3rd International Conference on Remediation of Chlorinated and Recalcitrant Compounds, Monterey, May 20-26, 2002.

HIESTER, U.; SCHRENK, V.; WEISS, T., 2003: Environmental Balancing of ´Cold' SVE and Thermally Enhanced Soil Vapour Extraction - Practical Support for Decision Makers, Proceedings of the ConSoil, ConSoil 2003, ICC, Gent, Belgium, May 12 - 16, 2003

KOSCHITZKY, H.-P., THEURER, T., SCHMIDT, R., WINKLER, A., FÄRBER, A., 2000: Pilot-scale study of steam injection for thermal in-situ remediation of the unsaturated zone below a hazardous waste site, Proceedings of ConSoil, Leipzig, Germany, September 18.-22., 2000, ISBN 0727729543, pp. 989 - 997.

SCHMIDT, R., KOSCHITZKY, H.-P. 1999: Pilothafte Sanierung eines BTEX Schadens an einem ehemaligen Gaswerksstandort mit der thermisch unterstützten Bodenluftabsaugung (TUBA) durch Dampfinjektion, Wiss. Bericht WB 99/5 (HG 262), Institut für Wasserbau, Universität Stuttgart.

THEURER, T., WINKLER, A., KOSCHITZKY, H.-P., SCHMIDT, R., 2000: Remediation of a landfill contamination by steam injection, Proc. of Groundwater 2000, Kopenhagen, Denmark, June 6.-8., 2000, ISBN 9058091333

THEURER, T.; WINKLER, A.; HIESTER, U.; KOSCHITZKY, H.-P., 2002: Developing thermally enhanced in-situ remediation technology by experiment and numerical simulation, International Conference Groundwater 2002, Berkeley, March 24-28, 2002, p 108-112.

THEURER, T.; HIESTER, U.; WINKLER, A.; KOSCHITZKY, H.-P., 2003: Mathematical and Numerical Modeling of Thermally Enhanced Remediation with Thermal Wells, Proceedings of ConSoil, ConSoil 2003, ICC, Gent, Belgium, May 12 - 16, 2003

UDELL, K.S., FITCH, J.S., 1985. Heat and Mass Transfer in Capillary Porous Media Considering Evaporation, Condensation and Non-Condensible Gas Effects. Paper presented at 23rd ASME/AIChE National Heat Transfer Conference, Denver, CO, 1985

WINKLER, A., THEURER, T., SCHMIDT, R., KOSCHITZKY, H.-P., 2000: Thermal In-Situ Remediation of Low Permeable Soils: Theory and Experimental Results, Proceedings of ConSoil, September 18.-22., 2000, Leipzig, Vol. 2, pp. 1127 - 1128.

WINKLER, A., CLASS, H., HELMIG, R., 2002: An Efficient Solution Technique for the Numerical Simulation of Thermally Enhanced Soil Vapour Extraction, International Conference Groundwater 2002, Berkeley, March 24-28, 2002, p 534-538.

WINKLER, A. 2003: Prozesse des Wärme- und Stofftransports bei der In-situ-Sanierung mit festen Wärmequellen. Mitteilungen, Heft 115, Institut für Wasserbau, Universität Stuttgart.

STIMULATING NATURAL ATTENUATION AT A BTEX-CONTAMINATED MEGASITE: THE SAFIRA ZEITZ PROJECT

Stefan Gödeke[1], Mario Schirmer[2], Carsten Vogt[3], Ralf Trabitzsch[1], Holger Weiß[1]
UFZ Centre for Environmental Research Leipzig – Halle, Germany
[1]Interdisciplinary Dept. of Industrial and Mining Landscapes, Permoserstr. 15, 04318 Leipzig
Phone: 0341-235-2333/2651/2127 ; Fax: 0341/235-2126
goedeke@pro.ufz.de, trabitzs@pro.ufz.de, weiss@pro.ufz.de
[2]Department of Hydrogeology, Theodor-Lieser-Str. 4, 06120 Halle (Saale)
Phone: 0345-5585201 ; Fax: 0345/558-5559
schirmer@hdg.ufz.de
[3]Department of Environmental Microbiology, Permoserstr. 15, 04318 Leipzig
Phone: 0341-235-2367 ; Fax: 0341-235-2247
vogt@umb.ufz.de

1 INTRODUCTION

The test site of the SAFIRA-Zeitz project is situated in the immediate vicinity of a former hydrogenation plant near Zeitz, Saxony-Anhalt, Germany. The acronym SAFIRA spells out to “Remediation research in regional contaminated aquifers”. The degradation of the contaminants at the site, under strictly anaerobic conditions in the aquifer, seems to be inhibited by a limited amount of nutrients and electron acceptors. Geochemical analyses have shown that sulfate is the terminal electron acceptor at the site (Wachter et al., 2001). BTEX (benzene, toluene, ethylbenzene, the xylenes), with benzene as the main pollutant, was found in the local aquifers to a depth of 50 m below ground, where benzene reaches concentrations of up to 200 mg/l. The project goal is to efficiently condition groundwater in order to enhance the degradation processes *in situ* (“Enhanced Natural Attenuation“). In its first phase, the project aims at the stimulation of the anaerobic degradation of the contaminants benzene and toluene in the aquifer.

Enhanced Natural Attenuation should be regarded as an alternative remediation strategy, when two lines of evidence exist: a) Natural Attenuation processes are taking place but are not sufficient to decrease the mass of the contaminant (e.g. when substances that are difficult to biodegrade contaminate the aquifer) and b) no potential receptor (e.g. well) downstream of the contamination is at immediate risk. The effectiveness of Natural Attenuation depends strongly on the processes of degradation and sorption. Natural and Enhanced Natural Attenuation (NA and ENA) can only be regarded as valid remediation strategies, when the cause – effect relationship between loss of contaminant and the mechanisms responsible for the loss are known (Macdonald, 2000). Therefore NA and ENA require a sound understanding of the geochemical and redox conditions at the site as well as a careful monitoring programme. It should be pointed out that the degradability or non-degradability of a compound depends on a variety of factors, such as the hydrogeologic, geochemical and microbiologic characteristics of the aquifer. Numerical modeling of the reactive contaminant transport at a site is a valuable technique to investigate if NA processes are ongoing and a necessary tool for making sensible, scientific decisions on the appropriate groundwater remediation strategies.

Injection of microorganisms (bioaugmentation) is a special way of trying to stimulate contaminant degradation in the aquifer, which already has been shown to be successful in field applications (Dybas et al., 1998). However, a major problem encountered with bioaugmentation is the limited spread of bacteria since they often adhere strongly to solid surfaces. A technique that tries to stimulate the transport of bacteria in the aquifer is the application of a direct current between two electrodes in the aquifer. Due to the electrokinetic transport of the bacteria, they can be transported laterally or even opposite to the groundwater flow direction (DeFlaun and Condee, 1997). Certainly, regulatory concerns over the application or injection of microorganisms need to be considered.

There are a variety of in-situ remediation techniques available. One of these options, which has gained a lot of attention, is the reactive barrier technology. The application of a reactive barrier attempts to minimise the use of mechanically operating systems, thus minimising long-term operation and maintenance costs. However, it is difficult to capture the full width of a large contaminant plume with a reactive wall and to reach depths greater than 15 m (Nyer et al., 1996). A special kind of reactive walls are in-situ microbial filters. This application involves the placing of sand mixed with non-indigenous microorganisms into a trench in the subsurface ahead of contaminant plumes. The contaminant is degraded by the microorganisms as it flows through the trench (Warith et al., 1999).

Crucial for the successful application of ENA as a remediation approach is a thorough understanding of the factors controlling the degradation of the contaminants. To evaluate these limiting factors, which depend largely on the geochemical- and redox-conditions of the groundwater, column and batch experiments in the laboratory are very important. The treatment method (e.g. aerobic or anaerobic or combinations of both) depend largely on the contaminants and their degradation products (Ndon and Randall, 1999). A long-term monitoring of observation wells is necessary to guarantee the success of the application. An advantage of the approach lies, besides the relatively low operating costs, in the utilisation of the aquifer volume, in which the stimulated degradation is taking place. Consequently, costly remediation techniques like “pump and treat” can be avoided (Effenberger at al., 2000).

2 LOCAL GEOLOGY

The local geology is very complex (Figure 1). The test site is located in a geological depression. The subsurface consists of two main aquifers, separated by a lignite and clay unit, whereas the lower aquifer is more sandy and consisting of less gravel than the upper aquifer. The lignite and clay unit is incomplete or non-existent in the immediate vicinity of the site. The lignite is mostly embedded in the clay, but in the contaminant source area, lignite is also in direct contact with the aquifer material. The aquifer material is made up of “braided-river” deposits. Typical sedimentological features are “fining upwards” sequences. Subrosion has caused significant vertical displacement throughout the stratigraphic units. Therefore the depth of the stratigraphic horizons is varying. The thickness of the different units is increasing towards the North and Northeast, where the center of the depression lies.

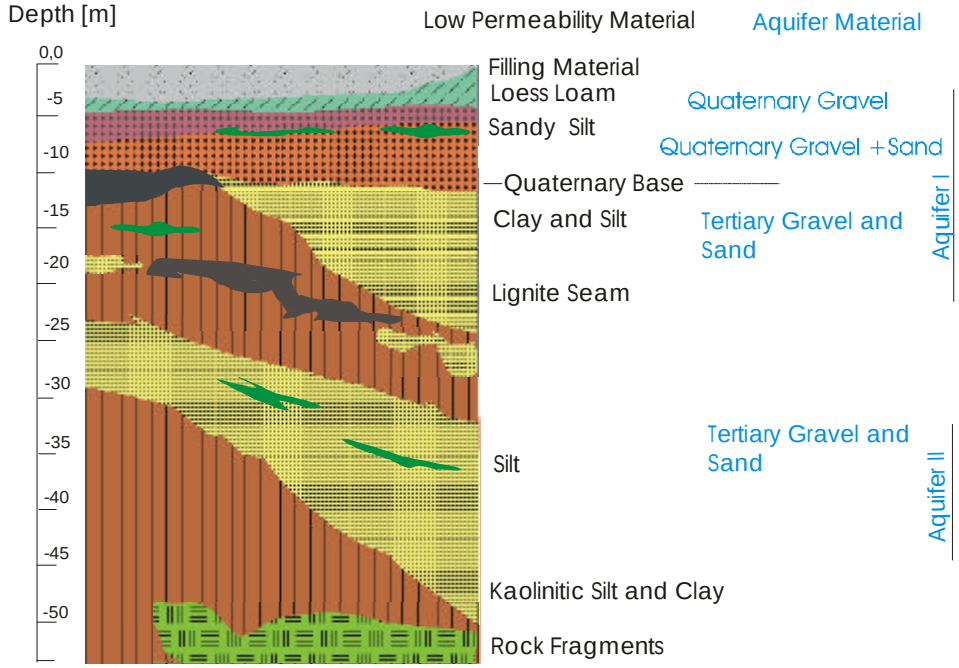

Figure 1. Schematic lithologic profile at the test site

3 GROUNDWATER CONDITIONING FACILITY

For the purpose of conditioning the groundwater, a below-ground facility was constructed, which allows to pump the groundwater from one or two extraction wells, pass it through a series of eight reactors (Figure 2), before re-infiltration of the water into the aquifer through one or several wells. The microbial degradation is monitored at different control planes consisting of observation wells. Electrical conductivity logs in the nearby wells have shown that the aquifer in this specific area is relatively homogenous. Further characteristics of the groundwater at the site are low Eh values (-200 mV and below) and a pH close to neutral (6,7-6,9 pH).
Before the groundwater enters the reactors, the water is pumped through a sand filter with a mesh-width of 0,1 mm. The water pressure is contained throughout the system to exclude any degassing and is finally released via a valve in the infiltration well, where the water can enter the aquifer over the full length of the well screen. The water is pumped from the lower aquifer via motor pumps, which are located at a depth of 25m. The motor pumps are frequency controlled. If the flow through the facility is

less than the target value, the frequency of the pump is automatically adjusted. Reactors, tanks and pipelines in the facility are all made of high-grade steel to prevent corrosion. Each reactor is 6 m long with a diameter of 25 cm. They are currently filled with granulated pumice. Pumice has been chosen as fill-material because of its high surface to volume ratio, which is ideal for microbial colonisation.
At different locations in the reactor chain, electron acceptors and nutrients can be added to the groundwater within the reactors. This is accomplished through revolving piston flow pumps, which have a maximum performance of 20 l/h. The adjusted amount of dosage is automatically controlled by a flow-meter. The introduced electron acceptors are fully mixed with the flowing groundwater while being pumped through the reactors. The electron acceptors have been dissolved beforehand in a dissolution unit (Figure 3). This unit is designed in a way that two different electron acceptors or nutrients can be dissolved simultaneously. It consists of a dissolution tank in combination with two storage tanks with a volume of 1600L. To optimise the dissolution process of electron acceptors and nutrients, the solution can be heated in the dissolution tank and kept in circulation between the tanks via a pump. Constant values of the electrical conductivity of the solution measured in the storage tank show a complete dissolution of electron acceptors and nutrients.
The reactors can be run in sequence so that the groundwater passes through all eight reactors, or the reactors can be used in parallel, in order to run different experiments simultaneously. The flow through the reactors can be varied between 0,2dm^3/h and 4m³/h. The parameters pH, Eh, dissolved oxygen, electrical conductivity and temperature of the groundwater can be measured at different locations within the facility. To assure anaerobic conditions, nitrogen is delivered to the tanks in the dissolution unit as well as to infiltration and extraction wells. This is important, since any oxygen entering the groundwater, e.g. due to leakages in the facility, could harm the population of sulfate reducing bacteria, which need strictly anaerobic conditions for growth (Fritsche, 1998).

4 GROUNDWATER FLOW CONDITIONS

The groundwater flow direction in the lower aquifer, the target aquifer of the project, is directed towards the NE (Figure 4). The field velocity estimated from the numerical model is approximately 1 m/d. The mean hydraulic conductivity from the sieve analyses of the lower aquifer is $5 \cdot 10^{-4}$ m/s.
Infiltration and extraction wells are approximately 60 m apart. A preliminary simulation of the pumping regime at the site was performed with the software Visual Modflow. Constant heads as boundaries were set perpendicular to the groundwater flow. The simulation showed that the distance between extraction and infiltration well should be not less than 50 m to prevent any short circuit flow between the wells due to the pumping in the extraction well. The nearest distance between infiltration well and the first observation well is 10 m. The draw down and increase of the water table due to pumping and infiltration was simulated for different scenarios using the software Wellz for Windows. Results showed that with the current pumping rate of 3.6 m³/h, water is pumped to the extraction well over a radius of about 100 m. Calculation were performed using the Theis-equation for confined aquifers and with typical transmissivity and storativity values for the aquifer in Zeitz. The maximum draw down or increase of the water table was about 10 cm . Since the governing equations for the calculation assume homogenous and isotropic conditions, the real draw down and increase of the water table will probably be a few cm higher due to heterogeneities. The groundwater velocity as a result of these forced gradient conditions was estimated to be around 5 m/d in the close vicinity of the infiltration well.

Figure 2. Reactors 1-4 of the facility.

Figure 3. Dissolution unit of the facility.

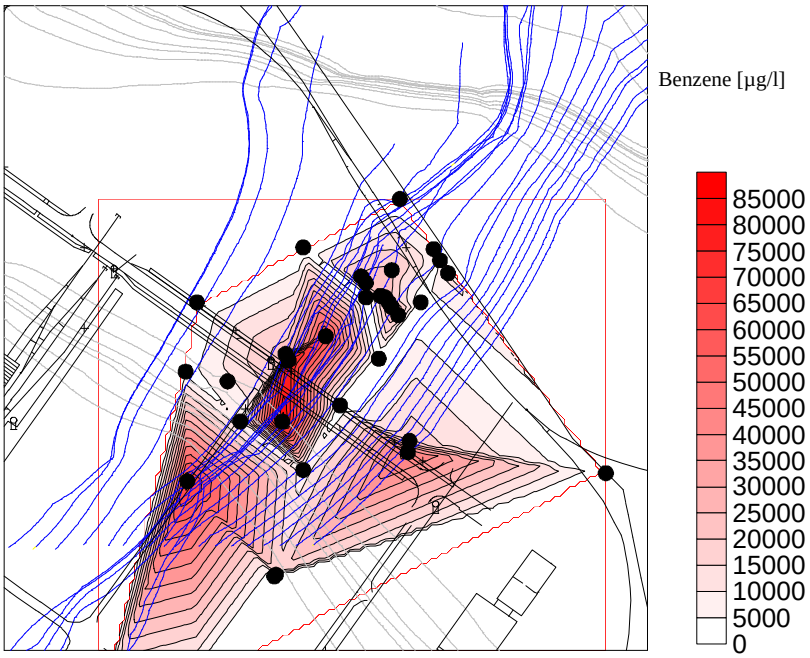

Figure 4: Benzene concentrations and groundwater pathlines of the lower aquifer

5 COMPLEMENTARY LAB EXPERIMENTS AND OPERATION OF FACILITY

Early dissolution and conditioning experiments with $MgSO_4 \cdot 7H_2O$ as electron acceptor and $NaNO_3$ and $NaPO_4$ as nutrients were run at the facility in Zeitz. The calculated field velocity from the addition of magnesium-sulfate agreed well with that of the numerical model and was in the range of 0.9 to 1 m/d. The usage of $NaNO_3$ in the experiments led to redox reactions in the reactors of the facility, which resulted in an oxidation of sulfide to elemental sulfur and the reduction of nitrate in the groundwater. Sulfide concentrations at the extraction well are in the range of 10 mg/l. To study the microbiological and geochemical effects of this, reaction batch experiments were performed. In this way it could be shown that the reaction was clearly a nitrate dependent biological oxidation of sulfide. The isolation of the responsible bacteria was not successful, but it is assumed that nitrate respiring sulfate reducing bacteria were involved, since sulfate is the main electron acceptor (Percheron 1999). In general, sulfate reducing bacteria have been accepted to inhabit a greater habitat range than previously thought (Stahl et al. 2002).
The dissolution and conditioning experiments also showed that the adding of ortho-phosphate (PO_4^-) as a nutrient is unsuitable for the groundwater at Zeitz. Due to the high Ca^{2+} concentrations (~ 6 mmol) in the groundwater (groundwater is saturated in regard to Calcite), very small amounts of phosphate lead to the instantaneous precipitation of amorphous hydroxy-apatite ($Ca_5(PO_4)_3OH$)).
Simulations with PhreeqC with the initial composition of the groundwater indicated that slight changes in pH (from 7 to 7,1) lead to an oversaturation with regard to hydroxyapatite. Bacterial growth experiments with meta-phosphate ($M_n[P_nO_{3n}]$; M = single charged metal) and two aerobic chlorobenzene degrading strains have proven the biological availability of meta-phosphate. Groundwater spiked with ortho- and meta-phosphate showed significant higher bacterial growth than groundwater without any additional phosphate. The advantage of meta-phosphate over ortho-phosphate as a nutrient is that a precipitation with ions like Ca^{2+} and Mg^{2+} can be ruled out, or occur at much lower levels.
Currently no additions are made to the groundwater. Subsequent tracer tests are in preparation. The duration of this first operating period depends on the results of the chemical analysis from the groundwater samples of the monitoring wells and the facility and on the laboratory experiments run in parallel. Groundwater samples are taken on a weekly basis. An option for a later operation phase could be the dosing of the strong oxidising agent peroxide (H_2O_2) into the groundwater flowing through the reactors. Two peroxide tanks with a volume of 1 m^3 each are situated in a shaft in front of the facility. The data obtained from sampling in the facility and at the observation wells is collected in a database to facilitate further evaluation.

6 RESULTS FROM THE FIRST OPERATION PERIOD

Results from time-series plots gave strong indications for the anaerobic degradation of benzene due to sulfate reduction (see circle in Figure 5). Benzene concentrations declined during a time-period of 15 days from 7.3 mg/l to 1.8 mg/l. Afterwards Benzene concentrations gradually inclined and reached a stable plateau, when the infiltrated groundwater reached a well located 52 m downstream of the infiltration well.

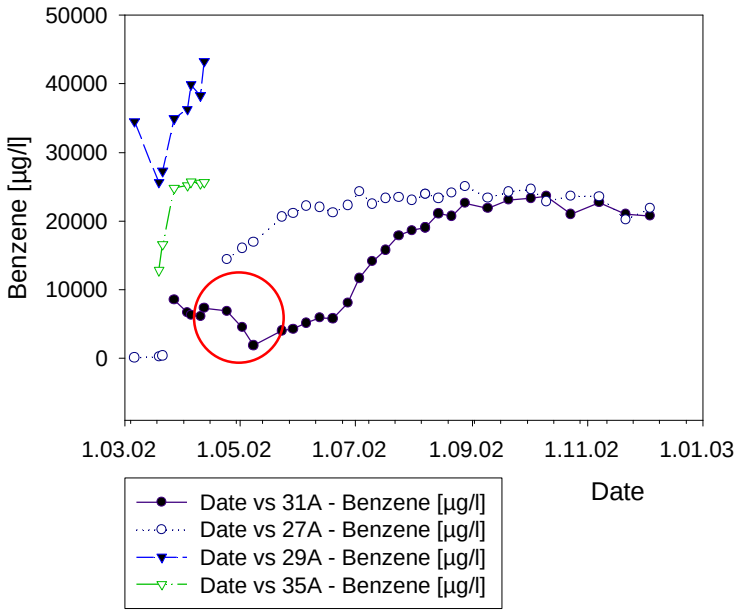

Figure 5. Development of benzene concentrations at downstream monitoring wells

The decline in benzene concentrations correlated with a decrease in sulfate concentrations and a rise in sulfide concentrations. Furthermore, pH values declined during this time-period and a significant rise of the water table was not observed. Benzene concentrations have now reached a stable plateau (see Figure 5), indicating stationary conditions at the downstream monitoring wells. It is possible that the higher benzene concentrations from the infiltrated groundwater inhibiteted the degradation processes.

Results from scatter plots (Figure 6 to Figure 8) clearly show that NA processes are ongoing at the site. For the construction of the scatter plots, data collected after an operation time of three months and after an operation time of 6 months of the facility were used. From Figure 6 it can be seen that m,p - xylene concentrations decreased in time relative to ethylbenzene concentrations. o – xylene concentrations are generally below detection limit.

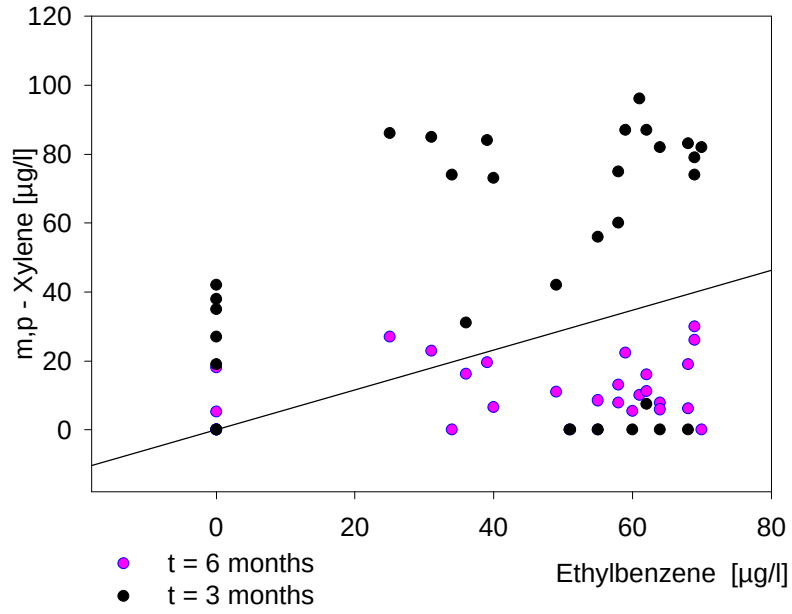

Figure 6. m,p-xylene concentrations vs. ethylbenzene concentrations from monitoring wells at the test-site

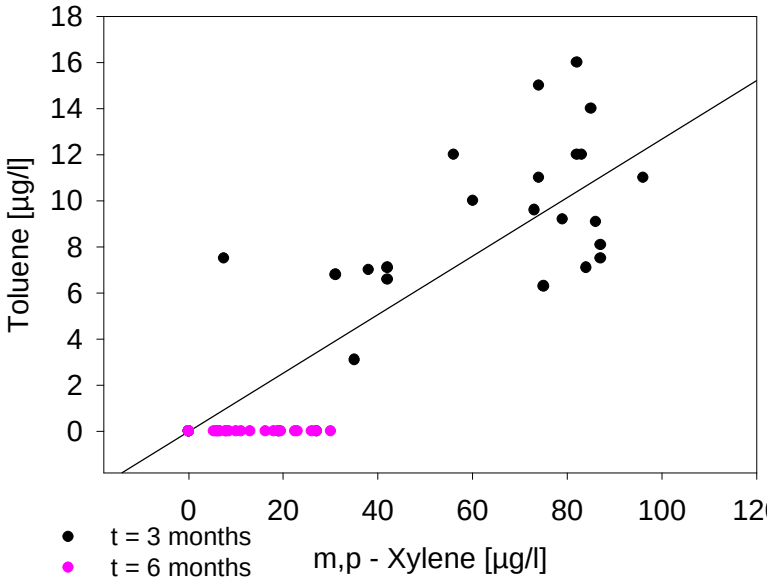

Figure 7. Toluene concentrations vs. m,p - Xylene concentrations from monitoring wells at the test-site

It is obvious from Figure 7 that toluene concentrations decrease in time relative to m,p - xylene concentrations. Despite the higher solubility of toluene in groundwater of approximately 600 mg/l (Montgomery, 1996) in comparison to m,p – xylene with approximately 200 mg/l, toluene concentrations in groundwater at the site are less than m,p – xylene concentrations. Figure 8 shows that ethylbenzene concentrations decrease in time relative to benzene concentrations. Benzene degradation is especially favorable in those locations where the preferentially degraded toluene, ethylbenzene and m,p-xylene already have been consumed by the responsible microorganisms. It can be seen that a preferential order of decay from easier to harder degradable compound exists, which is: toluene > m,p – xylene > ethylbenzene > benzene.

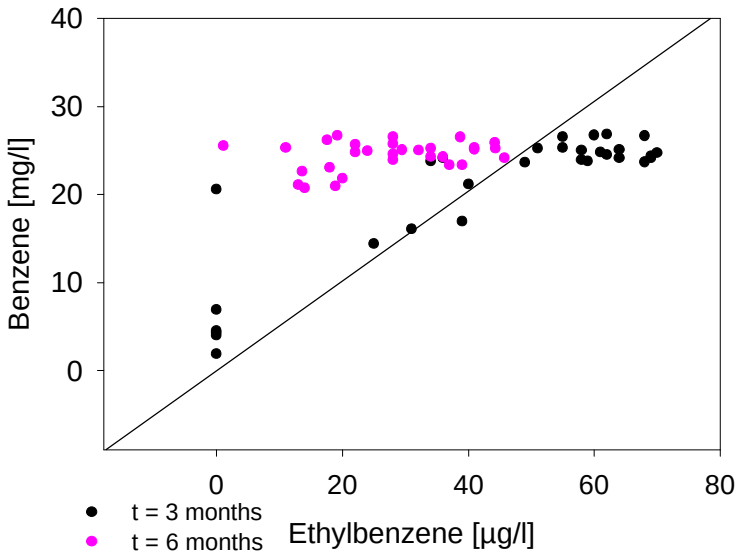

Figure 8. Benzene concentrations vs. ethylbenzene concentrations from monitoring wells at the test-site

In order to gain insight over consumed electron acceptors and electron donors, sulfate-, sulfide-, bicarbonate- and benzene-concentrations were compared between two control-planes orientated along the groundwater flow direction. Each control plane consisted of three monitoring wells, whereas the control planes are 50 m apart. The monitoring wells are screened over the full length of the aquifer (screen length between: 10 – 15 m). The spacing between the wells is approximately 9 m. The wells are located within the infiltrated contaminant plume. For the comparison of the concentration data, a time period with a length of 2 months (Nov.-Dec. 2002), was chosen, for which steady-state conditions could be assumed (Figure 5). For each control plane the arithmetic mean of the weekly concentration for each parameter was calculated and the differences compared. Table 1 shows the calculated differences for each parameter. A negative sign indicates the reduction of a parameter along the flow path. Dispersion has not been taken into account for this calculation.

Table 1. Calculated differences between control-planes

Parameter	**Difference (mmol)**
Benzene	- 0.012
Sulfate	- 0.28
Sulfide	0.24
Bicarbonate	0.56

It can be seen that sulfate reduction is taking place. Regarding the difference for sulfate of 0.28 mmol and taking the estimated groundwater flow-velocity of the numerical model of 1m/d into account, this value indicates a fairly high sulfate reduction rate (McGuire et al. 2002). Since a weak negative correlation (with a correlation coefficient of –0.42) between benzene and sulfate was observed at the infiltration well, the ratio of the differences of Table 1 was compared to the stoichiometry of the equation (Wiedemeier et al.1999),

$$7.5\ H^+ + 3.75\ SO_4^{2-} + C_6H_6 \rightarrow 6\ CO_2 + 3.75\ H_2S + 3\ H_2O \qquad (1)$$

which assumes benzene reduction due to sulfate reduction. Bacterial growth is neglected in this equation. The almost equal production of sulfide from the reduction of sulfate confirms the low concentrations of iron, which have been measured (~0.5 mg/l Fe). Higher dissolved iron concentrations would result in a greater loss of sulfide due to FeS_2 precipitation, since the

groundwater is highly oversaturated with regard to FeS_2 (SI : 11). The difference in bicarbonate concentration is higher than expected from equation 1, which indicates that other processes and parameters are also important. If the loss of benzene were due to sulfate reduction and not dispersion, the ratio of benzene consumed to sulfate reduced would be much higher than expected from the stoichiometry of Equation 1 (23 instead of 3.75). It is not unusual that higher amounts of consumed sulfate for the oxidation of benzene are observed (Reinhard et al. 1997, Anderson and Lovley 2000), but the large difference found and the differing ratio for bicarbonate demonstrates that other processes and parameters have to be considered. It is obvious that other, more easily oxidisable substances than benzene have not yet been taken into account. Toluene-, ethylbenzene- and xylene – (TEX) concentrations were negligible during this time-period. A process that might be important in this combination is the anaerobic oxidation of methane due to sulfate reduction (Valentine, 2002). The extraction well is located at a distance of approximately 40 m from the highest measured benzene concentrations (190 mg/l) of the lower aquifer, where methanogenesis may be expected. Since methane is subject to transport processes (Christensen et al. 2001), it is possible that groundwater with elevated methane concentrations is infiltrated into the aquifer, where it is oxidised according to equation 2:

$$CH_4 + SO_4^{2-} \rightarrow HCO_3^- + HS^- + H_2O \qquad (2)$$

7 CONCLUSIONS AND PERSPECTIVE

The facility offers the possibility for wide range of applications for the stimulation of the Natural Attenuation processes at the site. Different electron acceptors and nutrients can be dosed into the reactors and the groundwater. Furthermore, the reactors themselves can be used for experiments. The dissolution and conditioning experiments showed that $NaPO_4$ and $NaNO_3$ cannot be used as nutrients due to precipitation reactions. In microcosm experiments metaphosphate proofed to be a superior choice of nutrient compared to orthophosphate. The background geochemistry of the groundwater with low dissolved phosphate concentrations is an important factor influencing the natural attenuation rate at the site. Strong indications for the anaerobic degradation of benzene due to sulfate reduction have been found. From scatter plots it is apparent that a preferential order of degradation for the contaminants exists at the site. This preferential order of decay from easier to harder degradable compounds is: toluene > m,p-xylene > ethylbenzene > benzene. Under non-stimulated conditions, Natural Attenuation processes are slow. It has become evident that an active sulfate reducing population of microorganisms exists at the site. Future work will examine if other compounds beside BTEX may be oxidized via sulfate reduction at the site. In this respect, methane could be an important parameter. In order to assure that benzene is degraded along the flow path, dispersion needs to be quantified. Therefore a tracer-experiment with the conservative tracer KBr will be performed. For the investigation of the potential metabolites phenol and toluene of anaerobic benzene degradation (Coates et al. 2002), laboratory experiments and analyses will be performed.

8 ACKNOWLEDGEMENTS

The project is funded through the SAFIRA - (Remediation research in regionally contaminated aquifers) Programme of the UFZ Centre for Environmental Research Leipzig-Halle. Additional funding is provided by the German Federal Ministry of Education and Research (BMBF) under reference number 02WT0041.

9 REFERENCES

Anderson, R. T. and Lovley, D. R. (2000) Anaerobic Bioremediation of Benzene under Sulfate Reducing Conditions in a Petroleum-Contaminated Aquifer. Environ. Sci. Technol. 34, 2261-2266.
Christensen, T. H. et al. (2001) Biogeochemistry of landfill leachate plumes. Applied Geochemistry 16, 659-718.
Coates, J. D., Chakraborty, R. and McInerney, M. J. (2002) Anaerobic benzene biodegradation - a new era. Research in Microbiology 153, 621-628.
Dybas, M. J. e. a. (1998) Pilot-Scale Evaluation of Bioaugmentation for In-Situ Remediation of a Carbon Tetrachloride-Contaminated Aquifer. Environ. Sci. Technol. 32, 3598-3611.
DeFlaun M.F., Condee C.W. (1997): Electrokinetic transport of bacteria. Journal of Hazardous Materials 55, 263-277.

Effenberger M, Schirmer M., Weiss, H. (2000): Der Einfluss des Benzininhaltsstoffes MTBE auf den “Natural – Attenuation”- Ansatz bei Benzinschadensfällen. TerraTech 6, 58 – 63.
Fritsche W. (1998): Umweltmikrobiologie. Fischer, Jena.
Macdonald, J. A. (2000) Evaluating natural attenuation for groundwater cleanup. Environmental Science & Technology 34, 346A - 353A.
McGuire, J. T. et al. (2002) Evaluating Behavior of Oxygen, Nitrate, and Sulfate during Recharge and Quantifying Reduction Rates in a Contaminated Aquifer. Environ. Sci. Technol. 36, 2693-2700.
Montgomery, J. H. (1996) Groundwater chemicals desk reference. Lewis Publishers
Ndon U. J., Randall A. A. (1999): Periodic Aerated Treatment and In-Situ Bioremediation Strategies for Polyhalogenated Compounds. Water Research 33, (11), 2715-2720.
Nyer E. et al. (1996): In-situ Treatment Technology. Lewis Publishers, New York
Percheron, G., Bernet, N. and Moletta, R. (1999) Interactions between methanogenic and nitrate reduching bacteria during the anaerobic digestion of an industrial sulfate rich wastewater. FEMS Microbiology Ecology 29, 341-350.
Reinhard, M., Shang, S., Kitanidis, P. K., Orwin, E., Hopkins, G. D. and Lebron, C. A. (1997) In situ BTEX biotransformation under enhanced nitrate- and sulfate-reducing concentrations. Environ. Sci. Technol. 31, 28-36.
Stahl, D. A. et al. (2002) Origins and diversification of sulfate-respiring microorganisms. Antonie van Leeuwenhoek 81, 189-195.
Valentine, D. L. (2002) Biogeochemistry and microbial ecology of methane oxidation in anoxic environments: a review. Antonie van Leeuwenhoek 81, 271-282.
Wachter T., Dethlefsen F. Dahmke A. (2001): Neubewertung der Eisen (III)-Oxidationskapazität bei NA-Prozessen anhand von Literatur- und Feldstandort-Daten. 3. Symposium „Natural Attenuation – Umsetzung, Finanzierung, Perspektiven“, DECHEMA, Frankfurt/M., Germany, Dec 04-06.
Warith M., Fernandes L., Gaudet N. (1999): Design of in-situ microbial filter for the remediation of naphthalene. Waste Management 19, 9-23.
Wiedemeier, T. H., Rifai, H. S., Newell, C. J. and Wilson, J. T. (1999) Natural Attenuation of Fuels and Chlorinated Solvents in the Subsurface. New York: John Wiley & Sons, Inc. 617.

LCA METHODOLOGY FOR REMEDIATION STRATEGY SELECTION

F. Abeer Shakweer and C.Paul Nathanail
School of Chemical, Environmental and Mining Engineering (SChEME), University of Nottingham, University Park, Nottingham NG7 2RD, UK. Tel: + 49 8095 872 977, Enxafs@nottingham.ac.uk
Lecturer, School of Chemical, Environmental and Mining Engineering (SChEME), University of Nottingham, University Park, Nottingham NG7 2RD, UK. Tel: + 44 115 951 4099 Paul.nathanail@nottingham.ac.uk

Abstract
Although remediation activities used to reduce contaminated land related risks support sustainable development (SD) by helping to restore the land as a resource; preventing the spread of pollution to air and water; and reducing the pressure to develop on green field sites, those activities can result in harmful releases to different media. Consequently, a number of approaches and decision support systems (DSS) are being used for the selection of the preferred, most environmentally benign remedial action. However most of these approaches were developed for environmental assessment projects in general and not for remediation projects in particular. There is a need for more focused techniques to help in selecting the preferred remediation scheme within the context of SD.

A new methodology, based on Life Cycle Assessment (LCA) concept, was developed to help in remedy selection processes within the context of SD by considering its three components (environmental, social, and economic). A Detailed guidance on how to implement each phase within the new methodology together with a series of associated templates were developed to provide a comprehensive way for tackling the remedy selection process.

Introduction
Contaminated land problems have become an increasingly important issue in many areas of policy, research, and practice at both national and international levels. According to the UK Environmental Protection Act 1990, contaminated land is defined as “any land which appears to the local authority to be in such a condition by reason of substances in, on or under the land that

1. Significant harm is being caused or there is a significant possibility of such harm being caused or
2. Pollution of controlled waters is being or is likely to be, caused“.

Another definition by the North Atlantic Treaty Organization, Committee on the Challenges of Modern Society (NATO/CCMS) states that “contaminated land is any land which contains substances that, when present in sufficient quantities or concentrations, are likely to cause harm directly or indirectly to humans, the environment or on occasions to other targets“ (Bardos, 1994).

According to CLARINET, (2002) the contaminated land problem is a primarily post 1800s problem in terms of cause, and a post 1970s phenomenon in terms of the need for risk management. Contaminated land is a legacy of former industrial activity. Consequently, industrial countries, especially those who were subjected to early industrialization, suffer from contaminated land problems more than other countries. However, in many rural areas, intenive farming practices essential for food supply are the main causes of contamination (Christie et al., 1998, Bardos, 1994, and Petts et al., 1997).

Remediation of contaminated land is a field of technology that has developed and grown recently to assist in the reclamation of contaminated areas. Remediation techniques aim at protecting human health and the environment; enabling redevelopment; and limiting liabilities (Bardos et al., 1999b).

Over the past decade a large number of remediation techniques have been evolved, and a wide range of emerging as well as mature technologies are now available. However, as with any industrial process, remediation techniques can have harmful releases to different media. This has drawn the attention to the need for advanced techniques to help in selecting the preferred, most environmentally benign remedial action (Bardos et al., 1999b, Volkwein, 1997 and Varnes et al, 1999).

A number of approaches and Decision Support Systems (DSS) have been developed to assist in the remedy selection process. The most common remedy selection approaches and DSS are: Cost Benefit Analysis (CBA); Environmental Impact Assessment (EIA); Risk, Environmental merit, and Cost (REC) decision support system; Multi Criteria Analysis (MCA); and Life Cycle Assessment (LCA). However, there

is a need for more focused techniques for selecting the preferred remediation strategy within the context of sustainable development (Varnes et al. 1999, and CLARINET, 2002).

1.2 Background to the problem

Contaminated land risk may be considered in terms of a source of contamination, a pathway, and a receptor at risk, fig (1). The assessment of a contaminated land problem is a multi-stage process which includes: the suspicion that a certain site is contaminated followed by the appropriate site investigations, the determination of site contaminants and unacceptable risk to human health or the environment and the final decision on the necessary remediation (Ellis and Rees, 1995).

Due to the complexity of contaminants, more than one remedial method may be necessary for the treatment of a contaminated site. A combination of several treatment methods is usually required to achieve successful clean-up for the site as a whole. The series of remediation techniques form what is called a "remediation scheme or remediation strategy". In most cases it is possible to identify several remediation strategies, which are able to achieve the remediation objectives and overcome constraints for a contaminated site (Hester and Herbert, 1994 and CIRIA, 1995).

It should be clear that the use of remediation processes do not always lead to a positive environmental balance due to the use of different resources such as energy and water during the remediation process which may lead to the transfer of contaminants to another component (Okx, 1998). Therefore, attention should be given to the process of selecting the remediation strategy which minimizes unwanted impacts on the environment.

The available remediation strategy selection tools are focus, to a great extent, on the narrow aspects of solving the contamination problem and funding the proposed. This may lead to other problems in the future. Despite the number of analytical tools (e.g. LCA, MCA) which began to consider the wider environmental values within the remedy selection process, more effort should be exerted to consider the social and economical aspects of sustainable development for remedy selection process. The need for decision support techniques that consider sustainable development, risk management and stakeholders participation within the remedy selection process are recognized by several authors and environmental bodies (e.g CLARINET, 2002 and Bardos et al., 2001).

In this paper, a LCA based methodology is proposed as a solution to the above problem. The proposed methodology is a new LCA based Methodology for Remedy Selection (A*fr*S) within the context of SD. A*fr*S takes into account the three components of sustainable development (environmental, social, and economic). The output of A*fr*S is believed to be the preferred remediation alternative from an environmental, social, and economic point of view.

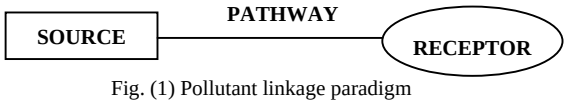

Fig. (1) Pollutant linkage paradigm
After Bardos, 1999b

The LCA approach studies the environmental aspects and potential impacts throughout a products' life (i.e. cradle-to-grave) from raw material acquisition though production, use and disposal. The approach consists of the following four phases: goal and scope definition; inventory analysis; impact assessment; and interpretation. While the goal and scope definition aims at identifying the goals of adopting the intended study, the inventory analysis phase involves data collection and calculation procedures to quantify relevant inputs and outputs of all processes under investigations.

Impact assessment phase evaluates the environmental impact cause by different resources and emissions. Finally the interpretation phase aims at representing the LCA results in terms of key issues which will be usable within the decision making process (Friedrich, 2002 and Curran, (1997).

2. Developed Methodology

Before designing the proposed A*fr*S methodology, a review on the existing techniques for remedy selection processes (e.g. Cost Benefit Analysis, REC Decision Support System, etc.) is presented. This covers the criteria considered within the remedy selection process for different remedy selection techniques, the advantages and disadvantages of each technique, and the feedback from the application of those techniques to real world case studies. In addition a detailed analysis for the application of LCA approach to environmental problems in general and to contaminated land problems in particular was carried out. Based on the adopted survey and analysis, the new A*fr*S methodology was developed.

While developing the A*fr*S methodology, the main aim was to develop a methodology for remedy selection that fits within the context of SD by considering the three aspects of SD (social, environment, and economic). Ease of use was another but secondary objective.

A*fr*S consists of eleven phases: Planning, Scope definition, Preliminary data collection, Screening, Data collection, Analysis, Ranking, Environmental interpretation, Economic interpretation, Final interpretation, and Evaluation, Fig (2). The Economic interpretation and Final interpretation phases were added to the methodology based on feedback from an initial pilot case study.

The methodology's eleven phases can be categorized into four main steps. Each main step consists of a number of phases which account for one component of the sustainable development concept, table (1).

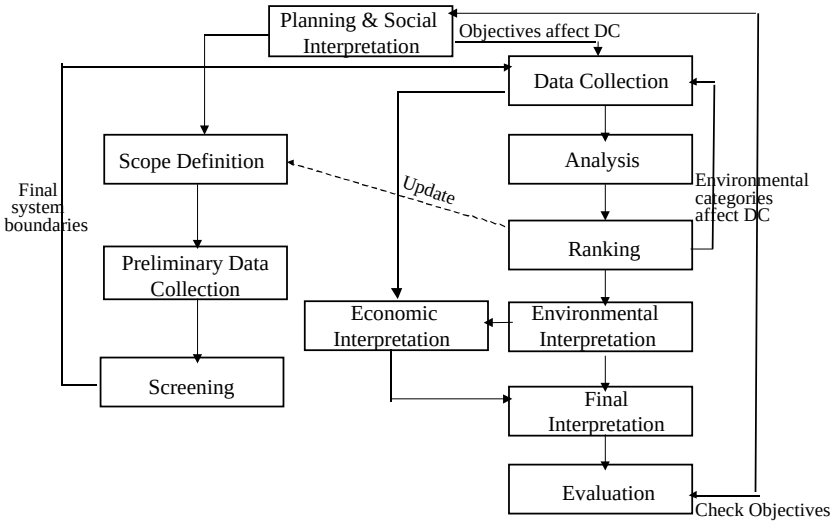

Fig (2) The new developed methodology for the selection of the preferred remediation scheme

Main Steps	**Phases within the main step**	**Sustainable development's element considered within the main step**
Planning and social interpretation	Planning and social interpretation	Social element
Environmental Interpretation	Scope definition, preliminary data collection, screening, data collection, analysis, ranking, and environmental interpretation	Environmental element
Economic Interpretation	Economic interpretation	Economic element
Final Interpretation	Final interpretation and evaluation	

Table (1) The main phases within AfrS methodology

2.1 Planning and social interpretation phase: The aim of the planning and social interpretation phase is to develop an overall framework for the whole remedy selection process by determining the objectives, constraints, and stakeholders of the selection process. In addition, a timeplan for the whole methodology should be developed by the end of this phase.

Public involvement takes place during this phase. Although public involvement raises the cost and delays the selection process, it brings local knowledge, fresh perspective, and hidden issues to the assessment process. In addition, it prevents misunderstanding between the developers and local residents. However, the following challenges may be encountered within the public participation process: the public is not a defined body, public are not experts, and communicating with public is complicated (IChem, 2002).

There are a number of innovative methods proposed for public participation, for example: workshops where meetings are held to provide information and discuss issues in detail; focus groups/ forums to gain understanding of perceptions. In addition, public participation through dialogue makes the process open, and transparent. All stakeholders are involved in the process from the beginning, all participants

contribute, any conflict can be dealt with constructively, all are treated equally, underlying needs and interests are explored and assumptions are teased out (IChem, 2002).

For the sake of this methodology, the two suggested techniques for communicating with stakeholders' representatives are meetings and questionnaires. A number of meetings should be arranged where the problem under investigation and the suggested solutions should be explained to stakeholders' representatives. Also the meaning of different environmental themes (e.g. global warming, ozone depletion) and the effect of the proposed remediation strategies on those themes should be clarified.

During the arranged meetings, stakeholders' representatives should be asked to state their own objectives, concerns and constrains with respect to the remedy selection process. In addition, they should be involved in evaluating the importance of different environmental themes that should be considered within the remedy selection process. This later step takes place by asking stakeholders' representatives to weight different environmental themes according to their importance. This may be done through a questionnaire.

The list of environmental themes "preliminary list of environmental themes" considered within the questionnaire was developed by combining and analyzing lists by the Society of Environmental Toxicology and Chemistry (SETAC) and the Center of Environmental Science (CML) at Leiden University Institute to be considered within any LCA study and one by Bardos et al., (1999a) to be considered within any remedy selection process. Finally, a timeplan for the remaining phases within A*fr*S methodology should be developed.

2.2 Scope definition: During this phase, the initial system boundary which includes all processes and activities that should be considered within the remedy selection should be set. In addition, whether the remedy selection process will be a screening or detailed study should be determined.

The functional unit which is defined as "the service or function on which alternative products or systems are to be compared" should also be identified within the screening phase (Clift, 1997). Although in most cases, the functional unit is taken as one unit of the product (i.e. output), it is more appropriate in the case of remediation strategies to take the functional unit as one unit of the input (i.e. contaminated soil). This is due to the fact that the output from different remediation strategies will not be of similar contents (i.e. percentage of contaminants in one unit of soil remediated using different remediation strategies are not exactly the same). Consequently considering the output as the functional unit will not provide a fair and uniform basis for the comparison process.

2.3 Preliminary data collection: This phase aims at collecting preliminary data on all processes and activities included within the initial system boundary. The collected data will be used for future calculations within the following screening phase. While data can be collected from generic sources and similar case studies, site specific data should be collected whenever possible.

The template developed for this phase includes a section where the sources of data can be documented. In addition, the collected data is stored in a data collection form, which is a part of the preliminary data collection template.

2.4 Screening: The screening phase aims at identifying significant and insignificant processes within each remediation alternative. A significant process is the one which affects the final result of the remedy selection process. For a remediation strategy, process with more than 5% contribution to the total environmental impact of the whole remediation strategy is considered as "significant process".

The environmental impact of each process within one remediation strategy is calculated as well as its relative contribution to the whole scheme. By the end of this phase, insignificant processes are excluded from the system boundary and the final system boundary for each remediation alternative is redrawn.

During the screening phase, calculations similar to those carried out during the analysis, ranking and interpretation phases are adopted. Consequently, it can be said that the screening phase is a prototype for the whole remedy selection process.

For simplicity within the screening phase, the environmental impact caused by energy consumption is not included in the calculated environmental impact caused by remediation strategies. However, the amount of energy consumed by each remediation alternative is calculated and presented as a stand alone piece of information where processes and activities with high environmental impact and/or high energy consumption are excluded from the system boundaries. A detailed explanation of the calculations carried

out to compute the environmental impact caused by a remediation alternative will be presented during the "analysis, ranking and interpretation" phases.

2.5 Data collection: After determining the final system boundary, more data on all processes and activities within this final system boundary is collected. At this stage, site specific data should be obtained as much as possible. In general, the collected data should be as accurate as possible. Similar to the preliminary data collection phase, data collection template includes a special data collection form to ease data storage and retrieval, figure (3).

5. Data Collection

5.1 Processes to be included	**Scheme 1**	Name of the remediation technique (e.g. Pump and treat)				
		Included		*Excluded*		
	Water pumping and treatment unit	*				
	Transportation			*		
	Energy consumption	*				
5.2 Required Data	**P&T**					
	Used Pump					
	Type of energy	Diesel				
	Energy consumption	15KW				
	Well excavation					
	Used rig	DANDO 2000				
	Energy consumption	13.4 kW				
	Treatment unit	Air stripping				
	Transportatio					
	No. of workers	20				
5.3Data Sources	Literature	Wong, J.W, Lim, C.H, and Nolen, G.L. (1997) Design of Remediation Systems. Lewis publishers, Florida, U.S.A. ISBN: 1 56670 217 8				
	Database	None				
	Internet	Personal environmental personal calculator, available from www.ans.neep.html.				
	Companies	Georemediation, DANDO				
5.4 Data Storage	**Process Name**	**Data Collection Form**				**Date**
	Mass Balance	**Inputs = Outputs + Emissions**				
		Inputs		**Added Substances**	**By products**	**Emissions From the treatment unit**
	Contaminants	microg/lit	mg/lit	None	None	To river (mg/lit) / To air (mg/kg)
	Benzene	2.6	0.0026	None	None	to be calculated / to be calculated
	TPH	256	0.256	None	None	N/A / N/A
	Energy Balance	**Inputs = Consumed + Output**				
		Inputs		**Consumed**		**Outputs**
	Dando2000 rig			13.4 KW		
	Total Energy consumption			0.06064MJ/Kg		
	Remarks	The output form the P&T pump was considered as the required standards				

site specific data

technique specific data

overlapping data

Fig (3) data collection template

2.6 Analysis: The data collected during the previous phase "data collection" is then processed to calculate the environmental impact caused by each remediation strategy. Those calculations are carried out through three main steps "mass and energy balances; classification; and characterization".

- *Mass and energy balance calculations:* The starting point of the analysis phase is to calculate mass and energy balances for all processes within the remediation alternatives under investigation. This step aims at completing any missing data by calculating the emissions released by all processes to different media.
- *Classification:* Using special classification tables emission (Van den Berg, 1995), emissions from each process are classified according to their contribution to different environmental themes (i.e. emissions contribute to a certain environmental theme form one category). One emission may contribute to more than one environmental theme. For example, benzene contributes to both aquatic toxicity and smog environmental themes.

- *Characterization:* The characterization process converts all emissions to their equivalent values of a theme's key emission. For example, CO_2 is the key emission of the "global warming" theme, consequently all emissions which contribute to the global warming theme are converted to their equivalent values of CO_2. This process is carried out using special conversion factors tables. Those conversion factors are the relation between each substance and a theme's key emission. The calculations are repeated for all emissions and all environmental themes. The output of each process is presented in terms of the themes' key emissions (Van den Berg, 1995).

At this stage, it is crucial to convert the calculated amount of different environmental themes' key emissions into dimensionless values in order to be able to compute the sum of those values. This conversion process is called the "normalization process". The normalization process is carried out by dividing the contribution of each remediation alternative to a certain environmental theme by the global contribution to that environmental theme. This global contribution represents the impact caused by different emissions form all processes and activities world wide to each environmental theme.

2.7 Ranking: Prior to this phase, the questionnaires distributed to stakeholders' representatives during the planning phase should be collected. The results of those questionnaires are analyzed to calculate the weights assigned to each environmental theme. Those weights are calculated as follows:

1. Stakeholders are clustered into groups (e.g. local residents, site workers, etc.) where each group is assigned a weight based on the number of participants in this group to the total number of participants.
2. For each group, the average weight assigned to an environmental theme is calculated by dividing the sum of the weights assigned to that environmental theme by all participants by the number of those participants. This calculation is repeated for all stakeholders' groups and all environmental themes
3. The average weights assigned by a stakeholder's group is then multiplied by the weight assigned to that group.
4. Finally, the weight assigned to each environmental theme is calculated by dividing the sum of the weighs assigned to that environmental theme by all groups by the number of stakeholders' groups.

The following table, table (2) represent the calculations carried out to assign weight the "Noise" environmental themes based on the assumptions that there are only two stakeholders groups (local resident and workers)

	No. of participants	Weight of stakeholder groups (W)
Local residents	6	6/10 =0.6
Workers	4	4/10=0.4
Total	10	

Weight assigned by Participants	Participant (1)	Participant (2)	Participant (3)	Participant (4)	Participant (5)	Participant (6)	Sum of weights
Local residents	8	7	10	9	9	8	51
Workers	6	7	3	9			25

	Average weight (X) = Sum of weights / no. of participants	Y= X* W	S =Sum of the weights assigned by all group	Average weight assigned to Noise = S / no. of stakeholder groups
Local residents	51/6 = 8.5	8.5 * 0.6 = 5.1	5.1 + 2.5 = 7.6	7.6/2 = 3.8
Workers	25/4 = 4.25	4.25 * 0.4 = 2.5		

Table (2), assigning weights to the "Noise" environmental theme

2.8 Environmental Interpretation: The output of the Environmental interpretation phase is a single score which represents the social (i.e. weight assigned by stakeholders to different environmental themes) and environmental impacts of each remediation scheme under investigation. This score is calculated by multiplying the weight assigned to each environmental theme during the previous phase „ranking" by the normalized value calculated for the same environmental theme during the analysis phase. Finally, the sum of the outputs from those multiplication processes for all environmental themes are calculated.

2.9 Economic Interpretation: At this stage the economic efficiencies of the remediation alternatives under investigation are calculated. The economic efficiency of a remediation strategy is calculated by dividing the environmental impact saved by carrying out the remediation strategy by the cost of that remediation strategy. The environmental impact saved by carrying out a remediation strategy is calculated by subtracting the environmental impact caused by carrying out a remediation strategy from the environmental impact caused by the presence of contaminants in the site "the no action option". The cost of a remediation strategy includes fixed costs (e.g. installation) and running cost (e.g. operation and maintenance).

2.10 Final Interpretation: The final single score which represents the social, environmental, and economic impacts of a remediation strategy is calculated at this phase. This final score is calculated by summing the environmental and social impact of a remediation strategy (i.e. the output from the „environmental interpretation phase“) and the inverse of the number which represents the economic efficiency (i.e. the inverse of the output from the economic interpretation phase). The preferred remediation strategy is the one with the lowest score.

2.11 Evaluation: This phase aims at providing future users with an overview of different tasks adopted while carrying out A*fr*S methodology. Weakness and strengths , public involvement techniques, easy and difficult tasks, used sources of data, usefulness and credibility of the used data sources, time consuming phases, etc. are highlighted in this phase.

2.12 Guidelines

To ease the use of A*fr*S methodology, detailed guidance for each phase was developed. In addition, several templates compatible with the guidance were developed. It is believed that both guidance and templates ease the use of A*fr*S methodology and allow users with low experience with remedy selection processes to reach the desired results by following the guidance and filling in its associated templates.

3. Risk Analysis

Because A*fr*S is a data intensive methodology, good attention should be given to data uncertainty issue. Consequently, it is important to adopt “Risk analysis” in order to calculate the probability distribution for the calculated environmental impact caused by different remediation alternatives. “Palisade Decision tool, @RISK for windows“ is a software which can be used to calculate those probability distributions. Probability Distributions Functions (PDFs) are used within the software to describe uncertain values. Each function represents a range of possible values that could occur for a certain variable, along with the probabilities that this value could occur.

Using @RISK allows for modeling and analyzing the real life situation. This model can be used to examine the real situation, and hopefully help in understanding what the future might bring. @RISK analysis results are presented in the form of probability distributions which the decision-maker must interpret and make a decision based on that interpretation.

4. Case Studies

Two case studies were carried out to examine the performance and practicality of the developed methodology, guidance, and associated templates. While the first one, “Stanbridge oil depot”, is a prototype simplified case study, “ Pumpherston site ” is a real world contaminated site.

4.1 Stanbridge Oil Depot

The “Stanbridge oil depot” case study was conducted to investigate the feasibility, practicality, and effectiveness of the developed methodology. A*fr*S, the draft user guidance and templates were amended based on the feedback from “ Stanbridge oil depot ”.

4.1.1Site Description

“Stanbridge oil depot” is a disused distribution depot close to a residential area, other industry, a farmland, and a river. The site was used for the storage and distribution of petroleum products. The main contaminants in soil and groundwater are: Benzene, Toluene, Ethylebenzene, Xylene, (BTEX) and Total petroleum Hydrocarbons (TPHs).

4.1.2 Results

Before applying AfrS to “ Stanbridge oil depot ”, a series of remediation alternatives which are able to remediate the site and meet the remediation project’s core objectives were identified. A*fr*S was applied to four alternatives. After collecting the required data and performing all necessary calculations, the alternative with the lowest final single score was selected as the preferred remediation alternative.

@ Risk was used to calculate the probability distribution of the environmental impact caused by the four remediation alternatives under investigation. Different PDFs were assigned to each variable with the help of literature (McMahon et al., 2001). Then the probability distributions of the environmental impact

caused by the remediation alternatives were calculated. The highest probability for the environmental impact caused by each remediation alternative indicates that the remediation alternative with the lowest environmental impact is the same alternatives which was selected using AfrS**.**

4.1.3 feedback

During the application of A*fr*S to " Stanbridge oil depot " the following remarks and alterations were made:

- It was found that the economic aspect of the SD concept was not given good attention within A*fr*S, consequently the "Economic interpretation and Final interpretation" phases were added to the methodology to allow for more consideration of the economic aspect.
- The screening phase was aimed at eliminating insignificant processes and activities from the system boundary of a remediation alternative. While adopting A*fr*S, it was found that eliminating remediation alternatives with high environmental impact and/ or energy consumption is more useful to the selection process as it saves time, effort, and money.
- Before adopting Stanbridge oil depot, the normalization step which is part of the analysis phase was though to be unnecessary. However, it was proven that this step is crucial for the calculation of the score which represents the environmental impact (the output from the environmental impact phase) of each remediation alternative.
- Before adopting "Stanbridge oil depot", mathematical models (e.g. rank sum, pair wise) were suggested to be used for ranking different environmental themes within the ranking phase. This was proven to be impractical, due to the fact that some mathematical models (e.g. rank sum, rank reciprocal) lack theoretical foundations and others (e.g. pairwise) are time consuming (Malczewski, 1999).
- In general, it was found that the total environmental impact of a remediation scheme is related to a great extent to the energy consumption of the scheme.
- Both user guidance and templates were modified based on the above mentioned remarks.

4.2 Pumpherston Site

After amending the developed methodology, guidance and templates based on the feed back form" Stanbridge oil depot", it was crucial to check the effect of those amendments on the feasibility, flexibility, and effectiveness of A*fr*S. Currently, another real world case study (i.e. Pumpherston site) is being carried out. Applying the developed methodology to a real world case study gives an indication of A*fr*S performance in real world.

4.2.1 Site description

"Pumpherston Works site" is located on the eastern outskirts of Livingston, West Lothian with an area of 29.5 ha. The site contains twelve hot spots, to be treated separately, thereby complicating the remediation selection process. A detailed site investigation and analysis (EPSRC, 1993a, EPSRC, 1993b, and EPSRC, 1993c) shows that both soil and ground water are contaminated with organic (e.g. TPH, phenols, benzene, toluene, ethylbenzene, xylen) and inorganic substances (e.g. arsenic, zinc, copper, mercury).

Four remediation strategies which are able to remediate the site and achieve the remediation project's core objectives were developed. Currently, AfrS is being applied to "Pumpherston Works site" to select the preferred remediation action from the available alternatives**.**

4.2.2 Feedback

"Pumpherston Works site" was found to be more complicated than "Stanbridge oil depot", however the amended methodology, guidance and templates ease the execution of the remedy selection process using A*fr*S. The amended methodology saved unnecessary efforts, time and money spent in collecting useless data or performing nonessential tasks.

It was necessary to design special templates for the remediation techniques which were not considered during "Stanbridge oil depot", figure (4). This process draws the attention to the need for designing different templates for different remediation techniques, however there is no big differences between those templates.

Summary and Conclusion

Land and groundwater contamination can seriously affect human health and the environment. In addition, the presence of contaminants in a certain piece of land may decrease the value of the land and limit possible land re-use alternatives. Consequently, the significance of contaminated land remediation has been recognized worldwide (CLARINET, 2002).

The use of remediation techniques is essential for land reclamation, however those remediation techniques can result in environmental, social, and economic impacts. Consequently, there is a need for decision support techniques that consider the wider issues of SD, and support stakeholder participation in the remedy selection process (CLARINET, 2002).

A*fr*S is an LCA based methodology, which was developed for remedy selection within the context of SD. The eleven phases of A*fr*S incorporate environmental, social, and economical elements within the remedy selection process. To ease the use of the proposed methodology, detailed user guidance and a set of compatible templates were developed to help and guide the user. Users with low experience in remedy selection processes should be able to use A*fr*S by following the developed guidance and using its associated templates to come out with the preferred remediation scheme.

4. Screening

Scheme 1	SW + (AS+CA) + P&T + MNA											
4.1 Emissions template	Soil Washing											
General Data	Assume any conc. Till I get the figure											
Area. of contaminated land	19.4 ha. = 194000 m² = 0.194 m2											
Max. depth of contaminats	8 m											
Vol. Of contaminated soil	1552000 m³											
Mass of contaminated soil	3.731E+09 kg											
Vol. Of hot spots	51325 m³											
Soil density =	2404 kg/m3 assumed											
Contaminated soil in hot spots	123385300 kg											
Average % Silt	22%											
Average % Clay	10%											
Average % Silt & Clay	32%											
Project duration =	5 years = 60 months = 1800 days = 43200 hrs.											
4.1.1 Mass & Energy Balances												
4.1.1.1Mass Balance	Inputs = Emissions + Outputs											
Used equations	Inputs = Emissions + Outputs											
Soil fed	24.7 t/hr = 24700 kg/hr											
Efficiency of the soil washing	85% = 0.85											
Hot spot name	Griffts tar Pond 1					Griffts tar Pond 2					Assessment levels-industrial	
Substance Name	Contaminan tConc. mg/kg	Cont. conc. in the output	Cont conc. Remain in soil mg/kg	Emissions - ass. Level in sludge (mg/kg)	in soil mg/kg	Contaminan tConc. mg/kg	Conc.of cont. in the output	Cont. conc. Remaining in soil	Emissions - ass. Level in sludge (mg/kg)	in soil mg/kg	Assessment levels-Soil-open space mg/kg	
Arsenic	0.009	0.00765	0.00135	-ve	-ve	0.009	0.00765	0.009	-ve	-ve	50	
Total PAH	20.991	17.84235	3.14865	- ve	- ve	20.991	17.84235	20.991	- ve	- ve	1000	
Total surfactants	40	34	6			40	34	40				
4.1.1.2 Energy Balance												
Used equations	*Total energy consumed by 3 pumps (MJ/hr)= energy consumption per pump/ hr (MJ/h)* number of pumps*											
	Energy consumptionby/ kg contaminated land (MJ/ contaminated land)= energy consumption (MJ/hr) / soil processed per hr (kg/ hr)											
Used Pumps												
No. of pumps	3 pumps											
Energy consumption/ hr	125 hp = 93.25 KW = 335.7 MJ/h = 335700 KJ/h											
Soil processed /hr	24.7 t/hr = 24700 kg/hr											
No. of hours required to processe contaminated soi	Mass of contaminated / Soil processed per hr											
	20.991 / 24700 = 0.00085 hrs											
Energy consumption to treat the soil kg contaminated land	Energy consumption /l * hr required to treat the / mass of contamonated soil											
	335700 * 0.000849838 / 0.01 = 28529.06 KJ/h											
Well excavation												
No. of wells	55 assumed											
Energy consumption	13.4 kW = 48.24 MJ/h = 48240000 J/h											
Used Rig =												
RPM =	6.1 l/hr											
Number of hrs required to dug a well =	Vol. Of well / RPM											
	= 21450 / 6.1 = 3516 hrs											
Energy consumption	13.4 KW = 48.24 MJ/h = 48240000 J/h											
Energy used to dug all wells =	3516 * 55 * 48.24 = 9329695 MJ/hr = 9.33E+09 KJ											
Energy consumption/kg =	9.33E+11 KJ/kg											
Total energy consumption	9.33E+11 KJ/Kg											
Diesel calorific value =	46 KJ/kg 38.5 MDI/l											
Mass of diesel used /kg =	Total energy consumption per kg of contaminated s / diesel calorific value =											
	9.3297E+11 / 46 = 2.028E+10 kg/kg contaminated soil											
Emissions caused by fuel combustion	**% in the vapour**				**Mass of diesel in kg /kg contaminated soil**					**Mass in the output vapour (kg)**		
CO2	7.1				20281946451					1440018198		
O2	15				20281946451					3042291968		
N	75				20281946451					15211459838		
Patriculate	0.006				20281946451					1216916.787		
Generall remarks												

Fig. (4) Template designed for the Soil washing remediation technique

The performance of the developed methodology was tested by applying it to two different case studies. Firstly, the practicality, feasibility, and effectiveness of A*fr*S was checked by applying the methodology to a prototype simplified case study. Necessary amendments were made to A*fr*S, its guidance and associated templates based on the feed back from this case study.

Secondly, the amended AfrS was applied to a real world case study to check the effect of the alterations made to the methodology, guidance, and templates. Finally, It is believed that the developed methodology will ease the remedy selection process and aid in selecting the preferred remediation strategy within the context of SD.

References

1. Bardos, R.P., Mariotti., C., Marot, F., and Sullivan., T. (2001) Framework for Decision Support Used in Contaminated Land Management in Europe and North America. *Land Contamination and reclamation.* (2001).Vol 9., No. 1.
2 Bardos, R. P, Nathanail, C.P., and Weenk, A. (1999a) Assessing the Wider Environmental Value of Contaminated Land remediation, A Review for Environmental Agency. R&D technical Report P5-023.
3. Bardos, R.P, Martin, I. And Kearney, T. (1999b) Framework for evaluating remediation technologies. In *IBC's 10th Conference*. Contaminated land. July 5th, Royal Marsden NHS Trust, London.
4. Bardos, P. (1994) Current Development in Contaminated Land Treatment Technology in the UK. In West Midlands Branch Symposium on Contaminated Land. Pb 402-408
5. CIRIA (1995) Remedial Treatment for Contaminated Land: Planning and Management, Vol. XI. CIRIA special publication 104. ISBN: 086017 406 9
6. Clift, R. (1997) Life Cycle Assessment. Proceedings of Environment 97'. University of Surrey. UK. Available from http://www.environment97.org/framed/reception/r/all_papers/t3.htm Accessed at 2/1/2000.
7. Contaminated Land Rehabilitation Network for Environmental Technologies (CLARINET, 2002) Sustainable Management of Contaminated Land; An Overview. August 2002. Available from www.clarinet.at Accessed at 12.10.2002
8. Curran, M. (ed.) (1997), Environmental life cycle assessment. MC-Graw Hill Publishers, New York, USA
9. EPSRC (1993a) BP International Ltd. Pumpherston Youngs Detergent Works. Desk Study
10. EPSRC (1993b) BP International Ltd. Pumpherston Youngs Detergent Works. Ground investigation, Phase 1.
11. EPSRC (1993c) BP International Ltd. Pumpherston Youngs Detergent Works. Phase 2-site investigation; Risk assessment and remediation report.
12. Friedrich, E.,, Life Cycle Assessment as an Environmental Management Tool in the Production of Potable Water. Published in Water Science and Technology. 46 (9) 29-36 (2002).
13. Institution of Chemical Engineers (IChem): Environmental Protection; Public Perception and the Consultative Process. Environmental Protection Subject group. March, 2001, London.
14. Malczewski, J. (1999) GIS and Multicriteria Decision analysis. John Wiely and sons, U.S. ISBN: 0-417-32944-4.
15. McMahon, A., Heathcote, J., Carey, M., Erskine, A., and Barker, J. (2001) Guidance on Assigning Values to Uncertain Parameters in Subsurface Contaminant Fate and Transport Modelling. Environment Agency National Groundwater & Contaminated Land Centre report Entec UK Ltd. ISBN: 1 857 05605 1
16. North Atlantic Treaty Organization (NATO): Evaluation of Demonstrated and Emerging Remedial Action Technologies for the Treatment of Contaminated Land and Ground Water. Available from www.nato.int/ccms/s13/report/intrmo1.html Accessed at 2.10.2001.
17. Palisade Corporation: @ RISK for Windows. Version 3.5.1, 1997.
18. Petts, J., Cairney, T., and Smith, M. (1997). Risk Based Contaminated Land Investigation and Assessment. Chichester: John Wiley & Sons. ISBN: 0471966088
19. Van den Berg, N.W., Dutillh, C.E., and Huppes, G. (1995) Beginning LCA: A Guide into Environmental Life Cycle Assessment. Published under the authority of: National Reuse of Waste Research Program (NOH). Humanities, Rotterdam. ISBN: 90-5191-088-6.